이학박사학위논문

Analogue Gravity : Quantum Backreaction and Quantum Many-Body Black Holes in a 1D Finite-Size Bose-Einstein Condensate

아날로그 중력 : 유한한 1차원 보즈-아인슈타인 응축체에서 양자 백리액션과 양자 다체계 블랙홀

2023년 2월

서울대학교 대학원

물리천문학부

박 상 신

Analogue Gravity :

Quantum Backreaction and Quantum Many-Body Black Holes in a 1D Finite-Size Bose-Einstein Condensate

지도교수 Uwe R. Fischer

이 논문을 이학박사 학위논문으로 제출함

2023년 1월

서울대학교 대학원

물리·천문학부

박 상 신

박상신의 박사 학위논문을 인준함

2023년 1월

위 원 장	정 성 훈	(인)
부위원장	Uwe. R. Fischer	(인)
위 원	신 용 일	(인)
위 원	김 지 훈	(인)
위 원	Caio Cesar Holanda Ribeiro	(인)

Analogue Gravity : Quantum Backreaction and Quantum Many-Body Black Holes in a 1D Finite-Size Bose-Einstein Condensate

by

Sangshin Baak

A Dissertation Submitted to the Faculty of the
Graduate School of Seoul National University in
Partial Fulfillment of the Requirements for the
Degree of Doctor of Philosophy

February 2023

Advisory Committee:

Professor Sunghoon Jung, Chair
Professor Uwe. R. Fischer, Advisor
Professor Yong-il Shin
Professor Jihoon Kim
Professor Caio C. Holanda Ribeiro

This dissertation contains contents of the following journal publications:
Caio C. Holanda Ribeiro, Sang-shin Baak, and Uwe R. Fischer, *Phys.Rev.D* 105, 124066 (2022);
Sang-shin Baak, Caio C. Holanda Ribeiro, and Uwe R. Fischer, *Phys.Rev.A* , To Appear (2022);

Printed in South Korea

Abstract

Analogue gravity is an interdisciplinary research program which simulates curved spacetime physics using tabletop experiments. This study concerns, in principle, the measurable analogue gravitational effect in quasi-1D finite-size dilute Bose-Einstein Condensate (BEC) whose inter-particle interaction is contact interaction. Because the Hamiltonian of the Bose gas has the global $U(1)$-symmetry, the total number of particle N is fixed. Hence, in the large N system, one can use $1/\sqrt{N}$ as a small expansion parameter for the field. A number-conserving Bogoliubov expansion in this thesis is done by simply including the $N^{-1/2}$-order field to the usual non-number-conserving Bogoliubov expansion which breaks $U(1)$-symmetry breaking. The included field is interpreted as a condensate correction induced by the Bogoliubov field. The expansion validity solely depends on the Bogoliubov assumption of the smallness of the depletion. And the analysis is done in a valid regime. Especially, the time scale of such a validity regime is investigated also.

The study covers two finite-size systems which are experimentally feasible in ultra-cold gas. Firstly, the 1D finite homogeneous BEC is investigated. Using the number-conserving Bogoliubov expansion, one can get the exact mode solution for the equations of motion up to $N^{-1/2}$-order field expansion for this model. The condensate is assumed to be noninteracting in the beginning, and in its ground state to ensure a well-defined initial vacuum state. By suddenly turning on the interaction, the condensate is driven out of equilibrium instantaneously. Notably, this assumption of the initial vacuum state allows one to avoid the ambiguity in choosing a vacuum state for interacting condensate which is due to phase diffusion and the consequent condensate collapse. Using the

exact solution of mode expansion in a given initial vacuum state, the depletion and condensate correction is calculated. It is revealed that the depletion and condensate density corrections cannot be disentangled by the measurement of the power spectrum. Furthermore, even though the initial condensate is at rest and the leading order condensate does not move, the quantum fluctuation of the depleted particles gives rise to a nontrivial condensate flux in the subleading order.

Moreover, the quantum backreaction force is identified as the deviation from the classical Eulerian force which can be obtained by using the Madelung representation. It is also shown that for the leading order condensate at rest, the classical force in the working order (N^0) is determined by only the total density of particles. Hence, the knowledge of total density as a function of time gives the viable route for experimental measurement of quantum backreaction force. In addition, the classical and total force can be written as a conservative form, i.e., one can find the scalar potential for them. Because the potential converges much faster than force, one can get the classical and total force potential in analytic form and can plot them, from which one can demonstrate that the quantum backreaction force attenuates a lot of the classical force near the boundaries.

Secondly, the 1D finite-size piece-wise homogeneous flow model is studied. The flow is sustained by the coherent source and drain placed at its boundary. The Mach number in each region is the ratio between the flow velocity and the sound speed in each region. Especially, the analogue event horizon is determined by the Mach number exceeding 1. It is shown that, regardless of the non-

Hermicity of the Bogoliubov Hamiltonian, it is, in principle, possible to sustain the stationary sonic black hole with a single event horizon.

The dynamical instabilities occur like black hole-white hole pairs. The black hole's lifetime is defined by the instabilities and the lifetime dependence on the system parameters is also investigated. Quantum depletion in this model is suggested as a diagnostic tool to validate the usage of Bogoliubov's theory and to describe the analogue Hawking process. One can find the clear signature of Hawking radiation in the depletion both inside and outside the event horizon. The relation between the Schiff-Snyder-Weinberg effect to the instability in the model is also investigated qualitatively.

Keywords: Bose-Einstein Condensate, Analogue Gravity, Depletion, Quantum Backreaction, Number-Conserving Bogoliubov Expansion

Student ID: 2012-20359

Contents

List of Figures

List of Tables

1 Introduction

Analogue gravity is the research program that investigates the phenomena coming from general relativity or the quantum field theory in curved spacetime in the analogous tabletop experiment. The analogous relation between gravity between other systems is noticed for a long time. Especially, in 1967, Sakharov noticed that many condensed matter systems are analogous to general relativity [61]. So, he suggests recognizing gravity not as a fundamental theory but as an emergent phenomenon from a more fundamental theory similar to the hydrodynamics that emerges from the motion of particles consisting of fluid. His idea is called the "induced gravity" or "emergent gravity" scenario of the quantum gravity model.

A few years later, Unruh showed that accelerating observers in flat spacetime can detect quanta even in the vacuum [73]. Especially, he showed that Hawking radiation is a general phenomenon of particle creation that can be obtained by appropriate boundary conditions. Moreover, he suggests the sonic analogue of the black hole, dumb-hole, which gives the same kinematic equations of motion for the sound wave and gives a sonic analogue of Hawking radiation [72].

From Unruh's suggestion, one can get an idea of getting around the difficulties of research in quantum field theory in curved spacetime and general relativity. For example, the observation of cosmological Hawking radiation is

notorious, because the thermal spectrum of usual massive black holes is extremely small so it is very weak and is hidden in the relatively high-temperature thermal bath. It can, in principle, be probed by the emission spectrum of the primordial black holes, but the primordial black holes themselves are not detected yet. But, in the analogue system, one can tune up the temperature of the Hawking radiation spectrum by controlling the experimental system parameters. Fascinated by this idea, analogue gravity is the research program that investigates the phenomena coming from general relativity or quantum field theory in curved spacetime in an analogous tabletop experiment is settled.

Because of its original suggestion from Unruh, the mainstream work was on exploring Hawking radiation. There was a lot of theoretical improvement in understanding Hawking radiation, and experimental suggestions on measuring it. Finally, researchers succeed in measuring the analogue Hawking radiation. Mainly, in the analogue models of Bose-Einstein condensate (BEC), not only the thermal spectrum of radiation but also the correlation between Hawking and its partner mode are observed by the Steinhauer group [51]. There is also a lot of increase and development in both theoretical and experimental aspects of analogue gravity in other phenomena also in recent years. It is stated that the new frontiers of analogue gravity are started and the new goals of investigating generalized quantum field theory in curved spacetime phenomena are settled [15].

The depletion is the first-order correlation function which tells how many of the Bose particles are not in the condensate state. Even though the concept is simple, measuring depletion is not easy and challenging. Theoretically, its smallness compared to the total particle tells the validity regime that the Bogoliubov approximation holds. In analogy with gravity, it is also related

to particle creation such as Hawking radiation and the backreaction effect. Hence, the investigation of the depletion measurement is not only hard but also important. The measurement of the depletion and its importance in analogue gravity is debated in this study.

The backreaction is how the matter field influences the background spacetime. In analogue gravity in BEC, the condensate is regarded as a background spacetime. Hence, one needs to include the condensate change caused by the sound wave or linear field. In order to describe that change properly, one needs to use the number-conserving theory for Bose gas. Moreover, not like real gravity, the quantum dynamics of Bose gas are known. Hence, one can calculate the analogue quantum backreaction for Bose gas dynamics. In this thesis, the well-defined notion of quantum backreaction in the linearization procedure is defined. The backreaction in analogue gravity is studied in [38, 55, 4, 74, 32]

In an actual tabletop experiment, we have a finite-size system. Moreover, Bose-Einstein condensates cannot exist in infinitely extended quasi-1D black hole models. This can be read, for instance, from the condensate perturbations of [33], which imply a (generic) logarithmic divergence of the quantum depletion with the system size at $T = 0$. At finite temperature, this divergence is stronger (linear in system size), as dictated by the Hohenberg theorem [28], showing that finite temperature effects as predicted by quasicondensate models might not be extendable to condensates. Nonetheless, henceforth our analysis is restricted to zero point (vacuum) fluctuations ($T \sim 0$), which pertain to the theory sector responsible for the quantum Hawking process. In this regime, a (weak) logarithmic divergence with the system size means that we can safely consider larger condensates while maintaining sufficient control of the system depletion.

Furthermore, another crucial aspect of infinite-size models is linked to the theory of $U(1)$ symmetry (in the absence of external sources). As the condensate existence breaks this symmetry, the theory always admits at least one zero-frequency excitation, and if the condensate is infinite in size, then the system spectrum is continuous. This is particularly important for black hole analogues, for the Hawking-like process is a low-energy phenomenon, and thus more sensitive to boundary conditions. Accordingly, to assume the robustness of the Hawking process with respect to the system size is a strong assumption that needs clarification. Indeed, the spectrum cannot even be continuous for finite-size configurations, and because the system is not homogeneous, nontrivial filtering of the excitations existent in infinite analogues should occur.

Hence, this thesis devotes to investigating finite-size systems. Two simple but important systems are investigated. The 1D finite-size uniform condensate at rest is the simplest system one can imagine. It corresponds to the 1D static finite-size universe. The backreaction in this model is analytically calculated, and the measurement is also suggested.

The other system is the 1D finite-size flow with two homogeneous regions which are called upstream and downstream. By varying the system parameter, one can control the Mach number of the system and the corresponding metric. Particularly, one can make the downstream Mach number to be supersonic to make the analogue Black hole. Not like the torus model, which has only one horizon. Because of the nonHermicity of the Bogoliubov Hamiltonian, the finite size flow model can be suffered from dynamical instability. The stability of the black hole system is investigated.

2 Quantum Field Theory in Curved Spacetime

2.1 Basic Formulation

Classical Field and Quantization — Quantum field theory in curved spacetime treats the quantum fields in curved spacetime. One can find the Lagrangian or equations of motion for the classical field theory. And one can also quantize the field without ambiguity [17]. For simplicity, let us see the massless scalar field ϕ coupled to gravity. The spacetime is defined as a 4-dimensional pseudo-Riemannian manifold $(M, \mathcal{O}, \mathcal{A}, \nabla, g)$ (See Sec. 8.1) The action is

$$S = -\frac{1}{2}\int \mathrm{d}^4x\sqrt{-g}(\nabla_\mu\phi\nabla_\nu\phi + m^2\phi^2 + \xi R\phi^2). \tag{2.1}$$

where $g \coloneqq \det g_{\mu\nu}$, R is the Ricci (curvature) scalar, and ξ is a dimensionless constant. $\xi = 0$ is called the minimal coupling and $\xi = 1/6$ is called the conformal coupling. One can easily get the Klein-Gordon (KG) equation by solving the Euler-Lagrange equation

$$\Box\phi + (m^2 + \xi R)\phi = 0, \tag{2.2}$$

where $\Box = g^{\mu\nu}\nabla_\mu\nabla_\nu$ is the covariant d'Alembertian operator. To get a general solution of Eq. (2.2), one needs to have a well-posed Cauchy problem. In other words, spacetime must be globally hyperbolic.

If a canonical formulation is desired, a decomposition of M in spacetime must be introduced. Concretely, one needs two ingredients:

- A Global time function $t : M \to \mathbb{R}$ defining a foliation of M in Cauchy hypersurfaces Σ_t labelled by the value of t.
- An "evolution" vector field t^μ, satisfying $t^\mu \nabla_\mu t = 1$, which provides an identification points in different leafs. It provides the "time flow"

For given t, t^μ, one can define the time derivative $\dot{\phi} \coloneqq t^\mu \nabla_\mu \phi$ and conjugate momentum

$$\Pi \coloneqq \frac{\delta S}{\delta \dot{\phi}} = \sqrt{h} n^\mu \nabla_\mu \phi, \tag{2.3}$$

where n^μ is the unit normal to Σ_t and $h \coloneqq \det[h_{\mu\nu}]$ where $h_{\mu\nu}$ is an induced metric on Σ_t by $g_{\mu\nu}$.

Given a fixed background metric $g_{\mu\nu}$, the KG equation is linear in ϕ. Hence, the space of complex solutions $\mathcal{S}^{\mathbb{C}}$ is a vector space. Given two solutions $\phi_1(x), \phi_2(x)$ one can define the KG current

$$j^{\mathrm{KG}}_\mu(\phi_1, \phi_2) \coloneqq \phi_1^* \nabla_\mu \phi_2 - (\nabla_\mu \phi_1^*)\phi_2. \tag{2.4}$$

And one can also define the KG-product

$$\begin{aligned}(\phi_1, \phi_2)_{\mathrm{KG}} &\coloneqq i \int_{\Sigma_t} \mathrm{d}\Sigma^\mu j^{\mathrm{KG}} \\ &= i \int \mathrm{d}^3 x (\phi_1^* \Pi_2 - \Pi_1^* \phi_2)\end{aligned} \tag{2.5}$$

where $\Pi_{1,2}$ is the conjugate momentum of $\phi_{1,2}$ each and $\mathrm{d}\Sigma^\mu = \mathrm{d}^3 x \sqrt{h} n^\mu$. The KG product is independent of the choice of Σ_t chosen in the foliation. It is a sesquilinear inner product in $\mathcal{S}^{\mathbb{C}}$.

Quantization such as canonical quantization, path integral or algebraic quantization can be done without ambiguity. For example, the canonical

quantization can be done by imposing

$$[\hat{\phi}(t,x), \hat{\Pi}(t,x')] = i\delta(x-x'). \tag{2.6}$$

Characterization of Quantum States and Physical Interpretation— As indicated by Fulling, the particle interpretation or Fock space representation is not adequate for general cases in quantum field theory in curved spacetime [19]. It is, however, more familiar and historically important. In this thesis, the Fock space representation is also adopted. The procedure is following

- Choose any splitting of positive/negative subspace such as $\mathcal{S}^{\mathbb{C}} = \mathcal{S}^+ \oplus \mathcal{S}^-$ satisfying:
  - $(\cdot,\cdot)_{\mathrm{KG}}$ being positive definite in $\mathcal{S}^+$.
  - $\mathcal{S}^- = (\mathcal{S}^+)^*$ so that $(\cdot,\cdot)_{\mathrm{KG}}$ is negative definite;
  - $\mathcal{S}^+ \perp \mathcal{S}^-$ i.e., for $\phi_1 \in \mathcal{S}^+, \varphi_2 \in \mathcal{S}^- : (\phi_1, \varphi_2)_{\mathrm{KG}} = 0$.

  If $\{\varphi_i(x)\}_{i=1}^{\infty}$ is a basis of $\mathcal{S}^+$, then $\{\varphi_i^*(x)\}_{i=1}^{\infty}$ is a basis of $\mathcal{S}^-$.
- Define the representation of "operator valued distribution" $\hat{\phi}(x)$ as

$$R_F[\,\hat{\phi}(x)\,] = \sum_i \varphi_i(x)\hat{a}_i + \varphi_i^*(x)\hat{a}_i^\dagger \tag{2.7}$$

  where $\hat{a}_i = (\varphi_i, R_F[\hat{\phi}])_{\mathrm{KG}}$ and $\hat{a}_i^\dagger = -(\varphi_i^*, R_F[\phi])_{\mathrm{KG}}$. The $R_F[\,\cdot\,]$ means the representation in Fock space. Hence, the commutation relation Eq. (2.6) implies

$$[\hat{a}_i, \hat{a}_j] = (\varphi_i, \varphi_j^*) = 0 \tag{2.8a}$$

$$[\hat{a}_i^\dagger, \hat{a}_j^\dagger] = (\varphi_i^*, \varphi_j) = 0 \tag{2.8b}$$

$$[\hat{a}_i, \hat{a}_j^\dagger] = (\varphi_i, \varphi_j) = 0 \tag{2.8c}$$

Note that Eq. (2.7) is not the operator, one can define the "smeared Heisenberg field operator" by introducing the test function and smearing on it [75].

- The vacuum state $|0\rangle$ associated to the choice of $\mathcal{S}^+$ is defined as

$$\forall \hat{a}_i : \hat{a}_i|0\rangle = 0. \tag{2.9}$$

- The one-particle Hilbert space $\mathcal{H}$ is the completion of $(\mathcal{S}^+, (\cdot\cdot)_{\mathrm{KG}})$ i.e., the space spanned by $\{\hat{a}_i^\dagger|0\rangle\}_{i=1}^\infty$.
- The symmetric Fock space $\mathcal{F}$ built from $\mathcal{H}$ is

$$\mathcal{F}(\mathcal{H}) \coloneqq \bigoplus_{n=0}^{\infty} \mathcal{H}^n = \mathbb{C} \oplus \mathcal{H} + \mathcal{H}^2 + \dots \tag{2.10}$$

where $\mathcal{H}^n = \underbrace{\mathcal{H} \otimes_{\mathrm{s}} \dots \otimes_{\mathrm{s}} \mathcal{H}}_{n \text{ times}}$ i.e., the space spanned by

$$\prod_{i=1}^{\infty} \frac{(\hat{a}_i^\dagger)^{n_i}}{\sqrt{(n_i)!}}|0\rangle$$

where $n_i \in \{0, 1, 2, \dots\}$.

Note that the concepts of vacuum and particles depend on the choice of $\mathcal{S}^+$ or equivalently the choice of representation. Hence, the particle concept is ambiguous and the physical interpretation of observables and quantum states is difficult [17].

2.2 Bogoliubov Transformation

Since there are infinitely many choices of representations, one needs to find the transformation connecting two different representations. Let the two different choices of representation as in Table. 2.1

Splitting	$\mathcal{S}^{\mathbb{C}} = \mathcal{S}_1^+ \oplus \mathcal{S}_1^-$	$\mathcal{S}^{\mathbb{C}} = \mathcal{S}_2^+ \oplus \mathcal{S}_2^-$
Basis of positive frequency	$\{\varphi_i^{(1)}\}$	$\{\varphi_i^{(2)}\}$
Annihilation operator	$\hat{a}_i^{(1)} = (\varphi_i^{(1)}, \hat{\phi})_{\mathrm{KG}}$	$\hat{a}_i^{(2)} = (\varphi_i^{(2)}, \hat{\phi})_{\mathrm{KG}}$
Vacuum state, Hilbert and Fock Space	$\|0\rangle_1$, $\mathcal{H}_1$, $\mathcal{F}_1$	$\|0\rangle_2$, $\mathcal{H}_2$, $\mathcal{F}_2$

Table 2.1 Table of notation in two different choices of splitting of the frequency in the positive and negative frequency.

Since $\{\varphi_i^{(1)}, \varphi_i^{(1)*}\}$ is a basis of $\mathcal{S}^{\mathbb{C}}, \exists \alpha_{ij}, \beta_{ij} \in \mathbb{C}$ such that

$$\varphi_i^{(2)} = \sum_j \alpha_{ij}\varphi_j^{(1)} + \beta_{ij}\varphi_j^{(1)*}, \tag{2.11}$$

where the coefficients $\alpha_{ij} = (\varphi_j^{(1)}, \varphi_i^{(2)})_{\mathrm{KG}}$, $\beta_{ij} = -(\varphi_j^{(1)^*}, \varphi_i^{(2)})_{\mathrm{KG}}$ are called the Bogoliubov coefficients.

Because each basis is orthonormal,

$$\sum_k \alpha_{ik}\alpha_{jk}^* - \beta_{ik}\beta_{jk}^* = \delta_{ij}, \tag{2.12a}$$

$$\sum_k \alpha_{ik}\beta_{jk} - \beta_{ik}\alpha jk = 0. \tag{2.12b}$$

And the inverse transformation for the Eq. (2.11) is

$$\varphi_i^{(1)} = \sum_j \alpha_{ji}^*\varphi_j^{(2)} - \beta_{ji}\varphi_j^{(2)*}. \tag{2.13}$$

Let us assume that there is a unitary operator $U : \mathcal{F}_1 \to \mathcal{F}_2$ by $R_{F_1}[\hat{\phi}] \mapsto UR_{F_1}[\hat{\phi}]U^{-1} = R_{F_2}[\hat{\phi}]$. Hence,

$$U^{-1}\hat{a}_i^{(2)}U = \sum_j \alpha_{ij}^*\hat{a}_j^{(1)} - \beta_{ij}^*\hat{a}_j^{(1)\dagger} \tag{2.14a}$$

$$U\hat{a}_i^{(1)}U^{-1} = \sum_j \alpha_{ji}\hat{a}_j^{(2)} - \beta_{ji}\hat{a}_j^{(2)\dagger} \tag{2.14b}$$

Hence, if $\beta_{ij} \neq 0$ for some i, j, then the vacuum is different. i.e.,

$$U|0\rangle \neq |0\rangle_2, \tag{2.15}$$

i.e., $U|0\rangle_1$ is not the vacuum in $\mathcal{F}_2$. Note that $\hat{a}_i^{(1)}|0\rangle_1 = 0$. Hence,

$$0 = U\hat{a}_i^{(1)}U^{-1}(U|0\rangle_1) = (\sum_j \alpha_{ji}\hat{a}_j^{(2)} - \beta_{ji}\hat{a}_j^{(2)\dagger})U|0\rangle_1. \tag{2.16}$$

The explicit form of the state $|0\rangle_1$ in $\mathcal{F}_2$ is

$$U|0\rangle_1 = N \exp\Big[\frac{1}{2}\sum_{i,j}\big(\sum_k \beta_{ik}^*\alpha_{kj}^{-1}\big)\hat{a}_i^\dagger\hat{a}_j^\dagger\Big]|0\rangle_2. \tag{2.17}$$

where N is a normalization factor. The number of particles (quanta) corresponds to the mode decomposition $\varphi_i^{(2)}$ contained in $U|0\rangle_1$ is

$${}_1\langle 0|U^{-1}\hat{a}_i^{(2)\dagger}\hat{a}_i^{(2)}U|0\rangle_1 = {}_1\langle 0|(U^{-1}\hat{a}_i^{(2)\dagger}U)(U^{-1}\hat{a}_i^{(2)}U)|0\rangle_1 = \sum_j |\beta_{ij}|^2. \tag{2.18}$$

is the main idea of understanding particle creation in quantum field theory in curved spacetime such as the Unruh effect. The nonzero β_{ij} for some i, j means a mode conversion between positive and negative frequency modes. In finite dimension, Stone-Von Neumann theorem guarantees that there is always a unitary operator defined as Eq. (2.14). If there is such a unitary operator, one calls two Fock representations are unitarily equivalent. In field theory, because of the infinitely many degrees of freedom, the Stone-Von Neumann theorem does not apply, and so, in general, Fock spaces are not unitarily equivalent. Practically, one can check whether two Fock spaces are unitarily equivalent by checking the total number of particles of vacuum states in the other Fock space representation [1]. The unitary operator U satisfying Eq. (2.14) exists iff

$$\sum_{i,j} |\beta_{ij}|^2 < \infty. \tag{2.19}$$

Mathematically, the existence of unitarily inequivalent representations is a significant problem since one cannot have a consistent formulation of the quantum theory. It is, however, still possible to construct the "physically equivalent" quantum theory for the finitely many measurements with finite accuracy if one considers only the measurable quantities in quantum field theory by Fell's theorem [75].

In Minkowski spacetime, there is a preferred vacuum corresponding to the inertial observer. If there is a globally timelike Killing vector field t^μ, there is a preferred vacuum [2]. But, in general spacetime, there is no globally timelike symmetry, so there is no preferred vacuum state. Since there is no preferred Fock space, the vacuum and particle concepts are equally meaningful and one cannot choose a specific configuration. What one can do is find a locally timelike Killing vector field (if there exists one) and use it to single out the preferred vacuum.

2.3 Unruh Effect and Hawking Radiation

The Minkowski spacetime admits global timelike Killing vector. Primarily, there is a preferred choice of observers who are called inertial observers. There is another choice of isometries. Especially, one can think about the Killing vector field of the form

$$b = a\left[X\frac{\partial}{\partial T} + T\frac{\partial}{\partial X}\right] \tag{2.20}$$

where T, X are global inertial coordinates, and a is an arbitrary constant which is interpreted as an acceleration of observer.

In Fig. 2.1, the Minkowski spacetime is divided into four regions. I and II regions represent the space where the value of the vector field b is timelike.

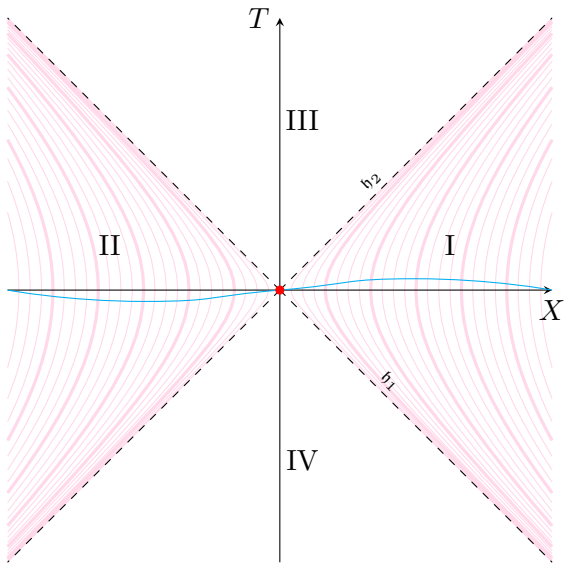

Figure 2.1 Spacetime diagram of Minkowski spacetime. T is the "ordinary" time direction, and X is chosen to be the spatial direction of the accelerating observer. Region I is the right Rindler wedge, and region II is the left Rindler wedge. The pink lines describe the trajectory of constantly accelerating observers. $\mathfrak{h}_1, \mathfrak{h}_2$ denotes the null plane. The red dot denotes the bifurcate Killing horizon. The cyan curve denotes the Cauchy surface in each wedge.

III and IV regions represent the space where the value of the vector field b is spacelike. $\mathfrak{h}_1, \mathfrak{h}_2$ lines show the horizon Killing horizon where the Killing vector field b is null. The congruence of integral curves of b in region I and II is shown as a pink curve. Each curve describes the trajectory of accelerating observers. Note that region I is globally hyperbolic (has a Cauchy surface), and the b is the timelike Killing vector in there. Hence, one can construct the Fock space $\mathcal{F}_{\mathrm{I}}$ in region I. Similarly, one can construct the quantum theory in region II in the same manner. Since in the whole Minkowski spacetime point of view, the whole cyan curve in Fig. 2.1 can be also understood as the Cauchy surface with a "bifurcation surface" (the red point) at the origin. In this case, one can construct $\mathcal{F}_1$ as the inertial observer Fock space in Minkowski spacetime and

$\mathcal{F}_2$ be

$$\mathcal{F}_2 = \mathcal{F}_{\rm I} \otimes \mathcal{F}_{\rm II}. \tag{2.21}$$

The basis expansion analogous to Eq. (2.11) is

$$\varphi_i^{(1)} = \alpha_i^{\rm I}\varphi_i^{(\rm I)} + \alpha_i^{\rm II}\varphi_i^{(\rm II)} + \beta_i^{\rm I}\varphi_i^{(\rm I)*} + \beta_i^{\rm II}\varphi_i^{(\rm II)*} \tag{2.22}$$

where $i = (\omega, k)$. Using lightcone coordinate, and conformal invariance of 2-dimensional subspace, one can get the mode solution [50].

Analogous to Eq. (2.17), one gets (for $1+1$-dimensional subspace)

$$\begin{aligned} U|0\rangle_1 &= N \exp\left[\frac{1}{2}\int \frac{{\rm d}\omega}{2\pi} {\rm e}^{-\pi\omega/a} \hat{a}_\omega^{(\rm I)\dagger} \hat{a}_\omega^{(\rm II)\dagger}\right] |0\rangle_{\rm I} \otimes |0\rangle_{\rm II} \\ &= N \prod_\omega \sum_{n=0}^{\infty} {\rm e}^{n\pi\omega/a} |n_\omega\rangle_{\rm I} \otimes |n_\omega\rangle_{\rm II}. \end{aligned} \tag{2.23}$$

where N is a normalization constant and n_ω is the notation for n particle with frequency ω. $\mathcal{F}_1$ is not unitarily equivalent to $\mathcal{F}_{\rm I} \otimes \mathcal{F}_{\rm RN2}$ [20]. But, one can construct the density matrix in $\mathcal{F}_{\rm I}$ by taking partial trace in $\mathcal{F}_{\rm II}$ for the density matrix $\rho_1 := U|0\rangle_{11}\langle 0|U$. In particular, the particle density with the energy ω is

$$n_\omega = \frac{1}{{\rm e}^{2\pi\omega/a} - 1}. \tag{2.24}$$

Since Eq. (2.24) is the Bose-Einstein distribution, the Minkowski vacuum is a thermal bath with the temperature

$$T_{\rm U} = \frac{a}{2\pi}. \tag{2.25}$$

The phenomenon of thermal particles noticed by the accelerated observer in the Minkowski vacuum is called the Fulling-Davis-Unruh effect, or simply the Unruh effect.

The simple point of view on Hawking radiation is interpreting Hawking radiation as a Fulling-Davis-Unruh effect where the accelerating observer is an observer who stays just outside of the horizon. In this simple view, one needs extended Schwarzschild spacetime.

In the formal derivation of the Fulling-Davis-Unruh effect, the main idea is to split the space into two subspaces with timelike Killing vector fields and construct the quantum theory on each subspace with the Cauchy surface in each subspace. The existence of a bifurcate Killing horizon shows the nontrivial attachment of two subspaces. Fig. 2.2 shows the same structure. Hence one can get the Fulling-Davis-Unruh effect with a black hole horizon, I.e., a black hole emits thermal radiation with the temperature.

$$T_{\mathrm{H}} = \frac{\kappa}{2\pi}. \tag{2.26}$$

where the acceleration being surface gravity $\kappa = 1/4M$ and M means the mass of the black hole.

As a final remark, even though the simple view of Hawking radiation as an example of the Fulling-Davis-Unruh effect is fascinating and gives the correct Hawking temperature, it is different from Hawking radiation in detail. The difference is that in a real black hole formed by a gravitational collapse, there is no region II, III. Hence, the extended Schwarzschild geometry explanation describes the Hawking radiation from the eternal black hole.

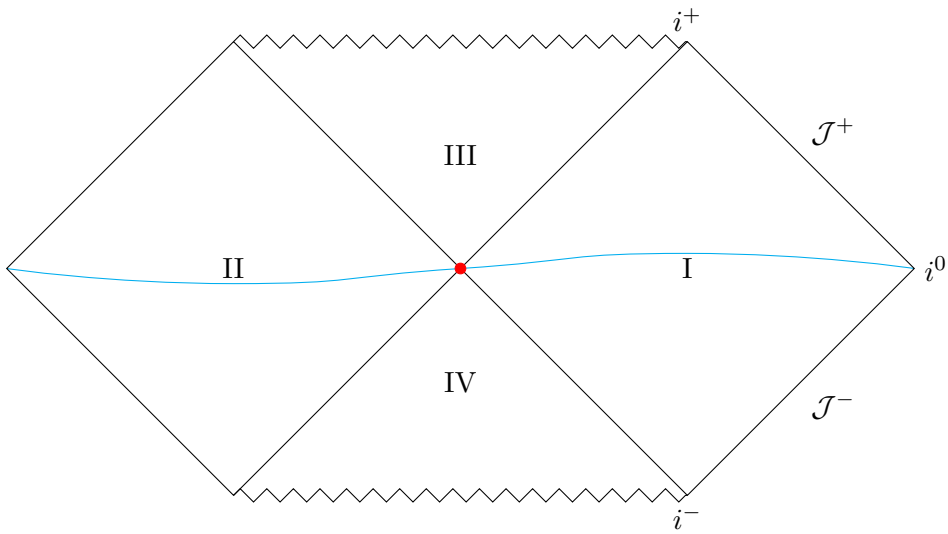

Figure 2.2 Penrose diagram for the extended Schwarzschild spacetime. The i^+, i^- is the future/past timelike infinity, and i^0 is the spatial infinity. $\mathcal{J}^+.\mathcal{J}^-$ is the future/past null infinity. The cyan curve is the Cauchy surface of each region I and II, and the red point is the bifurcate Killing horizon. The wiggled line describes the singularity at the center of the black hole.

3 Number-Conserving Bogoliubov Expansion

3.1 Expansion in Powers of N

The dynamics of the $1+1$ dimensional Bose gas comprising atoms or molecules of mass m within the s-wave approximation is described by the first-order Lagrangian density

$$\mathcal{L}(\partial_\mu\Psi,\Psi)=\frac{i}{2}(\Psi^*\partial_t\Psi-\partial_t\Psi^*\Psi)-\frac{1}{2m}|\partial_x\Psi|^2-U|\Psi|^2-\frac{g}{2}|\Psi|^4. \tag{3.1}$$

where g is the 1D contact interaction coupling constant. There is global U(1) symmetry in the Lagrangian density Eq. (3.1), which ensures that the total particle number of the system N is conserved. Namely, the conservation law $\partial_t\rho+\partial_x J=0$ holds, where $\rho=|\Psi|^2$, $J=(\Psi^*\partial_x\Psi-\Psi\partial_x\Psi^*)/2mi$ are the system particle density and current density respectively, and $N=\int \mathrm{d}x\rho$. In this thesis, only the system with a large particle number $N\gg 1$ is studied. Hence, one can expand the bosonic field Ψ in powers of the total particle number N as

$$\Psi=\phi_0+\chi+\zeta+\mathcal{O}(N^{-3/2}). \tag{3.2}$$

where $\phi_0=\mathcal{O}(N^{1/2}),\chi=\mathcal{O}(N^0)$, and $\zeta=\mathcal{O}(N^{-1/2})$. Especially, in the dilute gas limit, $N\to\infty$ with $gN=$ constant, the Lagrangian density Eq. (3.1) can be separated by the order of N also[68] (Note that for long range interactions other scalings appear in the expansion, cf.[66]). This condition is indeed required for

a rigorous derivation of the Gross-Pitaevskii energy functional [40], and for complete Bose-Einstein condensation to occur in the limit $N \to \infty$ [39]. Then the action is of the form

$$S = \int \mathrm{d}^2x \mathcal{L} = S_0 + S_1 + S_2 + S_3 + \mathcal{O}(N^{-1}). \tag{3.3}$$

The leading order of action is

$$S_0 = \int \mathrm{d}^2x \mathcal{L}_0 = \int \mathrm{d}^2x \frac{i}{2}(\phi_0^* \partial_t \phi_0 - \partial_t \phi_0^* \phi_0) - \frac{1}{2m}|\partial_x \phi_0|^2 - U|\phi_0|^2 - g|\phi_0|^4 = \mathcal{O}(N). \tag{3.4}$$

Using the action principle, one can get the usual Gross-Pitaevskii equation.

$$i\partial_t \phi_0 = \left(-\frac{\partial_x^2}{2m} + U + g\rho_0 \right) \phi_0. \tag{3.5}$$

where $\rho_0 = |\phi_0|^2 = \mathcal{O}(N)$. It will be assumed that the leading order field ϕ_0 satisfies the Gross-Pitaevskii equation. Note that the leading order Lagrangian is of the same form as the original Lagrangian Eq. (3.1), therefore,

$$\frac{\delta S_0}{\delta \phi_0^*} = 0 \implies \left[\partial_\mu \left(\frac{\partial \mathcal{L}}{\partial(\partial_\mu \Psi^*)} \right) - \frac{\partial \mathcal{L}}{\partial \Psi^*} \right] \Bigg|_{\Psi^* = \phi_0^*} = 0, \tag{3.6a}$$

$$\frac{\delta S_0}{\delta \phi_0} = 0 \implies \left[\partial_\mu \left(\frac{\partial \mathcal{L}}{\partial(\partial_\mu \Psi)} \right) - \frac{\partial \mathcal{L}}{\partial \Psi} \right] \Bigg|_{\Psi = \phi_0} = 0. \tag{3.6b}$$

One can easily get the higher order corrections to the action by Taylor expansion and the equations of motion Eq. (3.6). The first-order correction to the action is zero.

$$\begin{aligned} S_1 &= \int \mathrm{d}^2x \left(\left[\partial_\mu \left(\frac{\partial \mathcal{L}}{\partial(\partial_\mu \Psi^*)} \right) - \frac{\partial \mathcal{L}}{\partial \Psi^*} \right] \Bigg|_{\Psi^* = \phi_0^*} \right) \chi^* + \text{c.c.} \\ &= 0. \end{aligned} \tag{3.7}$$

where c.c. denotes the complex conjugate. The derivatives of Lagrangian by fields are

$$\frac{\partial^2\mathcal{L}}{\partial(\partial_t\Psi)\partial\Psi^*}=\frac{i}{2},\qquad \frac{\partial^2\mathcal{L}}{\partial\Psi^{*2}}=-g\Psi^2,\qquad \frac{\partial^3\mathcal{L}}{\partial\Psi^2\partial\Psi^*}=-2g\Psi^*,$$
$$\frac{\partial^2\mathcal{L}}{\partial(\partial_t\Psi^*)\partial\Psi}=-\frac{i}{2},\qquad \frac{\partial^2\mathcal{L}}{\partial\Psi^2}=-g\Psi^{*2},\qquad \frac{\partial^3\mathcal{L}}{\partial\Psi^{*2}\partial\Psi}=-2g\Psi$$
$$\frac{\partial^2\mathcal{L}}{\partial(\partial_x\Psi)\partial(\partial_x\Psi^*)}=-\frac{1}{2m},\qquad \frac{\partial^2\mathcal{L}}{\partial\Psi\partial\Psi^*}=-U-2g|\Psi|^2.$$

The second-order correction to the action is

$$\begin{aligned}S_2&=\left.\frac{\delta^2\mathcal{L}}{\delta\Psi\delta\Psi^*}\right|_{\phi_0,\phi_0^*}\chi^*\chi+\frac{1}{2}\left.\frac{\delta^2\mathcal{L}}{\delta\Psi^2}\right|_{\phi_0}\chi^2+\frac{1}{2}\left.\frac{\delta^2\mathcal{L}}{\delta\Psi^{*2}}\right|_{\phi_0^*}\chi^{*2}\\&=\int\mathrm{d}^2x\frac{i}{2}(\chi^*\partial_t\chi-\partial_t\chi^*\chi)-\frac{1}{2m}|\partial_x\chi|^2-U|\chi|^2-2g\rho_0|\chi|^2-\frac{g}{2}(\phi_0^{*2}\chi^2+\phi_0^2\chi^{*2}),\end{aligned}\tag{3.8}$$

and the third-order is

$$\begin{aligned}S_3=&\left.\frac{\delta^2\mathcal{L}}{\delta\Psi\delta\Psi^*}\right|_{\phi_0,\phi_0^*}(\chi^*\zeta+\zeta^*\chi)+\left.\frac{\delta^2\mathcal{L}}{\delta\Psi^2}\right|_{\phi_0}\chi\zeta+\left.\frac{\delta^2\mathcal{L}}{\delta\Psi^{*2}}\right|_{\phi_0^*}\chi^*\zeta^*\\&+\frac{1}{2}\left.\frac{\delta^3\mathcal{L}}{\delta\Psi^2\delta\Psi^*}\right|_{\phi_0,\phi_0^*}\chi+\frac{1}{2}\left.\frac{\delta^3\mathcal{L}}{\delta\Psi\delta\Psi^{*2}}\right|_{\phi_0^*}\chi^*\\=&\int\mathrm{d}^2x\frac{i}{2}(\zeta^*\partial_t\chi+\chi^*\partial_t\zeta-\partial_t\zeta^*\chi-\partial_t\chi^*\zeta)\\&-\frac{1}{2m}(\partial_x\chi^*\partial_x\zeta+\partial_x\zeta^*\partial_x\chi)-U(\chi^*\zeta+\zeta^*\chi)-2g\rho_0(\chi^*\zeta+\zeta^*\chi)\\&-g(\phi_0^{*2}\chi\zeta+\phi_0^2\chi^*\zeta^*)-g|\chi|^2(\chi^*\phi_0+\phi_0^*\chi),\end{aligned}\tag{3.9}$$

One gets the Bogoliubov equation from the action S_2 by

$$\frac{\delta S_2}{\delta\chi^*}=0\implies i\partial_t\chi=\left(-\frac{\partial_x^2}{2m}+U+2g\rho_0\right)\chi+g\phi_0^2\chi^*,\tag{3.10}$$

and the equation of motion for ζ can be obtained by the action S_3 by

$$\frac{\delta S_3}{\delta \chi^*} = 0 \implies i\partial_t \zeta = \left(-\frac{\partial_x^2}{2m} + U + 2g\rho_0 \right) \zeta + g\phi_0^2 \zeta^* + 2g|\chi|^2 \phi_0 + g\chi^2 \phi_0^* \tag{3.11}$$

One can also check the $\delta S_3/\delta\zeta$ for consistency and can easily notice that it gives the Bogoliubov-de Gennes equation. Hence, one can consistently expand the Bose field up to $N^{-1/2}$-order and can get the consistent equation of motion.

Recall that it is assumed that the ϕ_0 satisfies the Gross-Pitaevskii equation (3.5). The expansion is valid only in the regime of Bogoliubov assumption holds, i.e., $\delta N := \int \mathrm{d}x |\chi|^2 \ll N$. And by the Penrose-Onsager criterion, the ratio between condensate particle number and total particle number is finite nonzero value [57]. Because the total particle number is very big,

$$\frac{\delta N}{N} \approx \frac{1}{N} \approx \frac{1}{N_0} \ll 1 \tag{3.12}$$

where $N_0 = \int \mathrm{d}x \rho_0$. In this thesis, the only quantized field is the Bogoliubov field χ, and other fields are treated as classical fields i.e., the Bogoliubov field is promoted to satisfy the bosonic commutation relations.

$$[\chi(t,x), \chi^\dagger(t,x')] = \delta(x-x'), \qquad [\chi(t,x), \chi(t,x')] = [\chi^\dagger(t,x), \chi^\dagger(t,x')] = 0. \tag{3.13}$$

Especially, the only vacuum expectation value of the quantum operators $\langle \chi \rangle = 0$ is considered in this thesis.

3.2 Continuity Equations

Until now, the field is just expanded like the usual $U(1)$-symmetry-breaking approach and only the difference is the classical correction of the field ζ. To give a name "number-conserving" to the expansion, one needs to show that

the continuity equation holds. The continuity equation is the relation between the density and current which can be also expanded with the total particle number N

$$\rho := \langle \Psi^\dagger \Psi \rangle = \rho_0 + \rho_\chi + \rho_\zeta + \mathcal{O}(N^{-1/2}), \tag{3.14a}$$

$$J := \frac{1}{m} \Im[\Psi^\dagger \partial_x \Psi] = J_0 + J_\chi + J_\zeta + \mathcal{O}(N^{-1/2}). \tag{3.14b}$$

where

$$\rho_0 = \phi_0^* \phi_0, \qquad J_0 = \frac{1}{m} \Im[\phi_0^* \partial_x \phi_0], \tag{3.15a}$$

$$\rho_\chi = \langle \chi^\dagger \chi \rangle, \qquad J_\chi = \frac{1}{m} \Im[\langle \chi^\dagger \partial_x \chi \rangle], \tag{3.15b}$$

$$\rho_\zeta = 2\Re[\phi_0^* \zeta], \qquad J_\zeta = \frac{1}{m} \Im[\phi_0^* \partial_x \zeta + \zeta^* \partial_x \phi_0]. \tag{3.15c}$$

Note that the two leading-order contributions from χ and ζ are in the same order. More concretely,

$$\rho_\chi = \mathcal{O}(N^0), \qquad J_\chi = \mathcal{O}(N^0), \tag{3.16a}$$

$$\rho_\zeta = \mathcal{O}(N^0), \qquad J_\zeta = \mathcal{O}(N^0). \tag{3.16b}$$

For the leading order condensate, one can easily check from the equation of motion Eq.(3.5) that for the leading order,

$$\partial_t \rho_0 + \partial_x J_0 = 0, \tag{3.17}$$

the continuity equation holds.

But if one considers the next only the χ contribution, i.e., the depletion and phonon flux, which is done in the $U(1)$-symmetry breaking approach, one gets the relation

$$\partial_t \rho_\chi + \partial_x J_\chi = -ig(\phi_0^2 \langle \hat{\chi}^{\dagger 2} \rangle - \phi_0^{*2} \langle \hat{\chi}^2 \rangle). \tag{3.18}$$

By the way, the ζ contribution which is the subleading-order contribution on the condensate satisfies

$$\partial_t \rho_\zeta + \partial_x J_\zeta = ig(\phi_0^2 \langle \hat{\chi}^{\dagger 2} \rangle - \phi_0^{*2} \langle \hat{\chi}^2 \rangle). \tag{3.19}$$

Because the right-hand side of Eq. (3.18) and Eq. (3.19) is nonzero, the continuity equation for each contribution does not hold, and the number of each particle is not conserved. But by summing Eq. (3.18) and Eq. (3.19), one gets

$$\partial_t (\rho_\chi + \rho_\zeta) + \partial_x (J_\chi + J_\zeta) = 0. \tag{3.20}$$

or equivalently, for the whole density and current,

$$\partial_t \rho + \partial_x J = \mathcal{O}(N^{-1/2}) \simeq 0. \tag{3.21}$$

Hence, the continuity equation holds up to the $\mathcal{O}(N^0)$, if we consider the condensate and Bogoliubov field contribution consistently.

The physical situation here is the following. If one uses the $U(1)$-symmetry breaking approach, one neglects the effect of Bogoliubov field excitation to the condensate field. It means that even though the particles are excited to the Bogoliubov mode, the condensate particle number does not change. The ζ contribution is the condensate correction which is the reduction of condensate particles by the excitation to the depleted particles. Hence, by including the ζ contribution, the particle number is conserved in the working order $\mathcal{O}(N^0)$.

3.3 Comparison with Other Number-Conserving Expansion

Alternatively, there are different number-conserving approaches from the number-conserving Bogoliubov expansion in this study. For consistency, one should

compare the number-conserving Bogoliubov method here with others. In the working order $\mathcal{O}(N^0)$, the number-conserving Bogoliubov in this study is the same with others. Since the equivalence of other methods are already well-known [25, 22, 5] we can choose one of them to compare. Especially, I mention [68, 67] for original idea on the backreaction analysis in this study, and hence, the number-conserving expansion used in them will be compared.

The Girardeau-Arnowitt theory, which is also called the number conserving Hartree-Fock Bogoliubov theory, can be expressed by expanding the Bose field operator $\hat{\Psi}$ as

$$\hat{\Psi} = (\phi_c + \hat{\chi} + \hat{\zeta})\frac{\hat{A}}{\sqrt{\hat{N}}} \tag{3.22}$$

where $\phi_c = \mathcal{O}(N^{1/2})$ is condensate wave function, $\hat{\chi} = \mathcal{O}(N^0)$ is one-particle excitation, and $\hat{\zeta} = \mathcal{O}(N^{-1/2})$is the remaining higher order corrections. I keep a "hat" notation to distinguish the expansion of Girardeau-Arnowitt theory from the number-conserving Bogoliubov method used in this study. Note that in this expansion, we start with the fully quantized field in the beginning so that it is more explained in the language of many-particle quantum mechanics. By the Penrose-Onsager criterion, the condensate wave function macroscopically dominates so that the condensate particle number and total particle number are equivalent ($N_c \simeq N_{tot}$). If one carefully distinguishes the condensate and total particle, he/she must interpret the operator above in the Girardeau-Arnowitt theory as $\frac{\hat{A}}{\sqrt{\hat{N}}} \equiv \hat{A}_c\frac{1}{\sqrt{\hat{N}_c}}$ [22, 5]. The subscript c means that it corresponds to the condensate.

The dynamics of a full Bose field operator are governed by

$$i\frac{\partial\hat{\Psi}(t,x)}{\partial t} = \left(-\frac{\partial_x^2}{2m} + U - \mu\right)\hat{\Psi}(t,x) + g\hat{\Psi}^\dagger(t,x)\hat{\Psi}(t,x)\hat{\Psi}(t,x) \tag{3.23}$$

again, the order of coupling constant g must be $g = \mathcal{O}(N^{-1})$ to ensure that there is no depletion in the thermodynamic limit i.e., it is 100% condensed in the thermodynamic limit.[39, 40]

The most important feature of the condensate state and other fields such as one-particle excitation and higher order correction is that they are orthogonal [8]. Hence, the commutation relation for them is

$$[\hat{A}, \hat{\chi} + \hat{\zeta}] = 0. \tag{3.24}$$

Now one can get the equation of motion for the following expectation value of the field

$$\left\langle \frac{1}{\sqrt{\hat{N}}} \hat{A}^\dagger \hat{\Psi} \right\rangle = \phi_c + \langle \hat{\chi} + \hat{\zeta} \rangle = \phi_c. \tag{3.25}$$

In the last equality, the vacuum choice $\langle \hat{\chi} + \hat{\zeta} \rangle = 0$ is used.

Let us multiply $\frac{1}{\sqrt{\hat{N}}} \hat{A}^\dagger$ on the left of Eq. (3.23) and take expectation value

$$\begin{aligned} i\frac{\partial \phi_c}{\partial t} &= \left(-\frac{\partial_X^2}{2m} + U - \mu \right) \phi_c \\ &\quad + g \left\langle \left(\frac{1}{\sqrt{\hat{N}}} \hat{A}^\dagger \right)^2 (\phi_c^* + \hat{\chi}^\dagger + \hat{\zeta}^\dagger)(\phi_c + \hat{\chi} + \hat{\zeta}) \frac{\hat{A}}{\sqrt{\hat{N}}} (\phi_c + \hat{\chi} + \hat{\zeta}) \frac{\hat{A}}{\sqrt{\hat{N}}} \right\rangle \\ &= \left(-\frac{\partial_x^2}{2m} + U - \mu \right) \phi_c \\ &\quad + g \langle (\phi_c^* + \hat{\chi}^\dagger + \hat{\zeta}^\dagger)(\phi_c + \hat{\chi} + \hat{\zeta})^2 \rangle. \end{aligned} \tag{3.26}$$

Using the self-consistent mean field approximation,

$$(\hat{\chi}^\dagger + \hat{\zeta}^\dagger)(\hat{\chi} + \hat{\zeta})^2 \simeq 2\langle (\hat{\chi}^\dagger + \hat{\zeta}^\dagger)(\hat{\chi} + \hat{\zeta}) \rangle (\hat{\chi} + \hat{\zeta}) + \langle (\hat{\chi} + \hat{\zeta})^2 \rangle (\hat{\chi}^\dagger + \hat{\zeta}^\dagger) \tag{3.27}$$

One gets

$$i\frac{\partial\phi_c}{\partial t} = \left(-\frac{\partial_x^2}{2m} + U - \mu\right)\phi_c + g[\rho_c + 2\delta\rho]\phi_c + g\delta\sigma\phi_c^* \tag{3.28}$$

where the local density approximation applies

$$\rho_c \equiv |\phi_c|^2 \tag{3.29a}$$

$$\delta\rho \equiv \langle\delta\hat{\rho}\rangle = \langle(\hat{\chi}^\dagger + \hat{\zeta}^\dagger)(\hat{\chi} + \hat{\zeta})\rangle \simeq \langle\hat{\chi}^\dagger\hat{\chi}\rangle \tag{3.29b}$$

$$\delta\sigma \equiv \langle(\hat{\chi} + \hat{\zeta})^2\rangle \simeq \langle\hat{\chi}^2\rangle. \tag{3.29c}$$

Note that the second and third equations are just keeping the leading order term in the particle number expansion.

Hence, the condensate wave function ϕ_c satisfies the amended Gross-Pitaevskii equation [68]

$$i\partial_t\phi_{\rm c} = \left(-\frac{\partial_x^2}{2m} + U + g\rho_{\rm c} + 2g\langle\hat{\chi}^\dagger\hat{\chi}\rangle\right)\phi_{\rm c} + g\langle\hat{\chi}^2\rangle\phi_{\rm c}^*. \tag{3.30}$$

where $\rho_{\rm c} = |\phi_{\rm c}|^2$, and $\hat{\chi}$ is the corresponding Bogoliubov field. Note that the condensate in this amended Gross-Pitaevskii equation is related to the above number conserving expansion is simply $\phi_{\rm c} = \phi_0 + \zeta + \mathcal{O}(N^{-1})$ so that the Eq. (3.30) is equivalent to the Eq. (3.10) and Eq. (3.11) up to the order N^{-1}.

Now, let us multiply $\frac{1}{\sqrt{\hat{N}}}\hat{A}^\dagger$ to the Eq. (3.23) and eliminate terms using Eq. (3.26)

$$i\frac{\partial(\hat{\chi} + \hat{\zeta})}{\partial t} = \left(-\frac{\partial_x^2}{2m} + U - \mu\right)(\hat{\chi} + \hat{\zeta}) + g[\hat{\psi}^\dagger\hat{\psi}\hat{\psi} - \langle\hat{\psi}^\dagger\hat{\psi}\hat{\psi}\rangle \tag{3.31}$$

Or equivalently, using the self-consistent mean-field approximation Eq. (3.27), one can write

$$i\frac{\partial(\hat{\chi} + \hat{\zeta})}{\partial t} = \left(-\frac{\partial_x^2}{2m} + U - \mu\right)(\hat{\chi} + \hat{\zeta}) + 2g\rho(\hat{\chi} + \hat{\zeta}) + g\sigma(\hat{\chi}^\dagger + \hat{\zeta}^\dagger) \tag{3.32}$$

where the self-consistent density is

$$\rho := \langle \hat{\Psi}^\dagger \hat{\Psi} \rangle = |\phi_c(t,x)|^2 + \langle (\hat{\chi}^\dagger + \hat{\zeta}^\dagger)(\hat{\chi} + \hat{\zeta}) \rangle \equiv \rho_c + \delta\rho \simeq \rho_c \tag{3.33a}$$

$$\sigma := \langle \hat{\Psi} \hat{\Psi} \rangle = \phi_c^2 + \langle (\hat{\chi} + \hat{\zeta})(\hat{\chi} + \hat{\zeta}) \rangle \equiv \phi_c^2 + \delta\sigma \simeq \phi_c \tag{3.33b}$$

By sorting the equation by the order, one will get the same form of the Bogoliubov-de Gennes equation,

$$i\frac{\partial}{\partial t}\hat{\chi} = \left(-\frac{1}{2}\partial_x^2 + U + g|\phi_c|^2 \right) \hat{\chi} + g\phi_c^2 \hat{\chi}^\dagger \tag{3.34}$$

and corrected equation for $\hat{\zeta}$

$$\begin{aligned} i\partial_t \hat{\zeta} = &\left(-\frac{\partial_x^2}{2m} + U + 2g\rho_c \right) \hat{\zeta} + g\phi_c^2 \hat{\zeta}^\dagger \\ &+ 2g(\hat{\chi}^\dagger \hat{\chi} - \langle \hat{\chi}^\dagger \hat{\chi} \rangle)\phi_c + g(\hat{\chi}^2 - \langle \hat{\chi}^2 \rangle)\phi_c^*. \end{aligned} \tag{3.35}$$

Note that taking the expectation value for the Eq. (3.35) is

$$i\frac{\partial}{\partial t}\langle \hat{\zeta} \rangle \approx \left(-\frac{1}{2}\partial_x^2 + U + g|\phi_c|^2 \right) \langle \hat{\zeta} \rangle + g\phi_c^2 \langle \hat{\zeta}^\dagger \rangle, \tag{3.36}$$

which is just the same as the Bogoliubov de Gennes equation. So, the leading order of $\langle \hat{\zeta} \rangle$ can be absorbed into $\hat{\chi}$ and vanish. Hence,

$$\langle \hat{\zeta} \rangle = \mathcal{O}(N^{-1}) \tag{3.37}$$

And because $\langle \hat{\chi} + \hat{\zeta} \rangle = 0$, we get

$$\langle \hat{\chi} \rangle = \mathcal{O}(N^{-1}) \tag{3.38}$$

Now, let us define density and phase operator. The density operator is

$$\hat{\rho} = \hat{\Psi}^\dagger \hat{\Psi} = \phi_c^* \phi_c + (\hat{\chi}^\dagger + \hat{\zeta}^\dagger)\phi_c + (\hat{\chi} + \hat{\zeta})\phi_c^* + (\hat{\chi}^\dagger + \hat{\zeta}^\dagger)(\hat{\chi} + \hat{\zeta}) \tag{3.39}$$

where $\frac{\hat{A}}{\sqrt{\hat{N}}}$ are canceled in the beginning because of the bilinearity of ρ. By taking the expectation value, one can get

$$\langle\hat{\Psi}^\dagger\hat{\Psi}\rangle = \phi_c^*\phi_c + \langle(\hat{\chi}^\dagger + \hat{\zeta}^\dagger)(\hat{\chi} + \hat{\zeta})\rangle, \tag{3.40}$$

which is consistent with Eq. (3.33) and Eq. (3.29).

The leading order expression for $\langle\delta\hat{\rho}\rangle$ is

$$\langle\delta\hat{\rho}\rangle = \langle\hat{\chi}^\dagger\hat{\chi}\rangle + \mathcal{O}(N^{-1/2}) \tag{3.41}$$

One must note that, unlike the expectation value, the operator itself is

$$\delta\hat{\rho} = (\hat{\chi}^\dagger + \hat{\zeta}^\dagger)\phi_c + (\hat{\chi} + \hat{\zeta})\phi_c^* + \hat{\chi}^\dagger\hat{\chi} + \mathcal{O}(N^{-1/2}) \tag{3.42}$$

i.e., $\delta\hat{\rho} = \mathcal{O}(N^{1/2})$. Unfortunately, in this case,$\langle\delta\hat{\rho}\rangle \neq 0$. Of course one can force $\langle\delta\hat{\rho}\rangle = 0$, but in that case, $\langle\delta\hat{\Psi}\rangle \neq 0$.

The expectation value of density and current density is

$$\rho := \langle\Psi^\dagger\Psi\rangle = \rho_{\mathrm{c}} + \tilde{\rho}_\chi + \mathcal{O}(N^{-1/2}), \tag{3.43a}$$

$$J := \frac{1}{m}\Im[\Psi^\dagger\partial_x\Psi] = J_{\mathrm{c}} + \tilde{J}_\chi + \mathcal{O}(N^{-1/2}). \tag{3.43b}$$

where $\tilde{\rho}_\chi := \langle\hat{\chi}^\dagger\hat{\chi}\rangle$, and $\tilde{J}_\chi := \frac{1}{m}\Im[\langle\hat{\chi}^\dagger\hat{\chi}\rangle]$. In this case, the continuity equation does not hold each,

$$\partial_t\rho_c + \partial_x J_c = ig(\phi_c^2\langle\hat{\chi}^{\dagger 2}\rangle - \phi_c^{*2}\langle\hat{\chi}^2\rangle), \tag{3.44a}$$

$$\partial_t\tilde{\rho}_\chi + \partial_x\tilde{J}_\chi = -ig(\phi_c^2\langle\hat{\chi}^{\dagger 2}\rangle - \phi_c^{*2}\langle\hat{\chi}^2\rangle). \tag{3.44b}$$

The sum of both, however, satisfies the continuity equation

$$\partial_t(\rho_c + \tilde{\rho}_\chi) + \partial_x(J_c + \tilde{J}_\chi) = 0. \tag{3.45}$$

Hence the continuity equation holds for the expansion order $\mathcal{O}(N^0)$ again. Note that even though the expansion scheme is a little bit different from the number-conserving Bogoliubov method used here, the difference is less than the expansion order, i.e.,

$$\phi_c = \phi_0 + \phi_\zeta + \mathcal{O}(N^{-1})$$
$$\hat{\chi} = \chi + \mathcal{O}(N^{-1}).$$

Especially, the physical quantities are

$$\rho_c = \rho + 0 + \rho_\zeta + \mathcal{O}(N^{-1/2}) \approx \rho + 0 + \rho_\zeta \tag{3.47a}$$
$$J_c = J_0 + J_\zeta + \mathcal{O}(N^{-1/2}) \approx J_0 + J_\zeta \tag{3.47b}$$
$$\tilde{\rho}_\chi = \rho_\chi + \mathcal{O}(N^{-1/2}) \approx \rho_\chi \tag{3.47c}$$
$$\tilde{J}_\chi = J_\chi + \mathcal{O}(N^{-1/2}) \approx J_\chi. \tag{3.47d}$$

I will not distinguish the Bogoliubov field contribution from one-particle excitation i.e., drop the "tilde" from now.

4 Quantum Backreaction

4.1 Backreaction

To understand the terminology of "backreaction", I define two words for clear explanation. Typically, the "actor" is the small part of the full system one wants to describe and the "background" is the (large) rest of the full system. The background and actor give influence each other. Because the background is assumed to be very big (or heavy) compared to the actor and is negligibly affected by it. On the contrary to the typical case, the main target of the cosmology is the whole universe i.e., one wants to investigate the dynamics of the full system. It is, however, not possible to access the full system in cosmology because of the curved nature of the spacetime and not possible to get the data of whole universe because of the largeness of it. Fortunately, it is known as the cosmological principle that in the large scale, the universe is homogeneous and isotropic. Hence, one can solve the large background if they neglect the effect of the actor (small scale anisotropy or fluctuation) on the background.

The influence on the background by the actor is called the backreaction. The reason for neglecting the backreaction in general case is that as Hawking said in his paper, the backreaction problem is difficult problem [26]. In spite of its difficulty, the backreaction is inevitable in modern cosmology because

researchers want to get the more exact nontrivial phenomena in universe. The backreaction in cosmology can be broadly divided into three categories: classical backreaction, semi-classical backreaction, and quantum backreaction. The classical backreaction can be thought as a perturbative effect comes from classical inhomogeneities. The semi-classical backreaction comes out when one used the quantum field theory in curved spacetime. Since there is no settled quantum gravity theory, the quantum field theory in curved spacetime is usually used to describe the quantum mechanical phenomena in the cosmological system. In the quantum field theory in curved spacetime, the actor is the quantum field and the background is the classical gravitation field (spacetime metric). The expectation value of the energy-momentum tensor gives the correction on the background.

$$G_{ab} = 8\pi\langle T_{ab}\rangle. \tag{4.1}$$

where G_{ab} is the Einstein tensor defined with the classical gravitational field, and the $\langle T_{ab}\rangle$ is the quantum expectation value of the energy-momentum tensor. The quantum backreaction is the remaining contribution of the backreaction that one cannot obtain in the classical equation of motion. The difference between semi-classical and quantum backreaction is that the former comes from the classical equations of motion even though the source (actor) comes from the quantum fluctuation. In summary, the backreaction in cosmology is the effects of matter field or cosmological inhomogeneities on the homogeneous dynamical background degrees of freedom of cosmology [63].

4.2 Quantum Backreaction in Analogue Model

One of the main physical quantities in this study is the quantum backreaction of the analogue gravitational system of Bose-Einstein condensates. Because the exact equation of motion of Bose gas is known, one can obtain the backreaction at least formally. In this section, the nonzero leading order contribution for the quantum backreaction force will be derived.

The classical equation of motion Eq. (3.5) or Eq. (3.30) is equivalent to the fluid equation when one uses the polar representation. It is easier to start with the full quantum Hamiltonian. In the sense of fluid dynamics, one is tempted to write the Bosonic field operator with density-phase representation (quantum Madelung representation) i.e.,

$$\hat{\Psi} = e^{i\hat{\theta}}\sqrt{\hat{\rho}} \tag{4.2}$$

Using Eq. (3.23), one can get the time development of an expectation value of the current density,

$$\begin{aligned}\partial_t J &:= \langle \partial_t J(\hat{\Psi}, \hat{\Psi}^\dagger)\rangle \\ &= \frac{1}{m^2}\partial_x\left[\frac{1}{4}\partial_x^2\langle\hat{\Psi}^\dagger\hat{\Psi}\rangle - \langle\partial_x\hat{\Psi}^\dagger\partial_x\hat{\Psi}\rangle\right] - \frac{1}{m}\langle\hat{\Psi}^\dagger\hat{\Psi}\rangle\partial_x U - \frac{1}{2gm}\partial_x\langle g^2\hat{\Psi}^{\dagger 2}\hat{\Psi}\rangle.\end{aligned} \tag{4.3}$$

If one substitute Eq. (4.2) on this Eq. (4.3), one will get

$$\begin{aligned}\partial_t J(\rho,\theta) &= \frac{1}{m^2}\partial_x\left[\frac{1}{4}\partial_x^2\langle\hat{\rho}\rangle - \left\langle\partial_x(\sqrt{\hat{\rho}}e^{-i\hat{\theta}})\partial_x(e^{i\hat{\theta}}\sqrt{\hat{\rho}})\right\rangle\right] \\ &\quad -\frac{1}{m}\langle\hat{\rho}\rangle\partial_x U - \frac{1}{2gm}\partial_x\left[g^2\langle\hat{\rho}^2 - \delta(0)\hat{\rho}\rangle\right] \\ &= \frac{1}{m^2}\partial_x\left[\frac{1}{4}\partial_x^2\langle\hat{\rho}\rangle - \langle(\partial_x\sqrt{\hat{\rho}})^2\rangle - \left\langle\sqrt{\hat{\rho}}(\partial_x\hat{\theta})^2\sqrt{\hat{\rho}}\right\rangle\right] \\ &\quad -\frac{1}{m}\langle\hat{\rho}\rangle\partial_x U - \frac{1}{2gm}\partial_x\left[g^2\langle\hat{\rho}^2 - \delta(0)\hat{\rho}\rangle\right]\end{aligned}$$

$$= \left\langle \frac{\hat{\rho}}{m}\partial_x \left(\frac{-\partial_x^2\sqrt{\hat{\rho}}}{2m\sqrt{\hat{\rho}}} \right) \right\rangle - \frac{1}{m^2}\left\langle \sqrt{\hat{\rho}}(\partial_x\hat{\theta})^2\sqrt{\hat{\rho}} \right\rangle$$
$$-\frac{1}{m}\langle\hat{\rho}\rangle\partial_x U - \frac{1}{2gm}\partial_x\left[g^2\langle\hat{\rho}^2 - \delta(0)\hat{\rho}\rangle\right] \tag{4.4}$$

where $\delta(0)$ comes from the equal time commutation relation full bosonic field $[\hat{\Psi}(t,x), \hat{\Psi}^\dagger(t,x')] = \delta(x-x')$ which can be removed by renormalization i.e., normal ordering. One can get the Madelung equation which is a quantum hydrodynamic equation when one renormalizes and puts the expectation value for measurable quantities ρ, J to the Eq. (4.4), i.e.,

$$\partial_t J_{\rm c} = f_{\rm cl}(\rho_c, J_c) \tag{4.5}$$

where $J_{\rm c} := \frac{1}{m}\Im[\phi_{\rm c}^*\partial_x\phi_{\rm c}]$. The classical Eulerian force (per unit mass) is

$$f_{\rm cl}(\rho, J) := -\partial_x(\rho v^2) - \frac{\rho}{m}\left(\frac{-\partial_x^2\sqrt{\rho}}{2m\sqrt{\rho}} + U + g\rho \right). \tag{4.6}$$

where $v = J/\rho$. In other words, the condensate field which is treated as a classical field, satisfies the classical Euler equation, with the classical force defined with the measurable quantities.

From now, let us suppress the terms which are negligible in our working order. Note that, however, if the quantized fields are get involved, there is a modification to the Euler equation.

$$\partial_t J = f_{\rm cl} + f_{\rm q}. \tag{4.7}$$

Because J and $f_{\rm cl}$ are known, this can be interpreted as a defining equation for $f_{\rm q}$

$$f_{\rm q} := \partial_t J - f_{\rm cl}. \tag{4.8}$$

And because of Eq. (4.5), one only needs to use the terms which contain the Bogoliubov field, (See Sec. 8.2 for detailed calculation)

$$\begin{aligned} f_{\mathrm{q}} = {} & \partial_t J_\chi - v_c \partial_t \rho_\chi + \partial_x (J_\chi v_c - \rho_\chi v_c^2) - J_\chi \partial_x v_c - \frac{\rho_c}{2m} \partial_x \left(\frac{g G^{(2)}}{\rho_c} \right) \\ & + \frac{\rho_\chi}{m} \partial_x \left[- \frac{\partial_x^2 \sqrt{\rho_c}}{2m \sqrt{\rho_c}} + U + g \rho_c \right] \\ & - \frac{\rho_c}{4} \partial_x \left[\frac{1}{2} \frac{1}{\sqrt{\rho_c}} \partial_x^2 \left(\frac{\rho_\chi}{\sqrt{\rho_c}} \right) - \frac{\rho_\chi}{\rho_c^{3/2}} \partial_x^2 \sqrt{\rho_c} \right] . \end{aligned} \tag{4.9}$$

Note that there are no terms only with the classical field, i.e., terms with subscript c only. Hence, it is easy to find that in our working order N^0,

$$\begin{aligned} f_{\mathrm{q}} = {} & \partial_t J_\chi - v_0 \partial_t \rho_\chi + \partial_x (J_\chi v_0 - \rho_\chi v_0^2) - J_\chi \partial_x v_0 - \frac{\rho_0}{2m} \partial_x \left(\frac{g G^{(2)}}{\rho_0} \right) \\ & + \frac{\rho_\chi}{m} \partial_x \left[- \frac{\partial_x^2 \sqrt{\rho_0}}{2m \sqrt{\rho_0}} + U + g \rho_0 \right] \\ & - \frac{\rho_0}{4} \partial_x \left[\frac{1}{2} \frac{1}{\sqrt{\rho_0}} \partial_x^2 \left(\frac{\rho_\chi}{\sqrt{\rho_0}} \right) - \frac{\rho_\chi}{\rho_0^{3/2}} \partial_x^2 \sqrt{\rho_0} \right] . \end{aligned} \tag{4.10}$$

4.3 The Initial Condition

The two equations

$$\partial_t \rho = - \partial_x J, \tag{4.11a}$$

$$\partial_t J = f_{\mathrm{cl}} + f\mathrm{q}, \tag{4.11b}$$

compose the Cauchy problem for J and ρ, so that for a given initial condition, one can get a unique solution for ρ and J. It is, however, not simple to determine the initial conditions for the system since the quantum state for the field operator χ is also needed. Mathematically one can just split the density by $\rho = \rho_0 + \rho_\chi + \rho_\zeta + \mathcal{O}(N^{-1/2})$. But, it is hard to measure each

contribution experimentally. Because ρ_χ can only be separately measurable if it is distinguished from ρ_ζ. If one accepts the infinite size model, there is a stable vacuum state, and one can wait for the state to be stabilized to that vacuum state. But, for the finite-size gas, because there is phase diffusion that spontaneously destroys the off-diagonal long-range order, there is no stationary condensate. Therefore, there is no stationary vacuum state, and one must specify the instantaneous vacuum state.

5 Homogeneous Gas

The simplest system we can imagine is a homogeneous system that does not move. This thesis devotes to the finite-size model which is more experimentally realistic than the infinite-size model. Current technology allows us to treat the finite-size homogeneous condensate [23]. This might be realizable ever more accurately experimentally with new trapping techniques being developed (see [52] for an up-to-date review). In this section, one will treat the finite stationary homogeneous 1D condensate which does not move. As one will see later, however, it is not only simple but also has a great property, related to backreaction analysis.

5.1 Background Condensate

Now, let us find the preparation needed for having the homogeneous gas. The condensate dynamics are governed by the Gross-Pitaevskii equation (3.5). The stationary homogeneous but finite size-condensate wave function is

$$\phi_0 = \sqrt{\rho_0} e^{-i\mu t}, \qquad x \in]-\ell/2, \ell/2[, \tag{5.1}$$

where μ is the chemical potential. It is not hard to see that the potential whose solution is this wave function (5.1) is

$$U = \mu - g\rho_0, \qquad x \in]-\ell/2, \ell/2[. \tag{5.2}$$

One wants the condensate to vanish at the outside of this finite box so that to describe exactly χ and ζ analytically. So, it decays sharply at the boundary, more precisely, it is of the form

$$\phi_0 = \sqrt{\rho} e^{-i\mu t} \Theta(x + \ell/2)\Theta(\ell/2 - x). \tag{5.3}$$

where $\Theta(x)$ is the Heaviside step function. The potential which has a solution of this form is

$$U = \mu - g\rho_0 + \frac{1}{2m}\partial_x[\delta(x - \ell/2) + \delta(x + \ell/2)]. \tag{5.4}$$

By integrating near each boundary ($x = \pm\ell/2$), one gets *Neumann boundary conditions* for each region $\partial_x\phi_0 = 0$. Because this discontinuity (and Neumann boundary conditions) comes from the potential by the same procedure, one can easily notice that all the field Ψ and so that χ, ζ all satisfies the Neumann boundary conditions. From now on, the irrelevant outside of the finite region will be dropped, and only the inside of the finite region $x \in]-\ell/2, \ell/2[$ will only be written for simplicity. It is enough to say that at the boundary the field must satisfy the Neumann boundary conditions.

As explained in the previous section, it is not possible to have stationary finite condensate forever because of phase diffusion. Hence, the system will be prepared to be noninteracting ($g = 0$ at $t < 0$), and the interaction will be turned on instantaneously ($g = g_0 > 0$ at $t > 0$), so that the quantum fluctuation χ and the correction ζ to be activated at $t = 0$. And in addition to $\hbar = 1$, the units such that $m = g_0 = 1$ would be used. In consequence, the sound velocity is also normalized to unity i.e., $c_0 = \sqrt{g_0\rho_0/m}$. Equivalently, the spatial units will be the healing length $\xi_0 = 1/\sqrt{mg_0\rho_0} = 1$, and time is unit of ξ_0^2.

5.2 Canonical Quantization

Let $\chi = e^{-i\mu t}\psi$. From BdG equation (3.10), one gets the equation of motion for ψ,

$$i\partial_t\psi = -\frac{1}{2}\partial_x^2\psi + \frac{g}{g_0}(\psi + \psi^*). \tag{5.5}$$

Using Nambu spinor $\Phi = (\psi, \psi^*)^{\mathrm{t}}$, one can rewrite Eq. (5.5) in the spinor form

$$i\sigma_3\partial_t\Phi = \left(-\frac{\partial_x^2}{2} + \frac{g}{g_0}\sigma_4\right)\Phi = \sigma_3 H_{\mathrm{BdG}}\Phi, \tag{5.6}$$

where $\sigma_4 = \mathbb{1} + \sigma_1$, and σ_i for $i = 1, 2, 3$ is the usual Pauli matrices. And one can also notice easily from the form of the Nambu spinor that

$$\Phi = \sigma_1\Phi^*. \tag{5.7}$$

The quantization is done by forcing the field mode to satisfy the commutation relation

$$[\psi(t,x), \psi(t,x')] = [\psi^\dagger(t,x), \psi^\dagger(t,x')] = 0, \qquad [\psi(t,x), \psi^\dagger(t,x')] = \delta(x - x'). \tag{5.8}$$

which is the same as forcing Eq. (3.13).

Using the Nambu spinor, this Eq. (5.9) can be written as

$$[\Phi_a(t,x), \Phi_b^\dagger(t,x')] = \sigma_{3,ab}\delta(x - x'), \tag{5.9}$$

where the subscript a, b denotes the matrix component.

Moreover, the Neumann boundary condition also applies to the Nambu spinor,

$$\partial_x\Phi|_{x=\pm l/2} = 0. \tag{5.10}$$

Because of the σ_3-pseudoHermicity of $H_{\rm BdG}$, one can check the conservation of the pseudo inner product

$$\langle \Phi, \Phi' \rangle = \int \mathrm{d}x \Phi^\dagger(t,x)\sigma_3 \Phi'(t,x). \tag{5.11}$$

And because the system only has the real spectrum, all the field modes have a finite norm and can be normalized as

$$\langle \Phi, \Phi \rangle = \pm 1. \tag{5.12}$$

The sign distinguishes the positive/negative norm modes each. And because of Eq. (5.7), one has 1-1 correspondence between positive and negative norm modes. Let us write the positive norm modes with index by $\Phi_n, n \in \{0,1,2,\ldots\}$. Then the mode expansion is

$$\Phi(t,x) = \sum_0^\infty [a_n \Phi_n(t,x) + a_n^\dagger \sigma_1 \Phi^*(t,x)]. \tag{5.13}$$

The quantization Eq. (5.9) is equivalent to promote complex frequency $a_n = \langle \Phi_n, \Phi \rangle$ to be an operator satisfying

$$[a_n, a_{n'}^\dagger] = \delta_{n,n'}. \tag{5.14}$$

The vacuum state $|0\rangle$ is defined as usual, i.e.,

$$a_n |0\rangle = 0. \tag{5.15}$$

And using the explicit component of eigenvector $\Phi_n = (u_n, v_n)^t$, one gets

$$\psi(t,x) = \sum_0^\infty [a_n u_n(t,x) + a_n^\dagger v_n^*(t,x)]. \tag{5.16}$$

5.3 Initial Setup

One must note that the homogeneity of the condensate in the model is not caused by the repulsive interaction in a hard wall. The sharp derivative of the delta function wall (5.4) allows the condensate to be uniform in the finite region regardless of the interaction. Hence one can have noninteracting uniform gas. The initial setup ($t < 0$) is a simple Bose gas that does not interact with each other ($g = 0$). Hence, the BdG equation (5.6) in this region is simply

$$i\partial_t \sigma_3 \Phi = -\frac{\partial_x^2}{2}\Phi. \tag{5.17}$$

Note that corresponding Hamiltonian H_{BdG} in Eq. (5.6) in this case ($g = 0$) is not only pseudoHermitian but also Hermitian. Hence, one has real eigenvalues only in the noninteracting regime. The system is in a stationary regime so that the solutions of the form $\Phi(t, x) = e^{-i\omega t}\Phi_\omega(x)$ exist for $\omega \geq 0$, such that

$$\omega\sigma_3\Phi_\omega = -\frac{\partial_x^2}{2}\Phi_\omega. \tag{5.18}$$

The solution is just plane wave form $\Phi_\omega(x) = e^{ikx}\Phi_{\omega,k}$ where $\Phi_{\omega,k}$ is constant and the wave number k satisfies the dispersion relation

$$\omega = \pm\frac{k^2}{2}. \tag{5.19}$$

There are 2 real, and 2 imaginary solutions for $k : k_1 = \sqrt{2\omega}, k_2 = -\sqrt{2\omega}$ and $k_3 = i\sqrt{2\omega}, k_4 = -i\sqrt{2\omega}$. The corresponding basis as $\Phi_{\omega,k_1} = \Phi_{\omega,k_2} = (1, 0)^{\mathrm{t}}$, and $\Phi_{\omega,k_3} = \Phi_{\omega,k_4} = (0, 1)^{\mathrm{t}}$. The solution for Eq. (5.18) is

$$\Phi_\omega = A_\omega \left(e^{ik_1 x}\Phi_{\omega,k_1} + \sum_{i=2,3,4} S_{k_i} e^{ik_i x}\Phi_{\omega,k_i} \right), \tag{5.20}$$

where A_k is the normalization constant, and S_{k_i} is introduced to express the usual S-matrix form. This is just a convenient expression. By imposing Neumann boundary condition $\partial_x \Phi_\omega(\pm\ell/2) = 0$, one gets $S_{k_3} = S_{k_4} = 0$, and $S_{k_2} = (-1)^n$, and $k_1 = -k_2 := k_n = n\pi/\ell$, $n \in \{0, 1, 2, \ldots\}$. And from dispersion relation (5.19), one gets $\omega := \Omega_n = n^2\pi^2/2\ell^2$. And one can get $A_k = 1/\sqrt{2\ell(1+\delta_{n,0})}$ for each n from the normalization condition $\langle \Phi, \Phi \rangle = 0$ Because ω and k are determined by the integer n, let us use the index n. The solution (5.20) is then

$$\Phi_n(t,x) = \frac{e^{-i\Omega_n t}[e^{ik_n x} + (-1)^n e^{-ik_n x}]}{\sqrt{2\ell(1+\delta_{0,n})}}(1,0)^{\mathrm{t}} \tag{5.21}$$

with $n \in \{0, 1, 2, \ldots\}$ are positive norm modes. One can easily deduce from the Hermicity of H_{BdG} that the $\Phi_n(t,x)$ spans the whole space.

One can also show completeness directly by showing that the commutation relation Eq. (5.9) holds, or equivalently Eq. (5.8) holds. By using Eq. (5.16),

$$[\psi(t,x), \psi^\dagger(t,x')] = \sum_{n=0}^{\infty} [u_n(t,x)u_n^*(t,x') - v_n^*(t,x)v_n(t,x')]. \tag{5.22}$$

From Eq. (5.21) and the form of the Nambu spinor, one gets

$$[\psi(t,x), \psi^\dagger(t,x')] = \frac{1}{2l} \sum_{n=-\infty}^{\infty} \left[e^{in\pi(x-x')/\ell} + (-1)^n e^{in\pi(x+x')/\ell} \right]. \tag{5.23}$$

By using the Poisson's summation formula [12],

$$\frac{1}{2\ell} \sum_{n=-\infty}^{\infty} e^{in\pi y/\ell} = \sum_{n=-\infty}^{\infty} \delta(y - 2\ell n), \tag{5.24}$$

one obtains

$$[\psi(t,x), \psi^\dagger(t,x')] = \sum_{n=-\infty}^{\infty} [\delta(x - x' - 2\ell n) + \delta(x + x' - 2n\ell - \ell)]. \tag{5.25}$$

Since $x, x' \in]-\ell/2, \ell/2[$, one can easily get $x \pm x' \in]-\ell, \ell[$, so that

$$[\psi(t,x), \psi^\dagger(t,x')] = \delta(x-x'). \tag{5.26}$$

Accordingly, the general solution for (5.17) is

$$\Phi(t,x) = \sum_{n=0}^{\infty} [a_n \Phi_n(t,x) + a_n^\dagger \sigma_1 \Phi_n^*(t,x)]. \tag{5.27}$$

5.4 Interacting Regime

Now let us see the field when the interaction is on ($t > 0$). Let us first find mode expansion in this regime. Now, the field equation is

$$i\sigma_3 \partial_t \Phi = \left(-\frac{\partial_x^2}{2} + \sigma_4 \right) \Phi \tag{5.28}$$

Unfortunately, in this case, the corresponding Hamiltonian $H_{\rm BdG}$ is not Hermitian, but one can still find the orthonormal bases still in this case by explicitly finding the bases. Because of non-Hermicity, there is "zero norm modes" in Eq. (5.28). Note that

$$\Phi = \Pi_0 := (1,-1)^{\rm t} \tag{5.29}$$

is a solution of Eq. (5.28) i.e., it is the right eigenvector of $H_{\rm BdG}$ with eigenvalue zero. And one can easily find that its norm is zero ($\Pi_0^\dagger \sigma_3 \Pi_0 = 0$). Hence, it is one of the zero norm modes. Moreover, $\sigma_1 \Pi_0^* = -\Pi_0$, and hence, one cannot use the property of the Nambu spinor to find a second linearly independent solution. It is shown in [8] how to find the missing zero norm modes physically interpreted as a conjugate phase momentum. But, in the present case, it is enough to see that

$$\tilde{\Pi}_0 = \frac{1}{2}(1,1)^{\rm t} - it\Pi_0 \tag{5.30}$$

is also a zero norm mode which is orthogonal to Π_0. Note that $\tilde{\Pi}_0$ is not an eigenfunction of time translation generator $i\partial_t$: $i\partial_t\tilde{\Pi}_0 = \Pi_0$. Hence, the occurrence of this mode implies that the time translational symmetry is broken, and there is no stationary BEC without any external source sustaining BEC itself. It corresponds to the condensate phase diffusion which is negligible when one treat the infinite size model but gives a significant effect in the finite size model [8, 37, 29]. Also, one can observe in connection to analogue gravity in BECs that finite size black hole analogues present generic dynamical instabilities that also break the system time translation symmetry [59], and thus our quantum quench from a non-interacting regime offers a route for studying backreaction also in these systems.

One can get nonzero norm modes in a similar procedure to the noninteracting case. Now, the equation of motion for stationary mode is

$$\sigma_3\omega\Phi = \left(-\frac{\partial_x^2}{2} + \sigma_4\right)\Phi \tag{5.31}$$

The plane wave form $\Phi_\omega(x) = e^{ikx}\Phi_{\omega,k}$ solution then satisfies

$$\omega\sigma_3\Phi = \left(\frac{k^2}{2} + \sigma_4\right)\Phi. \tag{5.32}$$

To have a nontrivial solution for Φ, the eigenvalues must satisfy the dispersion relation

$$\omega^2 = k^2 + \frac{k^2}{4} \tag{5.33}$$

Because it is also a 4th-order equation, we have the mode expansion of the form Eq. (5.20). And imposing the Neumann boundary condition will give the same k_i and S_{k_i}. Again using the label of the field as integer n, we have the

solution

$$\Pi_n(t,x) = \frac{e^{-i\omega_n t}[e^{ik_n x} + (-1)^n e^{-ik_n x}]}{\sqrt{2l[1-(\omega_n - k_n^2/2 - 1)^2}}(1, \omega_n - k_n^2/2 - 1)^{\mathrm{t}} \tag{5.34}$$

where $\omega_n = \sqrt{k_n^2(k_n^2/4+1)}$ with $n \in \{1,2,\ldots\}$. We use Π_n to distinguish the field eigenmode in the interacting regime to distinguish from the noninteracting regime. Again, the normalization constant A_n is chosen to satisfy the $\langle \Phi_n, \Phi_{n'} \rangle = \delta_{n,n'}$. Because H_{BdG} is not hermitian, one needs to explicitly the completeness in the interacting case. But, because it is also normalized, and plane wave, it is trivial to check (5.26) holds. Hence, the set $\{\Pi_0, \tilde{\Pi}_0, \Pi_n, \sigma_1 \Pi_n^*\}$ spans the whole solution space. And because the external potential is constant in time and the interaction behaves as a step function in time, the eigenmode Φ_n is also continuous in time, eventhough it is not the eigenmode at $t > 0$ i.e, $\Phi_n(0^+, x) = \Phi_n(0^-, x) := \Phi_n^{(-)}$. Thus one can expand all Φ_n by

$$\Phi_n = \alpha_{n,0}\Pi_0 + \beta_{n,0} + \sum_{j=1}^{\infty}[\alpha_{n,j}\Pi_j - \beta_{n,j}\sigma_1 \Pi^*], \tag{5.35}$$

for $t > 0$ where each constants are

$$\alpha_{n,0} = \frac{\langle \tilde{\Pi}_0, \Phi_n^{(-)} \rangle}{\langle \tilde{\Pi}_0, \Pi_0 \rangle}, \qquad \alpha_{n,j} = \langle \Pi_j, \Phi_n^{(-)} \rangle, \tag{5.36a}$$

$$\beta_{n,0} = \frac{\langle \Pi_0, \Phi_n^{(-)} \rangle}{\langle \Pi_0, \tilde{\Pi}_0 \rangle}, \qquad \beta_{n,j} = \langle \sigma_1 \Pi_j^*, \Phi_n^{(-)} \rangle, \tag{5.36b}$$

where $j > 0$ and the functions Π_n are evaluated at $t = 0$. By performing the integrals one can find

$$\alpha_{n,0} = \frac{\delta_{n,0}}{2\sqrt{\ell}}, \qquad \alpha_{n,j} = \frac{\delta_{n,j}}{\sqrt{1-(\omega_n - k_n^2/2 - 1)^2}}, \tag{5.37a}$$

$$\beta_{n,0} = \frac{\delta_{n,0}}{\sqrt{\ell}}, \qquad \beta_{n,j} = \frac{(\omega_n - k_n^2/2 - 1)(-1)^n \delta_{n,j}}{\sqrt{1-(\omega_n - k_n^2/2 - 1)^2}}, \tag{5.37b}$$

with $j > 0$. Using these expansions, one can calculate the time evolution of the fields and can calculate the dynamical quantities (of quantized fields) in neglecting the backreaction effect.

5.5 Depletion

Note that if one pauses at this step, it is just the usual $U(1)$ symmetry-breaking approach. Hence, it is also meaningful to calculate the quantities one can calculate here. The depletion ρ_χ and phonon flux J_χ are two important subleading order quantities in the theory of low-temperature Bose gas. For $t < 0$, there is no interaction, and the depletion and phonon flux are

$$\rho_\chi(t < 0) = 0, \qquad J_\chi(t < 0) = 0. \tag{5.38}$$

which is a trivial result one can see easily by Eq. (5.21). Recall that $\chi = e^{-i\mu t}\psi$. By using mode expansion (5.16) and commutation relation (5.14), one can express expectation values in sum of mode functions. The depletion is

$$\rho_\chi = \langle \psi^\dagger(t,x)\psi(t,x)\rangle = \sum_{n=0}^{\infty} |v_n|^2, \tag{5.39}$$

and the phonon flux is

$$J_\chi = \Im[\psi^\dagger(t,x)\partial_x\psi(t,x)\rangle = \sum_{n=0}^{\infty} \Im[v_n\partial_x v_n^*] \tag{5.40}$$

Direct substitution of Eq. (5.37) to the Eq. (5.35), one gets for $n - 0$

$$v_0 = \frac{it}{\sqrt{\ell}}, \tag{5.41}$$

and for $n = 1, 2, 3, \cdots$

$$v_n = \frac{(\omega_n - k_n^2/2 - 1)}{\sqrt{2\ell}[1 - (\omega_n - k_n^2/2 - 1)^2]}$$

$$
\begin{aligned}
&\times \left[e^{-i\omega_n t}\left[e^{ik_n x} + (-1)^n e^{-ik_n x}\right] - (-1)^n e^{i\omega_n t}\left[e^{-ik_n x} + (-1)^n e^{ik_n x}\right]\right] \\
&= \frac{(\omega_n - k_n^2/2 - 1)}{\sqrt{2\ell}[1 - (\omega_n - k_n^2/2 - 1)^2]}\left[e^{-i\omega_n t}\right. \\
&\qquad \left. \times \left[e^{ik_n x} + (-1)^n e^{-ik_n x}\right] - e^{i\omega_n t}\left[(-1)^n e^{-ik_n x} + e^{ik_n x}\right]\right] \\
&= \frac{(\omega_n - k_n^2/2 - 1)}{\sqrt{2\ell}[1 - (\omega_n - k_n^2/2 - 1)^2]}\left[-2i\sin(\omega_n t)\right]\left[e^{ik_n x} + (-1)^n e^{-ik_n x}\right] \\
&= \frac{i\sin(\omega_n t)}{\sqrt{2\ell}\omega_n}\left[e^{ik_n x} + (-1)^n e^{-ik_n x}\right]. \qquad (5.42)
\end{aligned}
$$

In the last line, the dispersion relation $\omega_n^2 = (k_n^2/2 + 1)^2 - 1$ is used. Hence,

$$
|v_0|^2 = \frac{t^2}{\ell} \qquad (5.43)
$$

and for $n = 1, 2, \ldots$,

$$
\begin{aligned}
|v_n|^2 &= \frac{1}{2\ell\omega_n^2}\left[\sin^2(\omega_n t)\right]\left[2 + (-1)^n\left(e^{2ik_n x} + e^{-2ik_n x}\right)\right] \\
&= \frac{1}{2\ell}\frac{(-1)^n}{\omega_n^2}\left[(-1)^n + \cos(2k_n x)\right]\left[1 - \cos(2\omega_n t)\right]. \qquad (5.44)
\end{aligned}
$$

By substituting Eq. (5.43) and Eq. (5.44) to Eq. (5.39), we get

$$
\begin{aligned}
\rho_\chi &= \sum_{n=0}^{\infty} |v_n|^2 \\
&= \frac{t^2}{\ell} + \frac{1}{2\ell}\sum_{n=1}^{\infty}\frac{(-1)^n}{\omega_n^2}\left[(-1)^n + \cos(2k_n x)\right]\left[1 - \cos(2\omega_n t)\right]. \qquad (5.45)
\end{aligned}
$$

The first term t^2/ℓ which comes from the zero norm mode shows clearly that the depletion grows in time [8]. Because the zero norm mode is related to the condensate phase diffusion, it is the growth of depletion by condensate phase degrading. Moreover, because of the denominator, if the system size is infinity ($\ell \to \infty$), the phase diffusion does not occur, and this term goes zero. So, for an infinite system, one does not need to consider phase diffusion. It is, however,

problematic since the second term diverges. And there is no infinite quasi-1D condensate exists that satisfies the Hohenberg theorem[28].

Similarly, one can calculate

$$\partial_x v_0^* = 0 \tag{5.46a}$$

$$\partial_x v_n^* = \frac{(-1)^n k_n \sin(\omega_n t)}{\sqrt{2\ell}\omega_n}\left[e^{ik_n x} - (-1)^n e^{-ik_n x}\right] \qquad \text{for } n \neq 0. \tag{5.46b}$$

Hence substituting Eq. (5.41) and Eq. (5.42) to Eq. (5.40), one gets

$$\begin{aligned} J_\chi &= \sum_{n=0}^{\infty} \Im[v_n \partial_x v_n^*] \\ &= \frac{1}{2\ell}\sum_{n=0}^{\infty} \Im\left[i\frac{(-1)^n k_n \sin^2(\omega_n t)}{\omega_n^2}[e^{2ik_n x} - e^{-2ik_n x}]\right] \\ &= \frac{1}{\ell}\sum_{n=0}^{\infty} \Im\left[\frac{(-1)^n k_n \sin^2(\omega_n t)}{\omega_n^2}\sin(2k_n x)\right] \\ &= 0. \end{aligned} \tag{5.47}$$

Therefore $J_\chi = 0$ for all t, and there is no phonon flux in this model.

Hence, one only needs to concentrate on the depletion. And Because the system has symmetry under $x \to -x$, one needs to consider only half of the system. In Fig. 5.1, two depletion profiles with size $\ell = 40$ and $\ell = 100$ are shown. One can notice that when the interactions are turned on, the depletion increases from zero. There is a boundary effect coming from the Neumann boundary condition at the condensate wall which shows a higher increase in depletion. By comparing the left and right panels, one can also find that the boundary effect propagates slowly from the wall at almost the same speed regardless of the size of the condensate. Therefore, the depletion growth far from the wall i.e., near the center grows insensitively to the boundary effect, and one can keep it insensitive for more time by increasing the size of the

condensate. It is not related to the zero norm mode, since one can notice from Eq. (5.45) the first term that it has no spatial dependence. The boundary effect

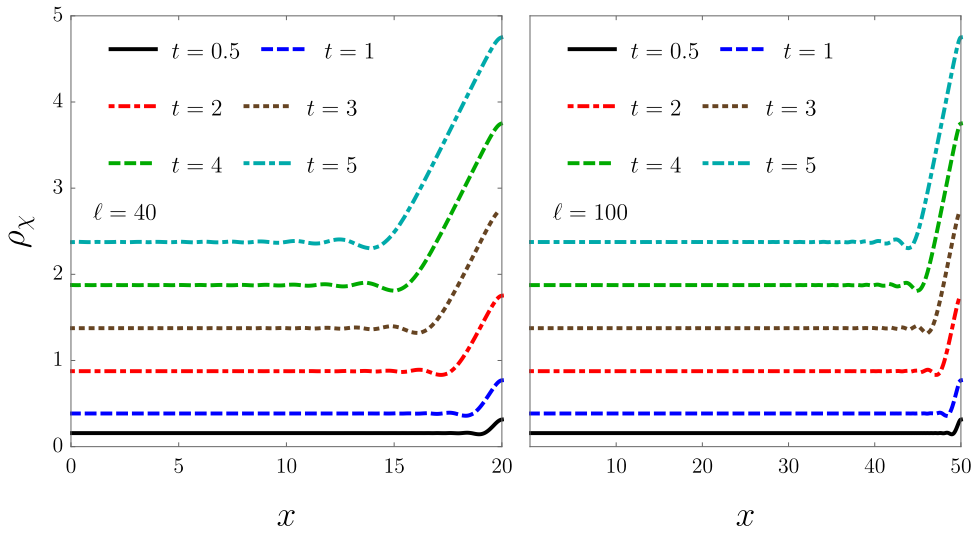

Figure 5.1 Left panel: Evolution of the condensate depletion for a condensate of size $\ell = 40$. The curves are plotted for $x \geq 0$ only, using that ρ_χ is an even function of x [see Eq. (5.45)]. As time passes, we observe an overall depletion increase, initially more pronounced at the condensate wall at $x = \ell/2$. Right panel: Depletion profile evolution for a system of size $\ell = 100$. We note that the bulk depletion increase is insensitive to the existence of the condensate walls for the time periods considered in the plots. Here and in the following plots, units are chosen such that we have the scalings $x = x[\xi_0]$, $t = t[\xi_0^2]$, densities $\rho_i = \rho_i[1/\xi_0]$ with $i = \chi, \zeta$, and for the current density $J_\zeta = J_\zeta[1/\xi_0^2]$.

not only has a similar speed but is also in the same form. In Fig. 5.2 left panel, we plot the depletion near right wall at $t = 5$. One can see that the depletion increase by boundary effect is almost congruent.

Because the growth time is independent of the system size in our parametrization, the time scale only depends on the chemical potential $g_0\rho_0$. Moreover, this fact reminisces that the quantum depletion in infinite size 3D condensate in its ground state is $\sqrt{g_{3\mathrm{D}}^3\rho_{3\mathrm{D}}}$. In the 1D case, there is no analogue formula for

infinite-size condensate, because of the infrared (IR) divergence. In the finite size case, there is no IR divergence so one can hope to obtain a similar relation necessarily model dependent. In the homogeneous condensate without flow, depletion grows with time, but one can obtain the growth rate dependence on the condensate chemical potential $g_0\rho_0$. Indeed, within the time $0 \leq t \leq 5$ shown in Fig. 5.1, the depletion grows linearly in time insensitive to the system size. Recall that the time scale used in this model is $t \sim \xi_0^2 = 1/g_0\rho_0$. Hence, if the units are revived correctly, one can conclude that within that time, $\rho_\chi \propto g_0\rho_0 t$ i.e., depletion is also linearly proportional to chemical potential[35, 43].

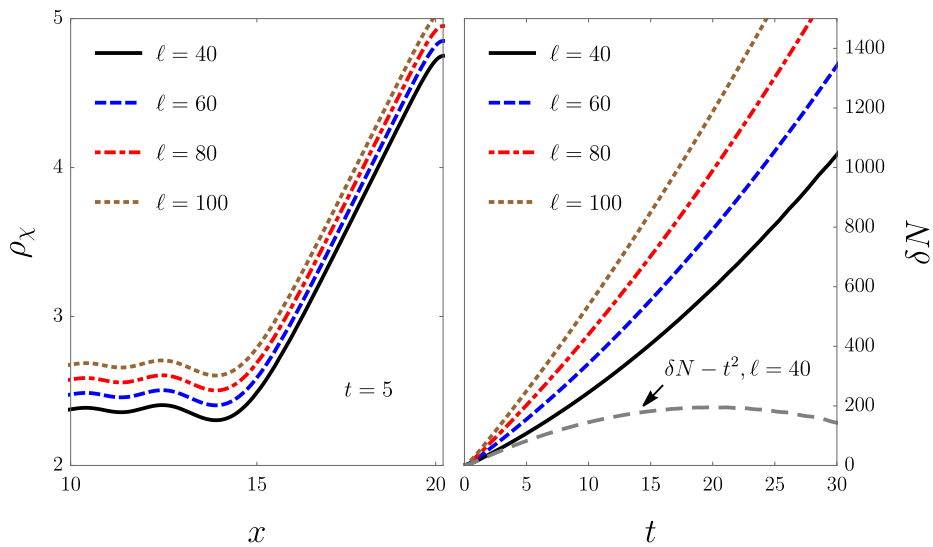

Figure 5.2 Left panel: Depletion near-boundary behavior for several system sizes at $t = 5$. The profiles corresponding to larger condensates are translated to the left and slightly shifted as to allow comparison with the smaller condensate profile. Right panel: Total number of particles in the depleted cloud as a function of time for several condensate sizes. Larger condensates correspond to faster growth of δN for fixed ρ_0. The long-dashed grey line depicts δN without the phase spreading contribution t^2 for $\ell = 40$ [cf. Eq. (5.48)], showing that δN is eventually dominated by condensate phase degradation.

Before proceeding more, one must check that the approximation we are using is valid. The assumption used here is just the Bogoliubov approximation i.e., $\delta N \ll N$ where

$$\delta N = \int_{=\ell/2}^{\ell/2} \mathrm{d}x \rho_\chi = t^2 + \frac{1}{2}\sum_{n=1}^{\infty} \frac{1}{\omega_n^2}[1 - \cos(2\omega_n t)] \tag{5.48}$$

is the whole number of depleted particles. In the right panel of Fig. 5.2, the number of depleted particles as a function of time is shown. One can see that δN increases faster if the system size is bigger. It is expected behavior since the bigger the size is, the more the condensate particle numbers are also since ρ_0 is kept constant. Furthermore, for a size $\ell = 40$ system, at $\delta N(t = 20) \sim 600$. By assuming a condensate with $N = 5000$ particles, $\delta N/N \sim 0.12$. For definiteness, $\delta N/N \lesssim 0.1$ is the chosen validity regime in this thesis. Thus, one needs to consider a smaller time for our theory valid. Fortunately, $t < 5$ which is in Fig. 5.1 is valid for all the model treated here.

5.6 Condensate Correction ζ

Now let us analyze the correction on the condensate ζ in the region $-\ell/2 < x < \ell/2$. One of the virtues of our homogeneous condensate without flow model is that it is analytically solvable. Let us multiply $e^{i\mu t}\sqrt{\rho_0}$ to the Eq. (3.11), where

$$U = \mu - g\rho_0. \tag{5.49}$$

Then we get

$$i\partial_t(e^{i\mu t}\sqrt{\rho_0}\zeta) = \left(-\frac{\partial_x^2}{2m} + g\rho_0\right)(e^{i\mu t}\sqrt{\rho_0}\zeta) + g\rho_0 e^{i\mu t}\sqrt{\rho_0}\zeta^* + g\rho_0(2\langle\hat{\psi}^\dagger\hat{\psi}\rangle + \langle\hat{\psi}^2\rangle) \tag{5.50}$$

Let us write a new spinor

$$F = \begin{pmatrix} e^{i\mu t}\sqrt{\rho_0}\zeta \\ e^{-i\mu t}\sqrt{\rho_0}\zeta^* \end{pmatrix}. \tag{5.51}$$

The equation of motion becomes

$$i\partial_t\sigma_3 F = -\frac{1}{2}\partial_x^2 F + \sigma_4 F + \begin{pmatrix} 2\rho_\chi + \langle\hat{\psi}^2\rangle \\ 2\rho\chi + \langle\hat{\psi}^{\dagger 2}\rangle \end{pmatrix}. \tag{5.52}$$

Because of the linearity of the equation, and also because the source is the sum of modes, we can write the solution in the sum $F(t,x) = \sum_{n=0}^{\infty} F_n(t,x)$, where each F_n satisfies

$$\left(i\partial_t\sigma_3 + \frac{1}{2}\partial_x^2 - \sigma_4\right) F_n = \begin{pmatrix} (u_n + 2v_n)v_n^* \\ (u_n^* + 2v_n^*)v_n \end{pmatrix}. \tag{5.53}$$

Note that in the view of a differential equation, this is just the BdG equation with source. We know the basis expansion of the general solution for this equation already. Therefore we will calculate the characteristic solution which also satisfies the Neumann boundary condition first. And then, because there is no correction on condensate also before turning on the interaction, we will use the initial condition $F(t=0) = 0$ to determine the general solution.

To get the characteristic solution, let us get the source term.

From substitution of Eq. (5.37) to the Eq. (5.35), one can also get

$$u_0 = \frac{1 - it}{\sqrt{\ell}} \tag{5.54}$$

Hence, with Eq. (5.41),

$$u_0 v_0^* = -\frac{t^2 + it}{\ell} \tag{5.55}$$

And

$$(u_0 + 2v_0)v_0^* = \frac{t^2 - it}{\ell} \tag{5.56}$$

For $n \neq 0$,

$$\begin{aligned}
u_n &= \frac{1}{\sqrt{2\ell}[1-(\omega_n - k_n^2/2 - 1)^2]} \\
&\quad \times \Big[e^{-i\omega_n t}\big[e^{ik_n x} + (-1)^n e^{-ik_n x}\big] \\
&\quad\quad -(\omega_n - k_n^2/2 - 1)^2 (-1)^n e^{i\omega_n t}\big[e^{-ik_n x} + (-1)^n e^{ik_n x}\big] \Big] \\
&= \frac{1}{\sqrt{2\ell}[-2\omega_n(\omega_n - \sqrt{\omega_n^2+1})]} \\
&\quad \times \Big[e^{-i\omega_n t}\big[e^{ik_n x} + (-1)^n e^{-ik_n x}\big] \\
&\quad\quad -(2\omega_n(\omega_n - \sqrt{\omega_n^2+1}) + 1) e^{i\omega_n t}\big[e^{ik_n x} + (-1)^n e^{-ik_n x}\big] \Big] \\
&= \frac{1}{\sqrt{2\ell}} \left(\frac{i\sin(\omega_n t)}{\omega_n(\omega_n - \sqrt{\omega_n^2+1})} + e^{i\omega_n t} \right) \big[e^{ik_n x} + (-1)^n e^{-ik_n x}\big] \\
&= \frac{1}{\sqrt{2\ell}} \left(\frac{-(\omega_n + \sqrt{\omega_n^2+1}) i\sin(\omega_n t)}{\omega_n} + e^{i\omega_n t} \right) \big[e^{ik_n x} + (-1)^n e^{-ik_n x}\big] \\
&= \frac{1}{\sqrt{2\ell}} \left(\frac{-(\sqrt{\omega_n^2+1}) i\sin(\omega_n t)}{\omega_n} + \cos(\omega_n t) \right) \big[e^{ik_n x} + (-1)^n e^{-ik_n x}\big]
\end{aligned} \tag{5.57}$$

Using dispersion relation,

$$u_n = \frac{1}{\sqrt{2\ell}} \frac{1}{\omega_n} \big[-(k_n^2/2 + 1) i\sin(\omega_n t) + \omega_n \cos(\omega_n t) \big] \big[e^{ik_n x} + (-1)^n e^{-ik_n x}\big] \tag{5.58}$$

With Eq. (5.42),

$$u_n + 2v_n = \frac{1}{\sqrt{2\ell}} \frac{1}{\omega_n} \big[(1 - k_n^2/2) i\sin(\omega_n t) + \omega_n \cos(\omega_n t) \big] \big[e^{ik_n x} + (-1)^n e^{-ik_n x}\big]$$

Hence,

$$(2v_n + u_n)v_n^* = \frac{1}{2\ell} \frac{1}{\omega_n^2} \big[(1 - k_n^2/2) \sin^2(\omega_n t) - i\omega_n \sin(\omega_n t) \cos(\omega_n t) \big]$$

$$\times \left[2 + (-1)^n \left(e^{2ik_n x} + e^{-2ik_n x}\right)\right]$$

$$= \frac{1}{2\ell}\frac{1}{\omega_n^2}\left[(1 - k_n^2/2)\left(1 - \cos(2\omega_n t)\right) - i\omega_n \sin(2\omega_n t)\right]$$

$$\times \left[1 + (-1)^n \cos(2k_n x)\right] \tag{5.59}$$

Using the dispersion relation again, one gets

$$(2v_n + u_n)v_n^* = \frac{1}{\ell}\frac{(-1)^n}{k_n^2(k_n^2+4)}$$

$$\times \left[(-1)^n + \cos(2k_n x)\right]\left[(2 - k_n^2)[1 - \cos(2\omega_n t)] - 2i\omega_n \sin(2\omega_n t)\right] \tag{5.60}$$

Now it is time to get the characteristic solutions. For $n = 0$,

$$(i\partial_t \sigma_3 - \sigma_4)\tilde{F}_0 = \frac{t^2 - it}{\ell}(1,1)^{\mathrm{t}}. \tag{5.61}$$

The characteristic solution is simply

$$\tilde{F}_0 = -\frac{t^2}{2\ell}(1,1)^{\mathrm{t}}. \tag{5.62}$$

Now one has to solve for $n \neq 0$. One can rewrite the Eq. (5.53) as

$$\left(i\partial_t \sigma_3 + \frac{1}{2}\partial_x^2 - \sigma_4\right) F_n$$

$$= \frac{(-1)^n\left[(-1)^n + \cos(2k_n x)\right]}{\ell k_n^2(k_n^2+4)}\left[(2 - k_n^2)\begin{pmatrix}1\\1\end{pmatrix}\right.$$

$$\left. -e^{2i\omega_n t}\begin{pmatrix}\omega_n - k_n^2 + 1\\ -\omega_n - k_n^2 + 1\end{pmatrix} - e^{-2i\omega_n t}\begin{pmatrix}-\omega_n - k_n^2 + 1\\ \omega_n - k_n/2 + 1\end{pmatrix}\right]. \tag{5.63}$$

Using the result in the Appendix App. 8.3, the characteristic solution for this equation is

$$\begin{aligned}\tilde{F}_n = \frac{(-1)^n}{\ell k_n^2(k_n^2+4)}\big\{(-1)^n\big[&(2-k_n^2)\tilde{F}_{n,0} - (1-k_n^2/2)\tilde{F}_{n,+1} - \omega_n\tilde{F}_{n,+2} \\ &- (1-k_n^2/2)\tilde{F}_{n,-1} - (-\omega_n)\tilde{F}_{n,-2}\big] \\ + \big[&(2-k_n^2)\tilde{F}_{n,3} - (1-k_n^2/2)\tilde{F}_{n,+4} - \omega_n\tilde{F}_{n,+5} \\ &- (1-k_n^2/2)\tilde{F}_{n,-4} - (-\omega_n)\tilde{F}_{n,-5}\big]\big\} \end{aligned} \tag{5.64}$$

Hence,

$$\begin{aligned}\tilde{F}_n = &-\frac{(-1)^n}{2\ell k_n^2(k_n^2+4)} \\ &\times\Bigg\{(-1)^n\left[(2-k_n^2)\begin{pmatrix}1\\1\end{pmatrix} - \frac{e^{2i\omega_n t}}{\omega_n}\begin{pmatrix}\omega_n - k_n^2/2\\ \omega_n + k_n^2/2\end{pmatrix} - \frac{e^{-2i\omega_n t}}{\omega_n}\begin{pmatrix}\omega_n + k_n^2/2\\ \omega_n - k_n^2/2\end{pmatrix}\right] \\ &+ 2\cos(2k_n x) \\ &\times\left[\frac{2-k_n^2}{2(k_n^2+1)}\begin{pmatrix}1\\1\end{pmatrix} + \frac{e^{2i\omega_n t}}{k_n^2}\begin{pmatrix}-\omega_n + k_n^2/2\\ \omega_n + k_n^2/2\end{pmatrix} + \frac{e^{-2i\omega_n t}}{k_n^2}\begin{pmatrix}\omega_n + k_n^2/2\\ -\omega_n + k_n^2/2\end{pmatrix}\right]\Bigg\}\end{aligned} \tag{5.65}$$

Now, let us find the general solution which satisfies the initial condition. At $t = 0$, the characteristic solution $\tilde{F}$ is

$$\tilde{F}(0,x) = \sum_{n=1}^{\infty}\tilde{F}_n(0,x) = \frac{1}{2\ell}\sum_{n=1}^{\infty}\left(\frac{1}{k_n^2+4} - \frac{(-1)^n}{k_n^2(k_n^2+1)}\cos(2k_n x)\right)\begin{pmatrix}1\\1\end{pmatrix}. \tag{5.66}$$

Linearity will be used again. The initial condition is $\zeta(t=0)=0$. Hence,

$$a_{n,0}\Pi_0 + b_{n,0}\tilde{\Pi}_0 + \sum_{j=1}^{\infty}\left[a_{n,j}\Pi_j - b_{n,j}\sigma_1\Pi_j^*\right] = -\tilde{F}_n \tag{5.67}$$

where

$$a_{n,0} = -\frac{\langle\tilde{\Pi}_0, \tilde{F}_n\rangle}{\langle\tilde{\Pi}_0, \Pi_0\rangle}, \quad a_{n,j} = -\langle\Pi_j, \tilde{F}_n\rangle \tag{5.68}$$

$$b_{n,0} = -\frac{\langle\Pi_0, \tilde{F}_n\rangle}{\langle\Pi_0, \Pi_0\rangle}, \quad b_{n,j} = -\langle\sigma_1\Pi_j^*, \tilde{F}_n\rangle \tag{5.69}$$

It is easy to get $a_{n,0}=0$ and

$$b_{n,0} = -\frac{1}{\ell(k_n^2+4)} \tag{5.70}$$

Using Eq. (5.34) one gets

$$\begin{aligned}
a_{n,j} &= -\frac{1}{2\ell}\frac{1}{\sqrt{2\ell[1-(\omega_j-k_j^2/2-1)^2]}}\begin{pmatrix}1 & \omega_j-k_j^2/2-1\end{pmatrix}\begin{pmatrix}1 & 0\\ 0 & -1\end{pmatrix}\begin{pmatrix}1\\ 1\end{pmatrix}\\
&\quad\times\int_{-\frac{\ell}{2}}^{\frac{\ell}{2}}\mathrm{d}x\left[e^{-ik_jx}+(-1)^je^{ik_jx}\right]\left(\frac{1}{k_n^2+4}-\frac{(-1)^n}{k_n^2(k_n^2+1)}\cos(2k_nx)\right)\\
&= -\frac{1}{2\ell}\frac{(-1)^n}{k_n^2(k_n^2+1)}\frac{\omega_j-k_j^2/2-2}{\sqrt{2\ell[1-(\omega_j-k_j^2/2-1)^2]}}\\
&\qquad\qquad\times\int_{-\frac{\ell}{2}}^{\frac{\ell}{2}}\mathrm{d}x\left[e^{-ik_jx}+(-1)^je^{ik_jx}\right]\left(\cos(2k_nx)\right)\\
&= -\delta_{j,2n}\frac{(-1)^n}{2k_n^2(k_n^2+1)}\frac{\omega_j-k_j^2/2-2}{\sqrt{2\ell[1-(\omega_j-k_j^2/2-1)^2]}}
\end{aligned} \tag{5.71}$$

and

$$\begin{aligned}
b_{n,j} &= -\frac{1}{2\ell}\frac{1}{\sqrt{2\ell[1-(\omega_j-k_j^2/2-1)^2]}}\begin{pmatrix}\omega_j-k_j^2/2-1 & 1\end{pmatrix}\begin{pmatrix}1 & 0\\ 0 & -1\end{pmatrix}\begin{pmatrix}1\\ 1\end{pmatrix}\\
&\quad\times\int_{-\frac{\ell}{2}}^{\frac{\ell}{2}}\mathrm{d}x\left[e^{ik_jx}+(-1)^je^{-ik_jx}\right]\left(\frac{1}{k_n^2+4}-\frac{(-1)^n}{k_n^2(k_n^2+1)}\cos(2k_nx)\right)
\end{aligned}$$

$$= \frac{1}{2\ell}\frac{(-1)^n}{k_n^2(k_n^2+1)}\frac{\omega_j - k_j^2/2 - 2}{\sqrt{2\ell[1-(\omega_j - k_j^2/2-1)^2]}}$$
$$\int_{-\frac{\ell}{2}}^{\frac{\ell}{2}} \mathrm{d}x\left[e^{-ik_jx} + (-1)^j e^{ik_jx}\right]\left(\cos(2k_nx)\right)$$
$$= \delta_{j,2n}\frac{(-1)^n}{2k_n^2(k_n^2+1)}\frac{\omega_j - k_j^2/2 - 2}{\sqrt{2\ell[1-(\omega_j - k_j^2/2-1)^2]}} \tag{5.72}$$

Therefore, from the solution of the form

$$F = \tilde{F}_0 + \sum_{n=1}^{\infty}\left(a_{n,0}\Pi_0 + b_{n,0}\tilde{\Pi}_0 + \sum_{j=1}^{\infty}\left[a_{n,j}\Pi_j - b_{n,j}\sigma_1\Pi_j^*\right] + \tilde{F}_n\right), \tag{5.73}$$

One gets

$$\begin{aligned}
e^{i\mu t}\sqrt{\rho_0}\zeta = -\frac{t^2}{2\ell} + \sum_{n=1}^{\infty}\Bigg[&-\frac{1}{2\ell(k_n^2+4)}(1-2it) \\
&- \frac{(-1)^n}{k_n^2(k_n^2+1)}\frac{\omega_{2n} - k_{2n}^2/2 - 2}{2\ell[1-(\omega_{2n} - k_{2n}^2/2-1)^2]} \\
&\qquad \times \cos(k_{2n}x)\left\{e^{-i\omega_{2n}t} + e^{i\omega_{2n}t}(\omega_{2n} - k_{2n}^2/2 - 1)\right\} \\
&- \frac{(-1)^n}{2\ell k_n^2(k_n^2+4)} \\
&\quad \times \Bigg\{(-1)^n\left[(2-k_n^2) - \frac{e^{2i\omega_n t}}{\omega_n}(\omega_n - k_n^2/2) - \frac{e^{-2i\omega_n t}}{\omega_n}(\omega_n + k_n^2/2)\right] \\
&\quad + 2\cos(2k_nx) \\
&\qquad \times \left[\frac{2-k_n^2}{2(k_n^2+1)} + \frac{e^{2i\omega_n t}}{k_n^2}(-\omega_n + k_n^2/2) + \frac{e^{-2i\omega_n t}}{k_n^2}(\omega_n + k_n^2/2)\right]\Bigg\}.
\end{aligned} \tag{5.74}$$

Because $k_{2n} = 2k_n$,

$$\begin{aligned}
e^{i\mu t}\sqrt{\rho_0}\zeta = -\frac{t^2}{2\ell} - \frac{1}{2\ell}\sum_{n=1}^{\infty}\Bigg[&\frac{1}{k_n^2(k_n^2+4)}\Bigg\{k_n^2(1-2it) \\
&+ \left((2-k_n^2) - 2\cos(2\omega_n t) + i\frac{k_n^2}{\omega_n}\sin(2\omega_n t)\right)\Bigg\}
\end{aligned}$$

$$
\begin{aligned}
&+\frac{(-1)^n}{k_n^2(k_n^2+1)}\frac{(\omega_{2n}-2k_n^2-1)-1}{[1-(\omega_{2n}-2k_n^2-1)^2]}\cos(2k_nx)\\
&\qquad\times\left\{e^{-i\omega_{2n}t}+e^{i\omega_{2n}t}(\omega_{2n}-2k_n^2-1)\right\}\\
&+\frac{(-1)^n}{k_n^2(k_n^2+4)}\left\{2\cos(2k_nx)\left[\frac{2-k_n^2}{2(k_n^2+1)}+\cos(2\omega_nt)-2i\frac{\omega_n^2}{k_n^2}\sin(2\omega_nt)\right]\right\}\Bigg]\\
=&-\frac{t^2}{2\ell}-\frac{1}{2\ell}\sum_{n=1}^{\infty}\frac{(-1)^n}{k_n^2(k_n^2+4)}\Bigg[2(-1)^n\left\{1-\cos(2\omega_nt)+ik_n^2\left(\frac{\sin(2\omega_nt)}{2\omega_n}-t\right)\right\}\\
&+\cos(2k_nx)\left\{\frac{2-k_n^2}{k_n^2+1}+2\cos(2\omega_nt)-4i\frac{\omega_n}{k_n^2}\sin(2\omega_nt)\right.\\
&-\frac{k_n^2+4}{k_n^2+1}\frac{1}{\omega_{2n}-2k_n^2}\Big\{(\omega_{2n}-2k_n^2)\cos(\omega_{2n}t)\\
&\qquad\left.+i(\omega_{2n}-2k_n^2-2)\sin(\omega_{2n}t)\Big\}\right\}\Bigg]
\end{aligned}
\tag{5.75}
$$

Using the dispersion relation, one gets

$$
\begin{aligned}
e^{i\mu t}\sqrt{\rho_0}\zeta=&-\frac{t^2}{2\ell}-\frac{1}{2\ell}\sum_{n=1}^{\infty}\frac{(-1)^n}{k_n^2(k_n^2+4)}\left[2(-1)^n\left\{1-\cos(2\omega_nt)+ik_n^2\left(\frac{\sin(2\omega_nt)}{2\omega_n}-t\right)\right\}\right.\\
&+\cos(2k_nx)\left[\frac{2-k_n^2}{k_n^2+1}+2\cos(2\omega_nt)-4i\frac{\omega_n}{k_n^2}\sin(2\omega_nt)\right.\\
&\left.\left.-\frac{k_n^2+4}{k_n^2+1}\left(\cos(\omega_{2n}t)+i\frac{(\omega_{2n}-2k_n^2-2)}{\omega_{2n}-2k_n^2}\sin(\omega_{2n}t)\right)\right]\right\}
\end{aligned}
\tag{5.76}
$$

Note that

$$
\begin{aligned}
\frac{(\omega_{2n}-2k_n^2-2)}{\omega_{2n}-2k_n^2}&=1-\frac{2}{\omega_{2n}-2k_n^2}\\
&=1-\frac{1}{k_n\sqrt{1+k_n^2}-1}\\
&=-\frac{k_n\sqrt{1+k_n^2}}{k_n^2}\\
&=-\frac{\omega_2 n}{2k_n^2}
\end{aligned}
\tag{5.77}
$$

Finally, one gets

$$e^{i\mu t}\sqrt{\rho_0}\zeta = -\frac{t^2}{2\ell} - \frac{1}{8\ell}\sum_{n=1}^{\infty}\frac{(-1)^n}{\omega_n^2}\left[2(-1)^n\left\{1-\cos(2\omega_n t) + ik_n^2\left(\frac{\sin(2\omega_n t)}{2\omega_n} - t\right)\right\}\right.$$
$$+\cos(2k_n x)\left\{\frac{2-k_n^2}{k_n^2+1} + 2\cos(2\omega_n t) - 4i\frac{\omega_n}{k_n^2}\sin(2\omega_n t)\right.$$
$$\left.\left. - \frac{k_n^2+4}{k_n^2+1}\left(\cos(\omega_{2n}t) - i\frac{\omega_{2n}}{2k_n^2}\sin(\omega_{2n}t)\right)\right\}\right] \tag{5.78}$$

where $4\omega_n^2 = k_n^2(k_n^2+4)$ is also used also.

Now it is time to calculate correction on the condensate density ρ_ζ and correction on current J_ζ. Note that they are corrections coming from the existence of the Bogoliubov field. Hence, they represent also the backreaction effect in the broad sense. The density correction is

$$\begin{aligned}\rho_\zeta &:= 2\Re[\phi_0^*\zeta] = 2\Re[e^{i\mu t}\sqrt{\rho_0}\zeta] \\ &= -\frac{t^2}{\ell} - \frac{1}{4\ell}\sum_{n=1}^{\infty}\frac{(-1)^n}{\omega_n^2}\left\{2(-1)^n[1-\cos(2\omega_n t)]\right. \\ &\qquad \left. +\cos(2k_n x)\left[\frac{2-k_n^2}{k_n^2+1} + 2\cos(2\omega_n t) - \frac{k_n^2+4}{k_n^2+1}\cos(\omega_{2n}t)\right]\right\}.\end{aligned} \tag{5.79}$$

Note first that

$$\int_{-\ell/2}^{\ell/2} \mathrm{d}x\,\rho_\zeta = -t^2 - \frac{1}{2}\sum_{n=1}^{\infty}\frac{1}{\omega_n^2}[1-\cos(2\omega_n t)] = -\delta N. \tag{5.80}$$

Hence, the total particle number is conserved as expected. But, also note that $\rho_\zeta \neq -\rho_\chi$ which shows that it is not the Bogoliubov field itself. In Fig. 5.3, the ρ_ζ corresponding to ρ_χ in Fig. 5.1 is shown. Note that even though they are not the same with the depletion ρ_χ, it shows similar behavior. Near the center, they are almost homogeneous and there is a boundary effect. The difference one

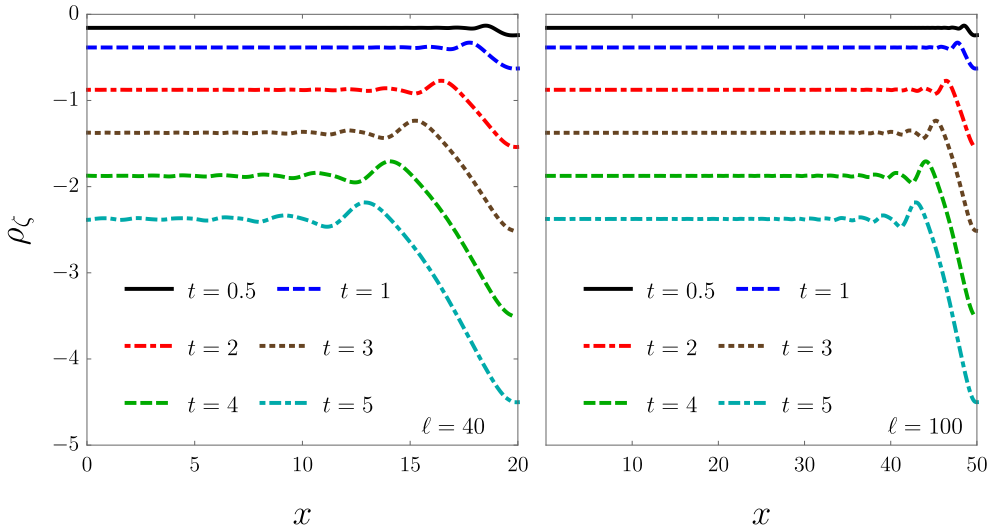

Figure 5.3 Left panel: Evolution of the condensate correction ρ_ζ for a condensate of size $\ell = 40$. The curves are plotted for $x \geq 0$ as ρ_ζ is an even function of x [see Eq. (5.79)]. As time passes, we observe an overall depletion increase, initially more pronounced at the condensate wall at $x = \ell/2$. Right panel: ρ_ζ profile evolution for a system of size $\ell = 100$. We note that the condensate bulk corrections are insensitive to the existence of the condensate wall boundary region for the time scales considered in the plots.

can directly from the plot is that they show more clearly noticeable oscillatory patterns.

Now, let us calculate the correction on the current J_ζ. In our model, because we have no leading order condensate flow ($\rho_0 = 0$), and no phonon flux ($\rho_\chi = 0$), this is the only existing current in our working order (N^0). Hence the current is

$$\begin{aligned} J_\zeta &:= \Im[\phi_0^* \partial_x \zeta] = \Im[e^{i\mu t}\sqrt{\rho_0}\partial_x \zeta] \\ &= \partial_x \Im[e^{i\mu t}\sqrt{\rho_0}\zeta] \\ &= -\frac{2}{\ell}\sum_{n=1}^{\infty} \frac{(-1)^n \sin(2k_n x)}{k_n}\left[\frac{\sin(2\omega_n t)}{2\omega_n} - \frac{\sin(\omega_{2n} t)}{\omega_{2n}}\right]. \end{aligned} \tag{5.81}$$

One can calculate the total current by

$$\int_{-\ell/2}^{\ell/2} J \mathrm{d}x = \int_{-\ell/2}^{\ell/2} J_\zeta \mathrm{d}x = 0 \tag{5.82}$$

which is expected from the $x \to -x$ symmetry of the system. In Fig. 5.4, the current density of the system with $\ell = 40$ is given.

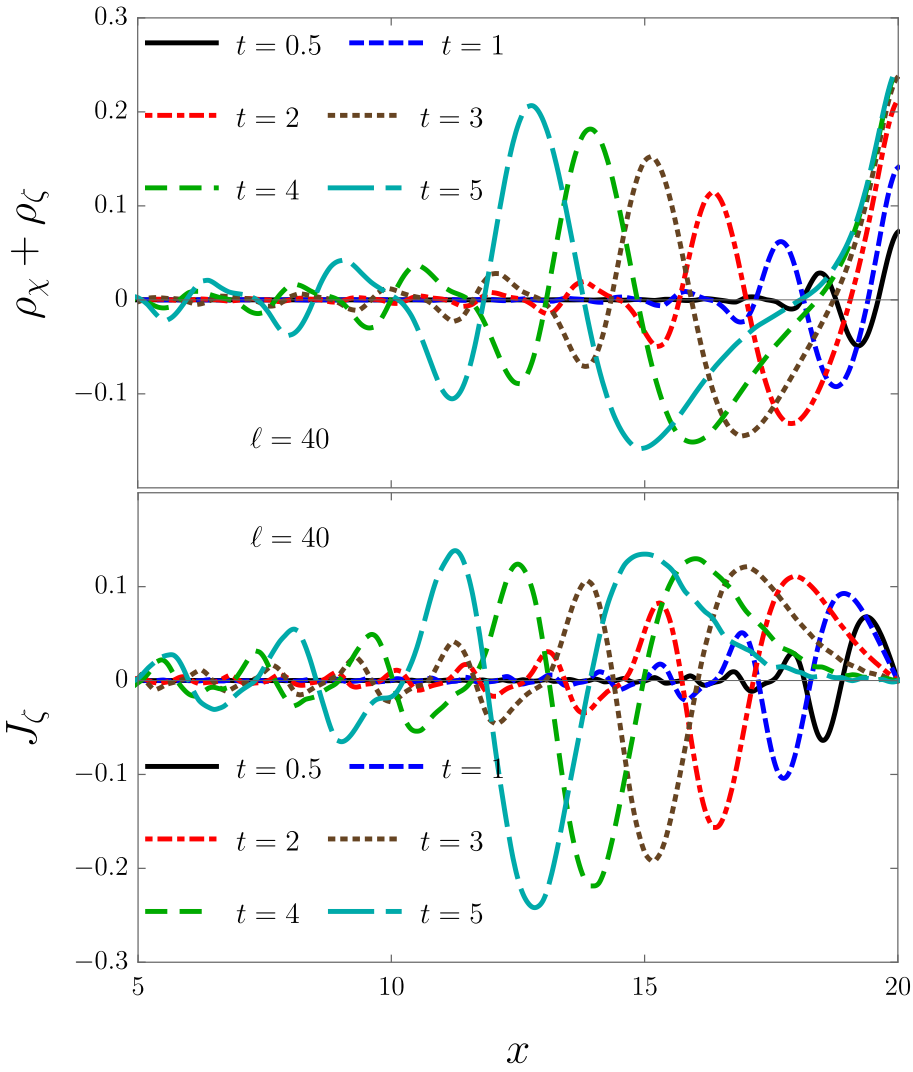

Figure 5.4 Upper panel: Evolution of the gas density on top of the condensate background ρ_0 for a system of size $\ell = 40$ and at several instants of time. These profiles represent the departure from a uniform density condensate profile as dictated by number-conserving backreaction effects. Lower panel: Evolution of the condensate flux J_ζ for a condensate of size $\ell = 40$ and at several instants of time. The positive plot range $5 < x < 20$ is motivated by the fact that J_ζ is an odd function in view of Eq. (5.81). Note that the flux of particles vanishes at the condensate walls, reflecting the fact that the particles are indeed trapped inside the box.

5.7 Measurement

In this subsection, the possibility of measurement on the contributions separately or not is investigated. For the flux, there is only one contribution J_ζ. Hence what one measures for the flux is the only current induced by the backreaction. But there are 3 distinct contributions on the density (ρ_0, ρ_χ, ρ_ζ) which are all nonzero. Because they have different physical meanings, one may ask the question of whether we can measure them separately. In [43], the authors measure quantum depletion ρ_χ separately. The main idea is that the condensate density ρ_0 is removed by the Bragg scattering technique, and one can see it by the power spectrum. In number conserving expansion, however, there is another contribution ρ_ζ. Hence, one needs to separate the correction of condensate from the depletion. But, at least in our knowledge, the power spectrum of ρ_χ and ρ_ζ are not simple to distinguish, and so it is not possible to determine ρ_χ or ρ_ζ independently. Hence, if one wants to measure ρ_χ only, one must suppress not only the ρ_0 but also the ρ_ζ. If not, one can measure only separately the leading order condensate density ρ_χ and the subleading order contribution $\rho_\chi + \rho_\zeta$. Fig. 5.4 shows the subleading order contribution to the density one can measure by using the Bragg scattering method.

Quantum Backreaction and Quantum Potential— Now, let us investigate the quantum backreaction more detail. Note that in our expansion, χ is the only quantized field. As explained in the previous section, the origin of J_ζ, ρ_ζ is affected by the existence of χ. Hence, the dynamic effect coming from the existence of ρ_χ and J_χ can be interpreted as a backreaction. Moreover, we also distinguish the part which satisfies the classical equation of motion $f_{\rm cl}$ and the remaining part $f_{\rm q}$ The leading order part of $f_{\rm cl}$ can be interpreted as a purely

classical expression. It comes from the classical equations of motion (Euler equation) with a classical source. The subleading order of $f_{\rm cl}$ also comes from the classical equation of motion but with a source determined from quantum fluctuation. This is the usual semi-classical approximation result, and we call this also the classical force. In quantum fluid mechanics, it is just the Madelung equation. The remaining one $f_{\rm q}$ comes from the quantum origin and does not appear in the classical equations of motion. Hence, it shows that if one considers the backreaction of the quantum effect, one needs to consider not only the effect on the source term from quantum fluctuation but also the correction of the dynamical equation of motion itself. In the system considered, the fact that $J = J_\zeta$ simplifies the analysis a lot. Let us calculate the classical force in that model. Because $v_0 = 0$ in the model, the first term of Eq. (4.6) is

$$\partial_x(\rho v^2) = \partial_x\big[\rho_0 v_0^2 - (\rho_\zeta + \rho_\chi)v_0^2 + 2(J_\chi + J_\zeta)v_0\big] = 0. \tag{5.83}$$

Therefore, classical force reduces to

$$f_{\rm cl} = -\partial_x\left(-\frac{\partial_x^2(\rho_\chi + \rho_\zeta)}{4} + (\rho_\chi + \rho_\zeta)\right) = \left(\frac{\partial_x^2}{4} - 1\right)(\partial_x\rho_\chi + \partial_x\rho_\zeta). \tag{5.84}$$

From the depletion Eq. (5.45), one gets

$$\partial_x\rho_\chi = -\frac{1}{\ell}\sum_{n=1}^{\infty}(-1)^n k_n \sin(2k_n x)\frac{[1-\cos(2\omega_n t)]}{\omega_n^2}. \tag{5.85}$$

Similarly, from the condensate density correction Eq. (5.79), one gets

$$\begin{aligned}\partial_x\rho_\zeta &= \frac{1}{2\ell}\sum_{n=1}^{\infty}\frac{(-1)^n k_n \sin(2k_n x)}{\omega_n^2}\left[\frac{2-k_n^2}{k_n^2+1} + 2\cos 2\omega_n t - \frac{k_n^2+4}{k_n^2+1}(\cos\omega_{2n}t)\right] \\ &= \frac{1}{2\ell}\sum_{n=1}^{\infty}\frac{(-1)^n k_n \sin(2k_n x)}{\omega_n^2}\left[-2[1-\cos(2\omega_n t)] - \frac{k_n^2+4}{k_n^2+1}[1-(\cos\omega_{2n}t)]\right]\end{aligned}$$

$$= -\frac{1}{\ell}\sum_{n=1}^{\infty}(-1)^n k_n \sin(2k_n x)\left[\frac{[1-\cos(2\omega_n t)]}{\omega_n^2} + 8\frac{[1-\cos(\omega_{2n} t)]}{\omega_{2n}^2}\right] \tag{5.86}$$

Substituting these to Eq. (5.84), we get

$$f_{\rm cl} = \frac{1}{\ell}\sum_{n=1}^{\infty}(-1)^n(1+k_n^2)k_n \sin(2k_n x)\left[2\frac{[1-\cos(2\omega_n t)]}{\omega_n^2} + 8\frac{[1-\cos(\omega_{2n} t)]}{\omega_{2n}^2}\right] \tag{5.87}$$

From induced current Eq. (5.81), one can easily get

$$\begin{aligned}\partial_t J_\zeta &= \frac{-2}{\ell}\sum_{n=1}^{\infty}\frac{(-1)^n \sin(2k_n x)}{k_n}\left[\cos(2\omega_n t) - \cos(\omega_{2n} t)\right] \\ &= \frac{2}{\ell}\sum_{n=1}^{\infty}\frac{(-1)^n \sin(2k_n x)}{k_n}\left\{[1-\cos(2\omega_n t)] - [1-\cos(\omega_{2n} t)]\right\}\end{aligned} \tag{5.88}$$

For convenience, it is better to write

$$\begin{aligned}\partial_t J_\zeta = &\frac{1}{\ell}\sum_{n=1}^{\infty}(-1)^n k_n(2+k_n^2/2)\sin(2k_n x)\frac{[1-\cos(2\omega_n t)]}{\omega_n^2} \\ &+ \frac{1}{\ell}\sum_{n=1}^{\infty}8(-1)^n k_n(1+k_n^2)\sin(2k_n x)\frac{[1-\cos(\omega_{2n} t)]}{\omega_{2n}}.\end{aligned} \tag{5.89}$$

By putting Eq. (5.87) and Eq. (5.89) to the Eq. (4.8), one gets

$$\begin{aligned}f_{\rm q} &= -\frac{3}{2\ell}\sum_{n=1}^{\infty}\frac{(-1)^n k_n^3 \sin(2k_n x)}{\omega_n^2}[1-\cos(2\omega_n t)] \\ &= -\frac{6}{\ell}\sum_{n=1}^{\infty}\frac{(-1)^n k_n \sin(2k_n x)}{k_n^2+4}[1-\cos(2\omega_n t)].\end{aligned} \tag{5.90}$$

One can get also this result by direct calculation.

Despite this simple analytic form, numerically plotting the $f_{\rm q}$ directly takes a too long time, because the series converges very slowly. Hence, in this thesis, this problem is detoured by calculating the potential. Note that in the system here, if one defines the potential to satisfy $f_{\rm cl} + f_{\rm q} := -\partial_s V$,

$$\partial_t J = \partial_t J_\zeta = -\partial_x V. \tag{5.91}$$

From Eq. (5.88), one can deduce that

$$V = -\frac{1}{\ell}\sum_{n=1}^{\infty}\frac{(-1)^n\cos(2k_n x)}{k_n^2}[\cos(2\omega_n t) - \cos(\omega_{2n} t)]. \tag{5.92}$$

Fortunately, this potential converges much faster. Since Eq. (5.83) holds for the condensate at rest is that the classical force $f_{\rm cl}$ can be determined by only the density i.e., $f_{\rm cl} = f_{\rm cl}(\rho, \partial_x\rho, \partial_x^2\rho, \partial_x^3\rho)$ in our working order (N^0). One can rewrite Eq. (5.84)

$$f_{\rm cl} = -\partial_x\left[\left(1 - \frac{\partial_x^2}{4}\right)(\rho_\chi + \rho_\zeta)\right]. \tag{5.93}$$

Hence, one can define classical potential which satisfies $f_{\rm cl} = -\partial_x V_{\rm cl}$ where

$$v_{\rm cl} = \frac{1}{\ell}\sum_{n=1}^{\infty}\frac{(-1)^n\cos(2k_n x)}{k_n^2}\left\{\frac{\omega_{2n}^2}{4\omega_n^2}[1 - \cos(2\omega_n t)] - 1 + \cos(\omega_{2n} t)\right\}. \tag{5.94}$$

In Fig. 5.5, it is shown that the total potential V and classical potential $V_{\rm cl}$ for the system size $\ell = 40$. Note that the $V_{\rm cl}$ is usually bigger than V. One can deduce that the quantum backreaction attenuates the classical backreaction effect. Especially, near the boundary, attenuation is a lot, and quantum potential exceeds the classical potential. And hence, the strong Eulerian force term at the boundary is reduced by the quantum backreaction force.

Note that the J_ζ in the model can be calculated from the continuity equation, and $f_{\rm cl}$ is also governed by the total density. Hence, if one measures the density, one can indirectly measure the quantum backreaction force.

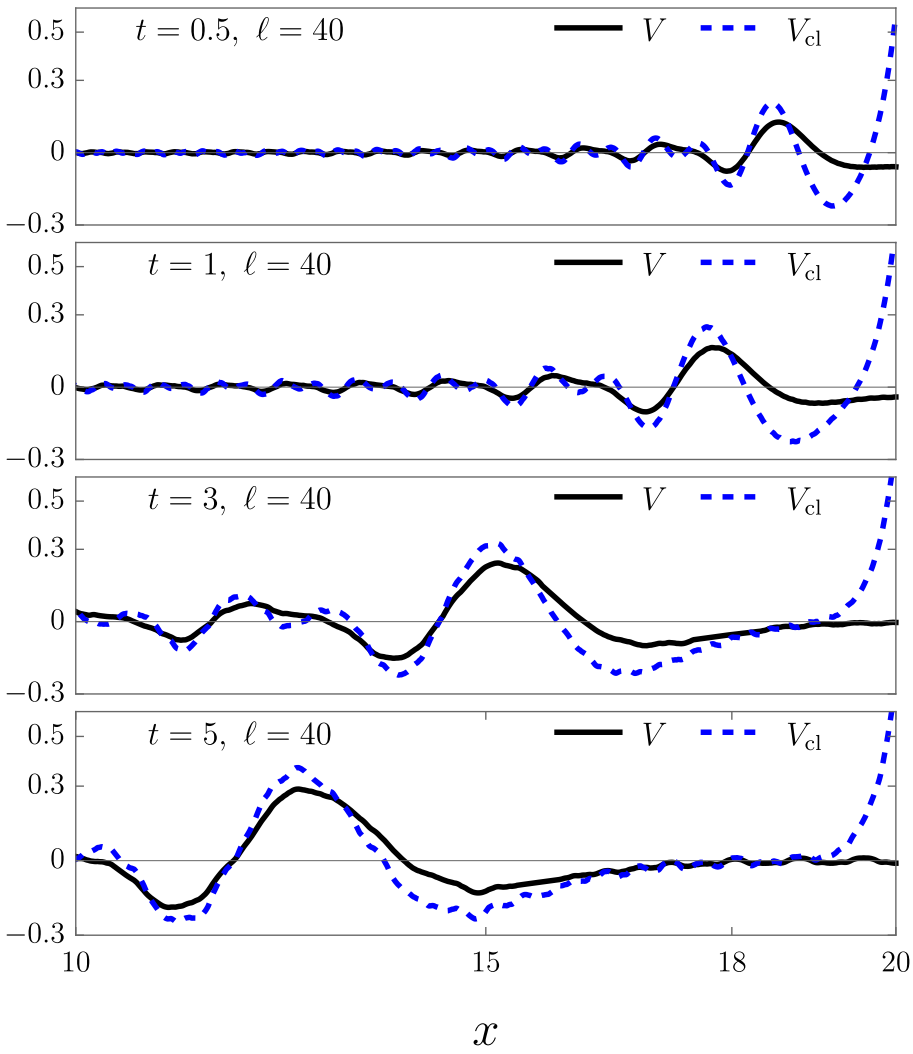

Figure 5.5 Evolution of the total and classical potentials V and V_{cl}, respectively, for a condensate of size $\ell = 40$ and at several instants of time. The slopes of the curves represent the local force density exerted on the system particles. We note that for the considered time interval, the quantum force has the effect of attenuating the classical Eulerian force and that this attenuation is more pronounced near the condensate walls.

6 Black Hole Model

One of the famous ways of making the black hole configuration in the BEC experiment is based on the Galilean invariance of the system[51, 31, 49]. In the laboratory frame, the condensate is at rest, and the moving blue-detuned laser acts as a moving potential step. In the comoving frame of the moving laser, the condensate moves through the potential step induced by the laser and one can think of it as a black hole configuration. The drawback of this model is that the stationary regime is difficult to establish and fully numerical analysis is therefore unavoidable. In particular, the moving horizon is responsible for the emergence of an inner horizon, and a black hole-white hole pair forms [31, 77, 78]. Different techniques possible to establish analogue event horizons include the condensate being released from a reservoir [53] by an outcoupling, and the flowing condensate in toroidal configurations [21], the latter always containing a black hole-while hole pair, as dictated by the very ring topology.

6.1 Background Condensate and Bogoliubov Field

The proposed model in this study is motivated by the atom laser experiment. To realize a finite-size (and therefore well-defined) quasi-1D black hole model, one can put the coherent sources and drains at the boundary of the condensate[21,

9]. So, one needs to add the term corresponding to the source

$$S_{\mathrm{s}} := \int \mathrm{d}x (J_{\mathrm{e}}\Psi^* + J_{\mathrm{e}}^*\Psi) \tag{6.1}$$

to the original action for the Bose gas which is defined as the integration of the Lagrangian Eq. (3.1). Here, J_e represents the external source and drains. From the total action, one gets an inhomogeneous Gross-Pitaevskii equation [56]

$$\left(i\partial_t - \frac{\partial_x^2}{2m} + U + g|\Psi|^2 \right) \Psi = J_{\mathrm{e}}. \tag{6.2}$$

Note that the source field J_{e} can be complex-valued. To understand the physical meaning of J_{e}, it would be better to rewrite the Eq. (6.2) in the Madelung representation $\Psi = \sqrt{\rho}e^{i\theta}$ where ρ is the density, and $v = \partial_x\theta/m$ is the fluid velocity[68]. One gets the continuity-like equation and the Madelung equation

$$\partial_t\rho + \partial_x(\rho v) = -2\Im[J_{\mathrm{e}}\Psi^*], \tag{6.3a}$$

$$m\partial_t\theta + \frac{mv^2}{2} - \frac{\partial_x^2\sqrt{\rho}}{2m\sqrt{\rho}} + U + g\rho = \frac{1}{\rho}\Re[J_{\mathrm{e}}\Psi^*]. \tag{6.3b}$$

The continuity-like equation Eq. (6.3a) shows that $-2\Im[J_{\mathrm{e}}\Psi^*]$ is the flux of particles being injected into the system, whereas the Eq. (6.3b) shows that the $\Re[J_{\mathrm{e}}\Psi^*]/\rho$ is the additional force density due to the source is turned on. It is more clear if we take ∂_x in both sides of Eq. (6.3b) to get the Euler-type equation [68]

$$(\partial_t + v\partial_x)v = -\frac{1}{m}\partial_x \left(-\frac{\partial_x^2\sqrt{\rho}}{2m\sqrt{\rho}} + U + g\rho - \frac{1}{\rho}\Re[J_{\mathrm{e}}\Psi^*] \right). \tag{6.4}$$

The analogue black hole considered here is prepared by adjusting the source field J_{e} and external potential U to produce the homogeneous flow with a piecewise homogeneous coupling constant. (See Fig. 6.1) Concretely, it

is assumed that the condensate density ρ_0 and the velocity $v_0 > 0$ are constant. And the coupling constant g is

$$g = g_{\mathrm{u}}\Theta(-x) + g_{\mathrm{d}}\Theta(x), \tag{6.5}$$

where $\Theta(x)$ is the Heaviside step function. The subscript "u" and "d" is used to denote the upstream/downstream each. In the view of analogue gravity, upstream is outside of the black hole and downstream is inside the black hole which is the same notion as the notion in the literature [3, 33, 11]. The condensate is trapped in the region $x \in [-\ell_1/2, \ell_2/2]$.

The model we discuss is the condensate with constant velocity $v > 0$ to the right. It can be modelled by letting $\theta = -\mu t + vx$, where μ is the chemical potential. One can make the finite solution as a limiting process. Let the system

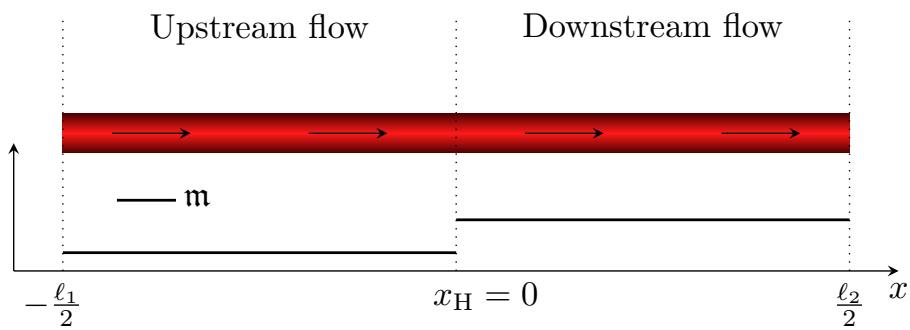

Figure 6.1 Schematics of the condensate under study, which is assumed to be a homogeneous quasi-1D condensate of size $(\ell_2 + \ell_1)/2$ flowing at constant velocity. The gas flow is sustained by continuous source and drain at $x = -\ell_1/2$ and $x = \ell_2/2$, respectively. At $x = x_{\mathrm{H}}$, the Mach number $\mathfrak{m}$ has a jump-like discontinuity, separating the system into two regions of different sound velocities.

density ρ be

$$\rho = \begin{cases} \rho_{\text{in}} & x \in [-\ell_1/2,\, \ell_2/2] \\ \rho_{\text{out}} & x \in \,]\infty, -\ell_1/2\,[\, \bigcup \,]\ell_2, \infty[\end{cases} \tag{6.6}$$

where $\rho_{\text{in}}, \rho_{\text{out}}$ are constants. Then the flux of particles can be obtained from Eq. (6.3a) as

$$\Im[J_{\text{e}}\Psi^*] = \frac{v(\rho_{\text{out}} - \rho_{\text{in}})}{2}[\delta(x + \ell_1/2) - \delta(x - \ell_2/2)]. \tag{6.7}$$

One also set the external potential as

$$U = \begin{cases} \mu - \frac{mv^2}{2} - g\rho_{\text{in}} & x \in [-\ell_1/2,\, \ell_2/2] \\ \gamma\rho_{\text{out}}^{-1/4} + \mu - \frac{mv^2}{2} - g\rho_{\text{out}} & x \in \,]\infty, -\ell_1/2\,[\, \bigcup \,]\ell_2, \infty[\end{cases} \tag{6.8}$$

where $\gamma > 0$ being a constant parameter. From Eq. (6.3b), one gets the additional force density

$$\begin{aligned} \frac{\Re[J_{\text{e}}\Psi^*]}{\sqrt{\rho}} &= \gamma\rho_{\text{out}}^{1/4}[\Theta(\ell_1/2 - x) + \Theta(x - \ell_2/2)] \\ &\quad + \frac{\sqrt{\rho_{\text{out}}} - \sqrt{\rho_{\text{in}}}}{2m}[\partial_x\delta(x + \ell_1/2) - \partial_x\delta(x - \ell_2/2)]. \end{aligned} \tag{6.9}$$

There are 8 free parameters $\{\mu, v, g_u, g_d, \ell_1, \ell_2, \rho_{\text{out}}, \rho_{\text{in}}\}$ for our piecewise homogeneous system. The finite size model can be obtained by letting $\rho_{\text{out}} \to 0$. Hence, the potential becomes

$$U = \begin{cases} \mu - \frac{mv^2}{2} - g\rho_{\text{in}} & x \in [-\ell_1/2,\, \ell_2/2] \\ \infty & x \in]\infty, -\ell_1/2[\cup]\ell_2, \infty[\end{cases} \tag{6.10}$$

and the associated force density term becomes

$$\frac{\Re[J_{\text{e}}\Psi^*]}{\sqrt{\rho}} = \frac{-\sqrt{\rho_{\text{in}}}}{2m}[\partial_x\delta(x + \ell_1/2) - \partial_x\delta(x - \ell_2/2)]. \tag{6.11}$$

The condensate particles enter the system at $x = -\ell_1/2$ and escape at $x = \ell_2/2$, similar to the external source considered in [56] As in the homogeneous model, ψ is defined as $\chi = e^{-i(\mu t - vx)}\psi$, i.e., ψ is the Bogoliubov wave in the comoving fluid. Because of the origin of Bogoliubov expansion, one also calls it linearized fluctuations. The BdG equation Eq. (3.10) then becomes

$$i\partial_t\psi = \left(-\frac{\partial_x^2}{2m} - iv\partial_x\right)\psi + g\rho_0(\psi + \psi^*). \tag{6.12}$$

Because the potential is infinity outside, the wave function must satisfy the Dirichlet boundary conditions: $\psi|_{x=\ell_1/2} = \psi|_{x=\ell_2/2} = 0$ [69]. From now on, only the finite region $x \in [-\ell_1/2, \ell_2/2]$ will be treated.

Because the model considers the piecewise homogeneous fluid[11], we have well-defined sound velocity in each region by $mc_{\mathrm{u,d}}^2 = g_{\mathrm{u,d}}\rho_0$. By dividing the Eq. (6.12) with $g\rho_{\mathrm{u}} = mc_{\mathrm{u}}^2$ and using dimensionless spatial unit by $x \to x/\xi_{\mathrm{u}}$, where $\xi_{\mathrm{u}} = 1/\sqrt{mg_{\mathrm{u}}\rho_0} = 1/mc_{\mathrm{u}}$, one will get

$$i\partial_t\psi = \left(-\frac{\partial_x^2}{2} - i\mathfrak{m}_{\mathrm{u}}\partial_x\right)\psi + \frac{g}{g_{\mathrm{u}}}(\psi + \psi^*). \tag{6.13}$$

Here, $\mathfrak{m}_{\mathrm{u}}$ denotes the upstream Mach number. The black hole is formed when $\mathfrak{m}_{\mathrm{u}} < 1 < \mathfrak{m}_{\mathrm{d}}$ holds. Hence, the remaining parameters governing the characteristics of the black hole configuration are $\{\mathfrak{m}_{\mathrm{u}}, \mathfrak{m}_{\mathrm{d}}, \ell_1, \ell_2\}$. The quantization is done in the same manner with homogeneous gas i.e., one forces the Bogoliubov field ψ to satisfy Eq. (5.8). One can also rewrite the same quantization using the Nambu spinor $\Phi = (\psi, \psi^*)^{\mathrm{t}}$ to satisfy Eq. (5.9). But, now the Nambu spinor must satisfy the equation

$$i\sigma_3\partial_t\Phi = \left(-\frac{\partial_x^2}{2} - i\mathfrak{m}_{\mathrm{u}}\sigma_3\partial_x + \frac{g}{g_{\mathrm{u}}}\right)\Phi. \tag{6.14}$$

Note that this can be written in the form

$$i\sigma_3\Phi = \sigma_3 H_{\rm BdG}\Phi.$$

and $H_{\rm BdG}$ is also σ_3-pseudoHermitian. But now, Φ must satisfy the Dirichlet boundary conditions

$$\Phi|_{x=-\ell_1/2} = 0 = \Phi|_{x=\ell_2/2}. \tag{6.15}$$

The pseudoHermicity of $H_{\rm BdG}$ allows one to have an orthonormal basis. Hence, the spinor can be spanned by the positive norm mode and its corresponding negative norm modes in the form Eq. (5.13) Or equivalently Eq. (5.16)

$$\psi(t,x) = \sum_{n=0}^{\infty}[a_n u_n(t,x) + a_n^\dagger v_n^*(t,x)]. \tag{6.16}$$

Because the leading order condensate is in the stationary regime, the solution of the Eq. (6.14) with the stationary form $\Phi(t,x) = e^{-i\omega t}\Phi_\omega$ exists where

$$\omega\sigma_3\Phi_\omega = \left(-\frac{\partial_x^2}{2} - i\mathfrak{m}_{\rm u}\sigma_3\partial_x + \frac{g}{g_{\rm u}}\right)\Phi_\omega. \tag{6.17}$$

By taking complex conjugate and using the anti-commutation relation of Pauli matrices, one can notice that $\sigma_1\Phi^*$ satisfies

$$-\omega^*\sigma_3\sigma_1\Phi_\omega^* = \left(-\frac{\partial_x^2}{2} - i\mathfrak{m}_{\rm u}\sigma_3\partial_x + \frac{g}{g_{\rm u}}\right)\sigma_1\Phi_\omega^*. \tag{6.18}$$

where $\sigma_4\sigma_1 = \sigma_1\sigma_4$, since $\sigma_4 = \mathbb{1} + \sigma_1$. If $\omega \in \mathbf{R}$, this shows that considering the $\omega > 0$ is enough to cover all the real frequencies.

But, now one can have, in principle, the complex frequency because $H_{\rm BdG}$ is not Hermitian. Fortunately, because the Hamiltonian for full Bose gas is Hermitian, if ω is in the spectrum, ω^* must also be in the spectrum[36]. Hence, one needs to solve Eq. (6.17) with $\Re[\omega] \geq 0 \wedge \Im[\omega] \geq 0$. Note that the $\Im[\omega] > 0$ mode exhibits dynamical instability.

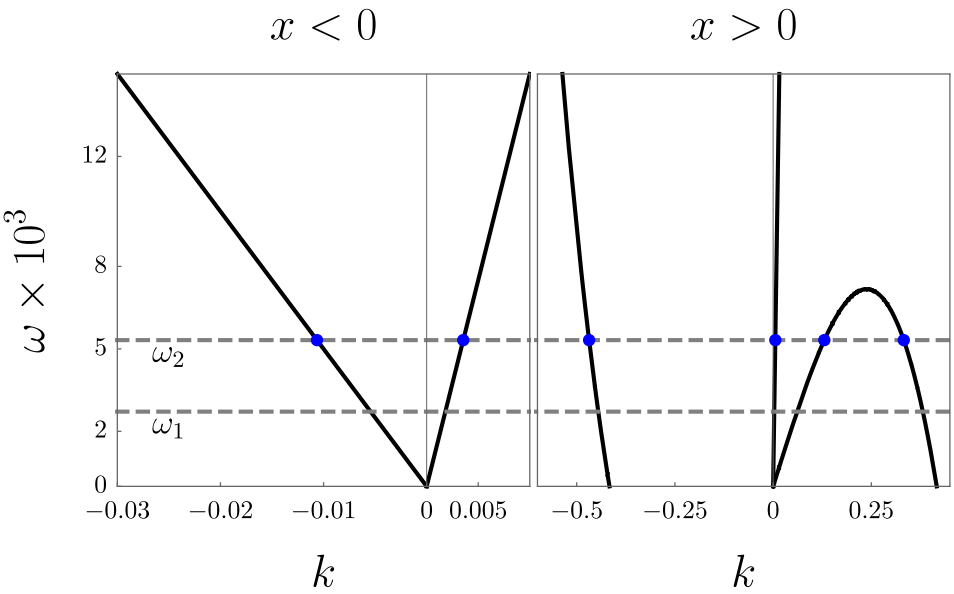

Figure 6.2 Bogoliubov dispersion relation $\omega = \omega(k)$. We set $\mathfrak{m}_\mathrm{u} = 0.5$, $\mathfrak{m}_\mathrm{d} = 1.1$, or $g_\mathrm{d}/g_\mathrm{u} \sim 0.2$. Left: Dispersion relation in the region $x < 0$. The grey dashed lines correspond to the eigenfrequencies within the plot range for a condensate with $-\ell_1/2 = \ell_2/2 = 60$. The blue points indicate the real solutions for k for ω_2. Right: Dispersion relation for the region $x > 0$. Because $\mathfrak{m}_\mathrm{d} > 1$, the negative branch of the dispersion relation presents a local maximum. We note that the field modes ω_1 and ω_2 are below this local maximum.

In each homogeneous region, one can use the plane wave form $\Phi_\omega = e^{ikx}\Phi_{\omega,k}$. And at the horizon ($x = 0$), the wave mechanics technique applied to Eq. (6.17) implies that Φ_ω and its first derivative are also continuous [13]. From Eq. (6.17), one can notice that the k must satisfy the Bogoliubov dispersion relation

$$(\omega - \mathfrak{m}_\mathrm{u})^2 = k^2\left(\frac{g}{g_\mathrm{u}} + \frac{k^2}{4}\right). \tag{6.19}$$

Because this is 4th order polynomial equation, we have 4 solutions for each ω which is shown in Fig. 6.2. For simplicity, p will denote the downstream wave

number instead of k. Then, the general solution for Φ_ω is

$$\Phi_\omega = \begin{cases} \sum_k s_k e^{ikx} \Phi_{\omega,k} & x < 0 \\ \sum_k s_p e^{ipx} \Phi_{\omega,p} & x > 0 \end{cases} \tag{6.20}$$

where constants s_k, s_p are the constants that can be obtained by solving the boundary conditions, and

$$\Phi_{\omega,k} = \begin{pmatrix} g/g_{\mathrm{u}} \\ \omega - \mathfrak{m}_{\mathrm{u}} k - k^2/2 - g/g_{\mathrm{u}} \end{pmatrix}. \tag{6.21}$$

In each ω, there are 8 boundary conditions total (4 from Dirichlet boundary condition, and 4 at $x = 0$ which comes from the continuity of Φ and $\partial_x \Phi$), and we have 8 unknowns s_p, s_k. In the scattering approach we let one of s_k(or s_p) to be nonzero. Hence, the 7 equations are used to determine the remaining unknowns, and the remaining one equation determines the ω in the system spectrum. Furthermore, because the system is finite-size and the equation is an analytic function of ω with s_k, s_p, k, p, the spectrum is discrete.

6.2 Black Hole Lifetimes

In the model, the Dirichlet boundary conditions show that the radiation of the Bogoliubov field is trapped in the two perfect mirrors. Therefore, the Hawking-like process also cannot radiate away infinitely and stays contained within the finite region, i.e., the condensate can be interpreted as a resonant cavity. In fact, resonance also occurs for the black hole-white hole pair[16]. They show black hole lasing effect comes from the resonance. But, it is also found that not all black hole-white hole pairs exhibit the black hole lasing effect, and are dynamically stable[21]. It is noteworthy that because of the complexity of black

hole-white hole analogues, the mechanisms leading to stabilization cannon in general be easily disentangled from one another [70, 30]. In the single black hole case in this study, one also has a similar interplay between the finite size and radiation process observed.

In a dynamically unstable case, a natural notion is the black hole's lifetime, which is determined by the instability time scale. The instability is investigated in the black hole-white hole configuration and also the dependence on system parameters. In this regard, the investigation was done in [21, 48, 47]. More recently, such an analysis has been pursued in [54] for a (more realistic) quasicondensate configuration. Because the background is condensate, the existence of a black hole is related to the time how long the condensate keeps in the same configuration or equivalently how long the Bogoliubov approximation holds. Therefore, by ensuring that the system starts from well-defined quantum fluctuations (e.g., by determining condensate depletion), the complex frequencies decide the black hole's lifetime. The analogue black hole lifetime is defined as

$$\tau := \min_{\omega\in\Sigma}(2\Im[\omega])^{-1} \tag{6.22}$$

where Σ is the set of mode frequencies ω with $\Im[\omega] \geq 0$. In the model, four parameters $\{\mathfrak{m}_{\rm u}, \mathfrak{m}_{\rm d}, \ell_1, \ell_2\}$ determines the black hole properties. One can investigate the black hole's lifetime with these 4 free parameters. In Fig. 6.3, the black hole lifetime is given as a function of $\mathfrak{m}_{\rm d}$ with fixed $\ell_1 = \ell_2 = 120$. For an infinite system $\ell_1 = \ell_2 \to \infty$, no dynamical instability exists, and the black hole lifetime is formally infinite, although of course the condensate is destroyed by phase fluctuations and is completely depleted [28]. Note that in the finite-size system, there is no monotonic behaviour. One can see from the

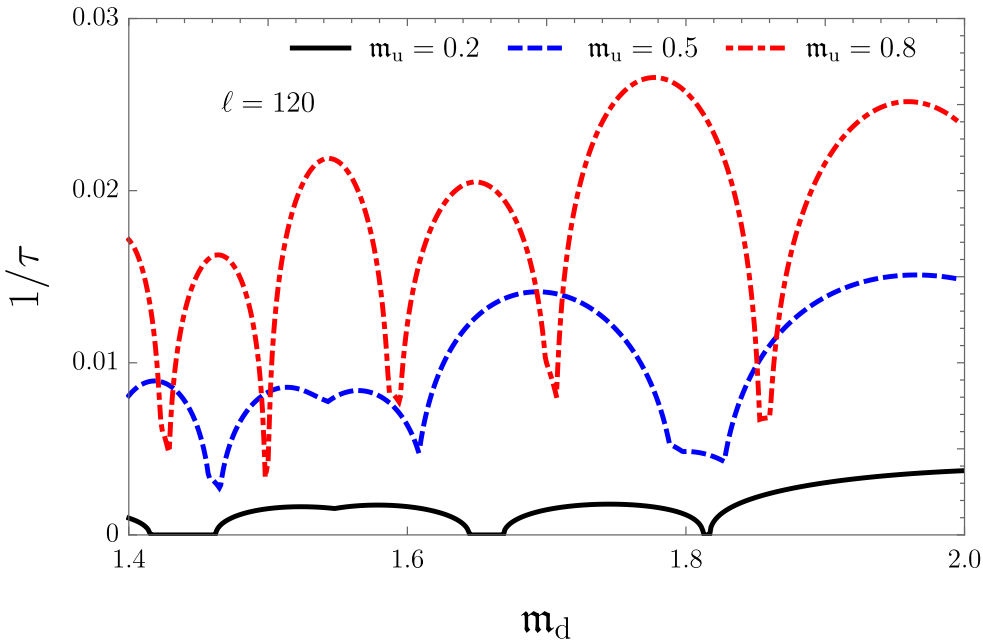

Figure 6.3 Black hole lifetimes as function of the downstream Mach number $\mathfrak{m}_d$ for several choices of $\mathfrak{m}_u$. Here we set $\ell = 120$. Notice that generally no monotonic behavior is observed. Moreover, the lifetimes diverge ($1/\tau = 0$) for $\mathfrak{m}_u = 0.2$ and some values of $\mathfrak{m}_d$, i.e., the black continuous curve then touches the $\mathfrak{m}_d$ axis.

figure that there are some parameter regimes that the $1/\tau$ curve that touches 0 which means that the black hole is stationary.

In Fig. (6.4), the black hole's lifetime with the system size is shown. Again, no clear functional dependence with the system parameters can be inferred, a feature also observed in the black hole-white hole calculations of [21, 48, 47, 54].

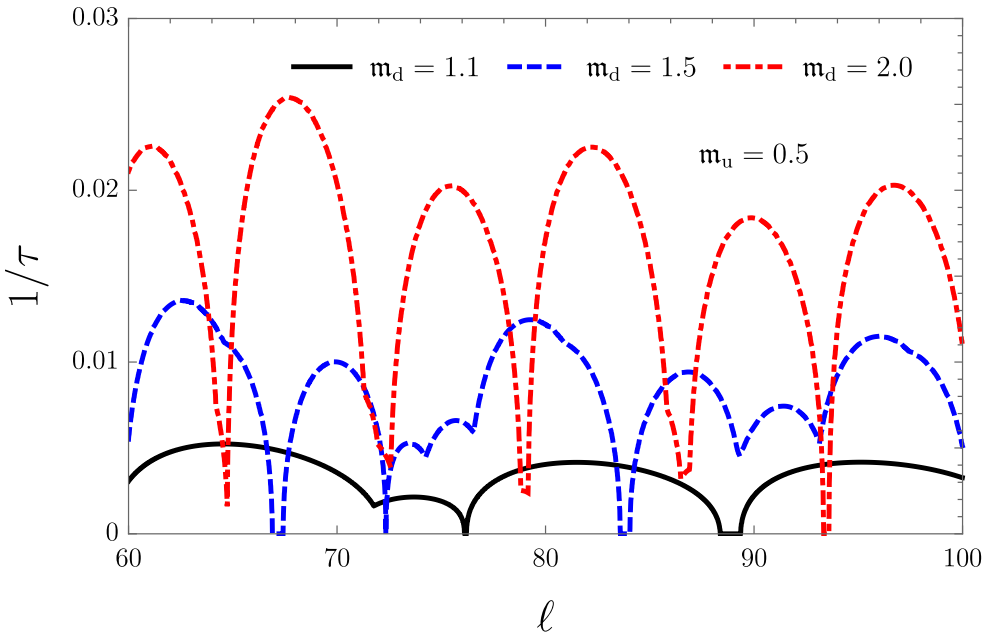

Figure 6.4 Black hole lifetimes as a function of the system size for the fixed upstream Mach number $\mathfrak{m}_\mathrm{u} = 0.5$ and several choices of $\mathfrak{m}_\mathrm{d}$. Similarly to what is observed in Fig. 6.4, there is no clear functional dependence of the lifetimes on the system size, and stability regions in the space of parameters exist.

6.3 Vacuum State with Instabilities and Black Hole Quenching

Field quantization in the presence of instabilities is a well-studied topic [36, 10, 60, 42, 41], and the canonical procedure also in such a case works in general. If there is no instability, one usually diagonalizes the Hamiltonian of the Bogoliubov field and defines vacuum to be $\langle\psi\rangle = 0$ The presence of instability precludes the choice of the preferred vacuum state[10]. Hence, it is not possible to find the vacuum state which allows a stationary state (eigenstate of $i\partial_t$) with a positive norm to span the field configuration. For infinitely extended 1D quasi-condensate analogue, the further details can be seen in

[45]. It is, however, possible to define the instantaneous vacuum state with complex eigenvalue states at a certain time $\langle\psi(t=0)\rangle = 0$. To understand more details about the instantaneous vacuum, let Ω, Ω^* be one of the complex frequency pairs in the spectrum, and the corresponding solution to be of the form $e^{-i\Omega t}\Phi_\Omega(x)$ and $e^{-i\Omega^* t}\Phi_{\Omega^*}(x)$, respectively, where $\Im[\Omega] \geq 0$. Because of the pseudoHermicity of the $H_{\rm BdG}$, one can show that both fields are zero norm fields, i.e., $(\Phi_\Omega, \Phi_\Omega)_{\sigma_3} = 0$. But, $(\Phi_\Omega, \Phi_{\Omega^*})_{\sigma_3} := \lambda e^{i\theta} \neq 0$, and we can define two orthogonal sets of fields by the linear combination as

$$\Phi^{(+)}_{\Omega,\alpha\beta} = \frac{\alpha}{\sqrt{\lambda}}\left[e^{-i\Omega t}\Phi_\Omega + \left(\frac{1}{2\alpha^2} + i\beta\right)e^{-i\theta - i\Omega^* t}\Phi_{\Omega^*}\right], \tag{6.23a}$$

$$\Phi^{(-)}_{\Omega,\alpha\beta} = \frac{\alpha}{\sqrt{\lambda}}\left[e^{-i\Omega t}\Phi_\Omega - \left(\frac{1}{2\alpha^2} - i\beta\right)e^{-i\theta - i\Omega^* t}\Phi_{\Omega^*}\right], \tag{6.23b}$$

for $\alpha > 0$ and $\beta \in \mathbb{R}$. The $(\pm)$ in the superscript denotes the sign of the norm explicitly, i.e., $(\Phi^{(+)}_{\Omega,\alpha\beta}, \Phi^{(+)}_{\Omega,\alpha\beta})_{\sigma_3} = 1 = -(\Phi^{(-)}_{\Omega,\alpha\beta}, \Phi^{(-)}_{\Omega,\alpha\beta})_{\sigma_3}$. If Ω is a pure imaginary number,i.e., $\Omega^* = -\Omega$, we can add $\Phi^{(+)}_{\Omega,\alpha\beta}$ and $\sigma_1\Phi^{(+)*}_{\Omega,\alpha\beta}$ as a positive-negative norm pair of field modes to the field expansion, whereas if $\Omega \in \mathbb{C}\setminus\mathbb{R}$, we must add $\Phi^{(+)}_{\Omega,\alpha\beta}, \sigma_1\Phi^{(-)*}_{\Omega,\alpha\beta}$ and the corresponding negative norm counterparts to the expansion. Note that any choice of pairs (α, β) does not affect the field norm, and all of them are equally acceptable as a basis of field expansion. Each choice, however, gives a distinct quantum field theory as one can see in the Bogoliubov transformation between different choices of (α, β). In particular, in principle, it is possible to have arbitrarily large depletion which makes our Bogoliubov approximation fails.

Black Hole Quenching— Because there is no preferred stationary vacuum state, one needs physical reasoning to choose the instantaneous vacuum. One of the elegant ways of choosing the vacuum state is the use of quenching the black

hole. Since the system is stationary before the formation of the supersonic region, one can start with fluid without a horizon, and make downstream supersonic at $t = 0$. For instance, in the system in this thesis, one can start with a configuration with the parameters such that $\mathfrak{m}_{\rm u}, \mathfrak{m}_{\rm d} < 1$ for $t < 0$. Then, at $t = 0$, by using the Feshbach resonance, one can tune the coupling at downstream $g_{\rm d}$ such that $\mathfrak{m}_{\rm d} > 1$ i.e., quench the black hole. As we work in the Heisenberg picture, the initial vacuum remains well-defined throughout the system's evolution. Specifically, the quantum field Φ has positive norm expansion in the region $t < 0$,

$$\Phi_n(t, x) = e^{-i\nu_n t}\Phi_{\nu_n} \tag{6.24}$$

where $\forall n : \nu_n > 0$. Because the black hole is quenched at $t = 0$, $\Phi_n(t = 0)$ can be represented as a linear combination of the complete set of field modes discussed such as

$$\Phi_n = \sum_{m=1}^{\infty}[\alpha_{n,m}e^{-i\omega_n t}\Phi_{\omega_m} + \beta_{n,m}e^{i\omega_m t}\sigma_1\Phi^*_{\omega_m}] + \sum_{j\in\Sigma_\Omega}\gamma_{n,j}e^{-i\Omega_j t}\Phi_{\Omega_j} \tag{6.25}$$

where Σ_Ω is the set of the complex frequency spectrum. Note that we do not have any discontinuity in time on the BdG equation. Hence, Φ is continuous about t, which amounts to the Fourier expansion

$$\sum_{m=1}^{\infty}[\alpha_{n,m}\Phi_{\omega_m} + \beta_{n,m}\sigma_1\Phi^*_{\omega_m}] + \sum_{j\in\Sigma_\Omega}\gamma_{n,j}\Phi_{\Omega_j} = \Phi_{\nu_n}. \tag{6.26}$$

Thus by using the orthonormality of the field mode, one can find the coefficients $\alpha_{n,m}, \beta_{n,m}$ and $\gamma_{n,j}$ uniquely so that the Bogoliubov field is fixed. By using this approach instead of instantaneous field quantization at the instability already existing, the vacuum state is defined to be the quasiparticle vacuum $a_n|0\rangle = 0$, which has a clear interpretation as it is uniquely defined.

6.4 Quantum Depletion and Validity of Bogoliubov Expansion

The quantum depletion in black hole configuration is defined as $\delta\rho = \langle\hat{\psi}^\dagger\hat{\psi}\rangle$. The interpretation of quantum depletion is that even at $T = 0$, a finite fraction of the condensed particles leave the condensate due to the inherent quantum fluctuations caused by the interaction of the particles constituting the system [58].

The depletion is the fundamental quantity that is necessary to validate the Bogoliubov expansion. The ratio between depleted particles and condensate particles should be small to make Bogoliubov expansion consistent. Different upper bounds for the Bogoliubov expansion applicability can be adopted, depending on the characteristics of each particular system. For instance, the simulations that follow are such that the largest number of depleted particles occurs near the analogue event horizon, roughly when (reinstating units for clarity) $\xi_{\mathrm{u}}\delta\rho \sim 2$. For a condensate which has $\xi_{\mathrm{u}}\rho \sim 60$, this corresponds to 3% of depleted particles near the event horizon. In the present work we fix by convention that the Bogoliubov theory predictions are considered to be accurate as long as depletion remains below 10%. From the mode expansion Eq. (6.16), one can write the depletion as

$$\delta\rho(t,x) = \sum_{n=1}^{\infty} |v_n(t,x)|^2 \tag{6.27}$$

Before the black hole formation— In Fig. 6.5, the depletion of the piecewise homogeneous flow with the parameters which does not exhibit the black hole is given with different system size. For simplicity, we use $\ell \equiv \ell_1 = \ell_2$, ad rescale x to fit the ends. The infrared (IR) logarithmic divergence is a well-known

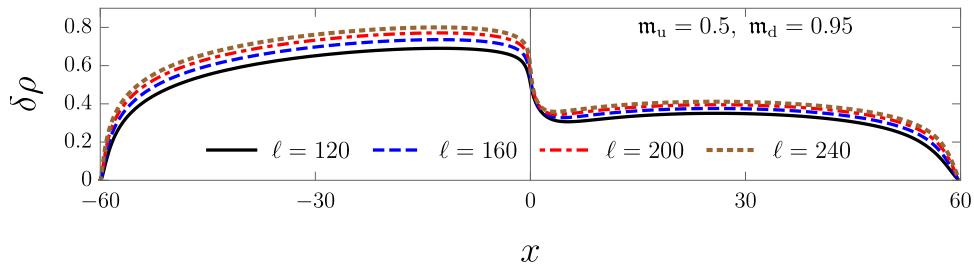

Figure 6.5 Quantum depletion for several condensate sizes in the absence of a black hole $\mathfrak{m}_d = 0.95$. Here, $\ell_1 = \ell_2$, and we recall that $\ell \equiv (\ell_2 + \ell_1)/2$. The curves are scaled in x to fit in the same plot. The effect of the system size is to increase the overall depletion logarithmically.

property of the infinite-size homogeneous system (see also for instance [33]). Hence, one expects the depletion increases with the system size. One can see the effect in Fig.6.5. Moreover, because $g_d < g_u$, the depletion in the downstream is smaller than the upstream. One can see that the depletion goes to zero at the boundary. This is just the result of Dirichlet boundary conditions at the boundaries. Note that because of the external flow which keeps the phase of the condensate, there is no zero mode, and this depletion is really constant not like in the homogeneous case without a source before.

Depletion of a Stationary Black Hole— When the black hole is formed, the depletion curves are qualitatively distinct, and let us consider the first quantum depletion in stationary (dynamically stable black hole configurations. In Fig. 6.6, depletion profiles for a fixed upstream Mach number $\mathfrak{m}_u = 0.5$ and different $\mathfrak{m}_d$ is given. The black and red, blue dotted lines correspond to the case that black hole is not formed. One can see that before the black hole is formed, the upstream configuration far from the horizon ($|x| \gg 1$) does not affect it at all. And the downstream depletion decreases when the $\mathfrak{m}_d$ increases, and the shape of it is almost the same. Hence, the depletion is indeed only

locally affected by the sound barrier: It is not possible to detect its presence by measurements of the depleted cloud if $|x| \gg 1$.

It is possible to directly correlate the imprint on the upstream depletion cloud far from the analogue event horizon to the Hawking-like radiation if we assume that the condensate is extremely elongated, by using, for instance, the field modes of [33]. Such a calculation, however, requires the use of frequency cutoffs to render depletion finite in our quasi-1D setup; such cutoffs can be inferred from our finite size model.

When the black is formed, the upstream depletion far from the horizon ($|x| \gg 1$) is also increased, and it can be interpreted that the Hawking-like radiation affects the upstream. And downstream, there are intricate patterns now. One can suspect the pattern downstream comes from the Bogoliubov-Čerenkov-Landau (BCL) radiation [7]. Recently, it is one of the popular signatures in analogue gravity experiments [31]. The BCL radiation is the zero frequency mode propagating away from the obstacle with respect to the obstacle frame[78], where the obstacle is downstream boundary $x = \ell_2/2$ in our system. But, because the external source and drain in the system keep the phase of the system to be sustained, there is no zero frequency mode in our system[8]. Hence, there is no BCL effect, and this pattern must be a new effect that comes from the horizon formation.

Depletion of an Unstable Black Hole— For the dynamically unstable black hole configuration, one needs to be more careful to make interpretations and experiments. Because depletion grows exponentially without restriction, it will continuously extract particles from the condensate, and the whole system will eventually go to a new configuration. Hence, a fully self-consistent backreaction analysis is required, but because the external source and drain break the

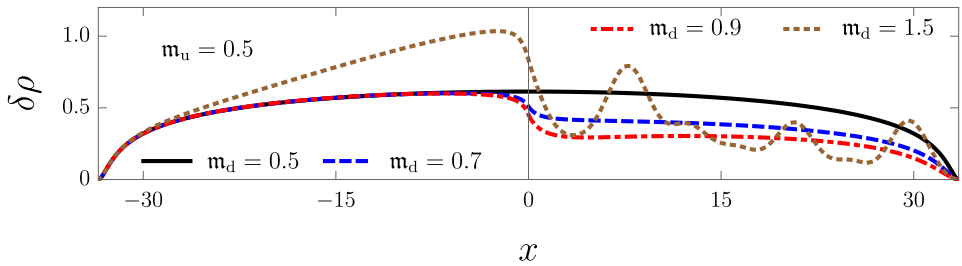

Figure 6.6 Several depletion profiles for fixed $\mathfrak{m}_u = 0.5$, and $\ell = 67$. The continuous black, dashed blue, and dot-dashed red curves correspond, respectively, to $\mathfrak{m}_d = 0.5$, $\mathfrak{m}_d = 0.7$, and $\mathfrak{m}_d = 0.9$, whereas the dotted brown curve depicts depletion for the stationary, stable configuration with $\mathfrak{m}_d = 1.5$. Deep into the upstream region we see that the sound barrier at $x = 0$ leaves no imprint in the black hole's absence, but as the analogue event horizon forms, the upstream noncondensed cloud changes due to the analogue black hole Hawking radiation. We also note the intricate depletion behavior at the downstream region after the black hole formation, which is in sharp distinction to the featureless depletion profile without the black hole.

$U(1)$ symmetry, one needs to be more careful in taking a number-conserving approach.

As discussed in Sec. 6.3, there is no stationary vacuum, and hence, one needs to specify the instance of quantization. In order to gain further insight, this thesis shall treat an explicit example. Consider the case $\mathfrak{m}_u = 0.5, \mathfrak{m}_d = 1.1$, and $\ell_1 = \ell_2 = 120$. It has six complex frequencies in the Bogoliubov spectrum, obtained from $\Omega_1 \sim i8 \times 10^{-4}$ and $\Omega_2 \sim (70.76 + 3i) \times 10^{-4}$. Therefore, from the discussion that leads to Eq. (6.23), we see that the space of possible choices for the system vacuum is parametrized by four real parameters, i.e., α and β for $\Omega_{1,2}$ each. Because the depletion is given as a mode sum, it can be split into time-dependent terms which come from the complex frequencies, and time-independent term $\delta\rho_s$ which is independent of the vacuum choice. Following the notation of Eqs.(6.16) and (6.23), the depletion is

$$\delta\rho = \delta\rho_s + |v^{(+)}_{\Omega_1,\alpha,\beta}|^2 + |v^{(+)}_{\Omega_2,\alpha',\beta'}|^2 + |u^{(+)}_{\Omega_2,\alpha',\beta'}|^2, \tag{6.28}$$

where $\alpha, \alpha' > 0$ and $\beta, \beta' \in \mathbb{R}$ are the arbitrary parameters we choose. This shows that the depletion will vary with time, and the Bogoliubov assumption breaks down. One can visualize this by counting the total number of depleted particles, $\delta N = \int \mathrm{d}x \delta\rho$, which in view of Eq. (6.28) splits into stable one and contribution from Ω_1, Ω_2 sectors. In Fig. 6.7, the contribution to the number of depleted particles in the Ω_2 sector, for different choices of α', β' is shown. Inspection of Fig. 6.7 reveals that depending on the parameters α', β', the predictions of Bogoliubov theory cannot be expected to be completely reliable. For instance, for a system with a total of 6000 particles, 1000 depleted particles correspond to 16% of the particles, not in the condensate. This is bigger than our small depletion criterion (10%), and the Bogoliubov expansion is not valid.

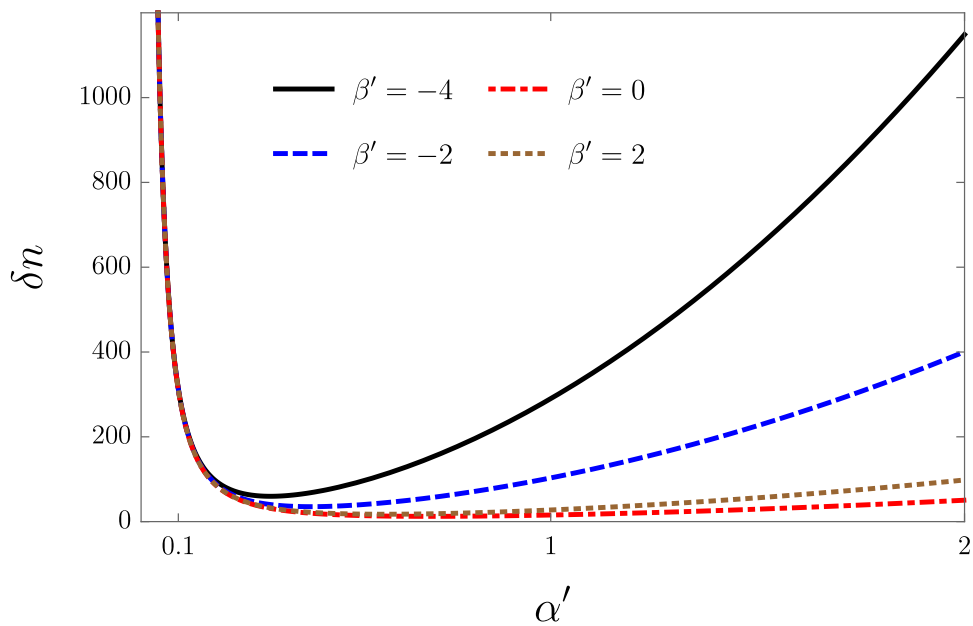

Figure 6.7 Quantum-depleted number of particles coming from different choices of instantaneous vacuum states for the sector Ω_2. System parameters are $\mathfrak{m}_{\mathrm{u}} = 0.5$, $\mathfrak{m}_{\mathrm{u}} = 1.1$, and $\ell = 120$.

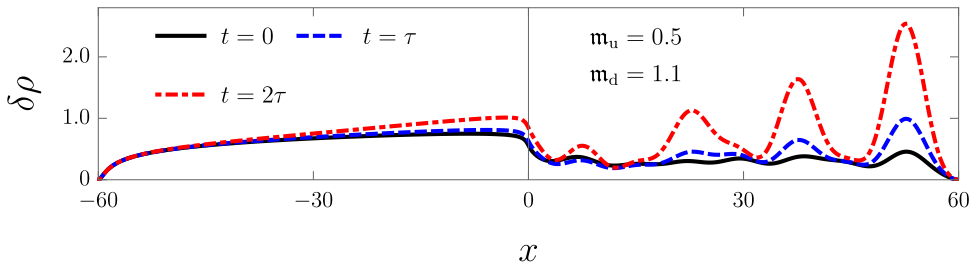

Figure 6.8 Depletion profiles as a function of time for a black hole characterized by $\mathfrak{m}_u = 0.5, \mathfrak{m}_d = 1.1$, and $\ell = 120$, with the system in its vacuum state of minimum depletion. Three major features are observed: Initially (black curve) the depletion profile inside the black hole does not resemble the stable curves of Fig. 6.5; as time passes, the number of depleted particles increases outside the black hole; an oscillatory pattern emerges inside the black hole. Here, the lifetime τ is defined in (6.22).

A regime of "Initially" large depletion corresponds to cases where the instability already played a relevant role, and de-stabilization processes are taking over the condensate evolution.

On the other hand, as the number of depleted particles is bounded below, there must be a vacuum state with the smallest depletion. Because each Ω_i contributions to the depletion are independent, one can find the smallest depletion vacuum by minimizing the number of depleted particles $\alpha, \alpha', \beta, \beta'$.

In Fig. 6.8, the evolution of depletion in time with the initial vacuum as a minimal depletion vacuum is shown. Note that at the initial time, the downstream is different from the stable black hole configuration, As time passes, the upstream depletion grows which can be interpreted as a Hawking-like process. And also note that there is an oscillatory pattern that arises downstream. In the theoretical approach, it is annoying that instability occurs, because the breaking of time translation symmetry makes one cannot use the approach to the asymptotic region, at late times. Moreover, the growth

of depletion means the condensate decrease, and our background is not the same as what one started. But, this is only of theoretical importance. In experimental realizations, the condensate and the black hole setting must have an initial value, which defines the system vacuum (and therefore the condensate) throughout its evolution. This is done by quenching the black hole configuration. In Fig. 6.9, the quenching of the unstable black hole configuration from the initially stable non-black hole configuration is shown. More precisely, the system with parameters $\ell_1 = \ell_2 = 120$, $\mathfrak{m}_{\rm u} = 0.5$ and $\mathfrak{m}_d = 0.95$ is prepared. At $t = 0$, the black hole is turned on by increasing the downstream Mach number to be $\mathfrak{m}_d = 1.1$ suddenly. By using Ref. [51] and its experimental parameters as a guide, and returning to dimensionful units, one can find $\tau \approx 8\,\mathrm{s}$ for a chemical potential of 70 Hz.

As advocated above, by starting from a truly stationary system in its uniquely defined quasiparticle vacuum, one can study the system evolution in a consistent and self-contained way when the Hawking process is switched on. In Fig. 6.9, the interference pattern downstream can be seen and there is a continuous increase in the overall number of depleted particles in the whole system. It is different from the non-black hole case (Fig. 6.5) since the depletion of downstream monotonously decreases when the $\mathfrak{m}_{\rm d}$ increases. This is just because the increase of $\mathfrak{m}_{\rm d}$ corresponds to a decrease of interaction strength $g_{\rm d}$. So, the interference pattern, and increase of downstream depletion is a clear notion of black hole formation. And in the upstream, the emergence of depletion is also the signal of the Hawking effect.

One can follow the ramp-up of the Hawking radiation with a better resolution by taking analogue models with higher downstream Mach numbers, which corresponds to stronger radiation[33]. In Fig. 6.10, the system with

$\mathfrak{m}_{\rm d} = 2$ is used keeping other parameters are the same with Fig. 6.9. Now, the lifetime is $\tau \sim 1\,\mathrm{s}$ for the experimental guiding parameters which are about ten times smaller than Fig. 6.9. Fig. 6.10 shows that, as the Hawking-like process is switched on, the cloud of depleted particles increases in a manner directly correlated to the radiated signal. One can see that the depletion growth propagates from the horizon. The increase makes the depletion break the small depleted ion assumption and finally, the Bogoliubov approximation does not hold.

Power spectrum of quantum depletion— Using the Bragg scattering, one can measure the momentum distribution of the particle. Denoting Fourier transform of depletion as $\tilde{\rho}(k) = \int \mathrm{d}x e^{-ikx}\rho(x)$, and simlarly, $\tilde{\delta\rho}(k) = \int \mathrm{d}x e^{-ikx}\delta\rho(x)$, Ref. [43] exploits the fact that in some configurations $\tilde{\rho}(k)$ decays faster for large k in comparison to the polynomial decay of $\tilde{\delta\rho}(k)$. In the previous homogeneous model, the condensate correction shows indistinguishable behaviour with the

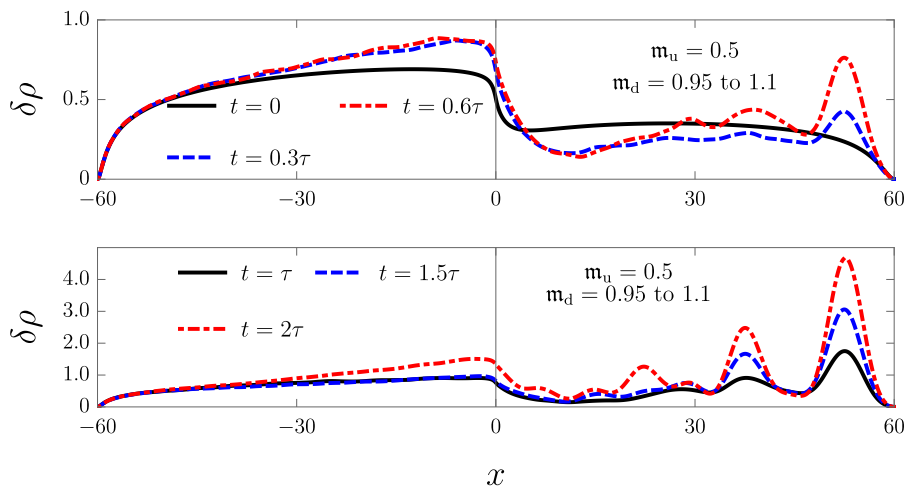

Figure 6.9 Several depletion profiles as a function of time for a quenched black hole. The system is set to have $\mathfrak{m}_{\rm u} = 0.5$, $\mathfrak{m}_{\rm d} = 0.95$, and $\ell = 120$ for $t < 0$, and we change $\mathfrak{m}_{\rm d} = 1.1$ after the quench at $t = 0$.

depletion. But if one suppresses the condensate correction, one obtains a large k window sensitive to the depletion. The interference pattern downstream suggests that there must be a peak in the power spectrum as time passes. In Fig. 6.11, the power spectrum of the black hole configuration for unstable/stable black hole configuration is shown.

Again, the interference pattern has no relation to BCL radiation, since there is no zero frequency mode in the obstacle frame, i.e., the LAB frame. One can see easily from the right panel which corresponds to the stable configuration, that the zero frequency mode is about $k \sim 0.75$. But one can see there is no peak in there. In the unstable configuration, it is more subtle. The zero frequency mode is $k \sim 0.42$ and it seems that there is such mode. But it is not

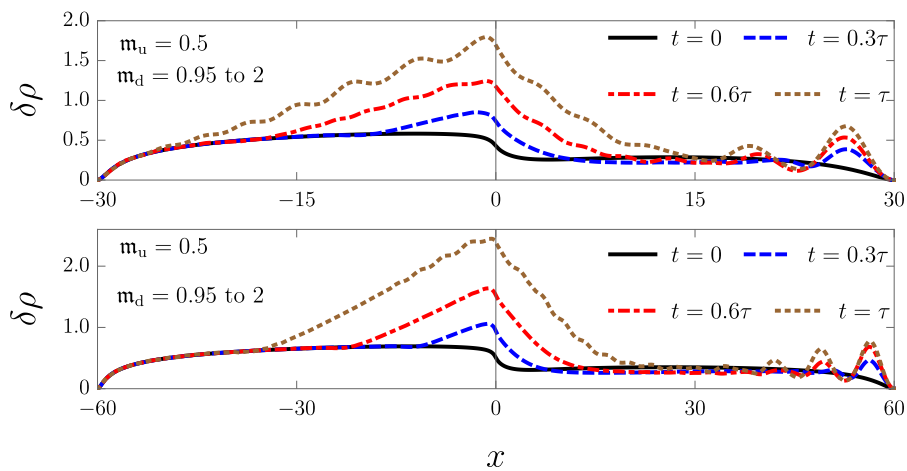

Figure 6.10 Quantum depletion for quenched black holes of different sizes. The black holes have $\mathfrak{m}_u = 0.5$, and the quench changes $\mathfrak{m}_d$ from 0.95 to 2 at $t = 0$. The increased downstream Mach number leads to a stronger radiation [33]. Upper panel: $\ell = 60$. Lower panel: $\ell = 120$. Both systems present similar depletion behavior, with the emergence of an oscillatory pattern inside the black hole, and the peculiar upstream-depleted cloud signal which forms at the analogue event horizon ($x = 0$) and then propagates against the condensate flow.

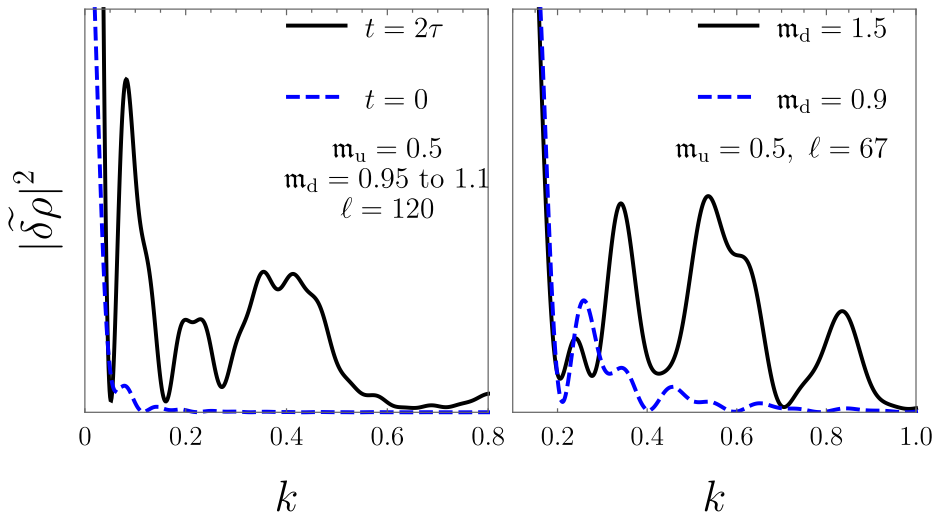

Figure 6.11 Power spectrum of the depletion profile for two black hole analogues. Left panel: The two curves represent the observed spectrum at different instants of time for an unstable black hole configuration, both at the beginning of the quench, and after a time $t = 2\tau$, for a black hole characterized by $\mathfrak{m}_u = 0.5$, $\ell = 120$, and $\mathfrak{m}_d = 0.95$ for $t < 0$, $\mathfrak{m}_d = 1.1$, $t > 0$. The black continuous curve shows the formation of a bump near $k \sim 0.4$, absent before the black hole forms, as indicated by the blue dashed curve. Right panel: Power spectrum for the stable black hole (continuous black curve) of Fig. 6.6. The blue dashed curve shows the power spectrum before the black hole formation.

valid, since it grows with time, hence, in fact, even though it has $\Re[k] \sim 0.42$, its imaginary part is nonzero, and it is not the zero frequency mode. Hence, it is also not related to BCL radiation at all.

In the many-body problem, elementary excitations often divide into two general types: 'quasi-particles' and 'collective excitations'[46]. Roughly, the fluctuations of density can be understood as a collective excitation. One may interpret the instability as collective excitations if higher-order interaction is considered. It is however beyond our analysis since we do not include higher than linearized fluctuation in this model.

6.5 Schiff-Snyder-Weinberg effect

In 1940, Schiff, Snyder, and Weinberg investigated the radial part of the Klein-Gordon equation with a static external electrostatic field with the simple step potential model. By varying the step size, they found the phenomenon that as the step size increases, two frequencies merges to one value and disappear, and then the two complex frequency arises[64]. Later, in 1976, Fulling investigate the same phenomenon with a one-dimensional box in a region [18] $x \in \{-L_-, L_+\}$. The Klein-Gordon equation is

$$[\omega_j - eA_0(x)]^2\phi_j(x) = (-\nabla^2 + m^2)\phi_j(x) \tag{6.29}$$

where the electrostatic potential is simple step potential

$$eA_0(x) = \begin{cases} -V & x \in]-L_-, 0[\\ 0 & x \in [0, L_+[. \end{cases} \tag{6.30}$$

He found that the same merging frequency phenomenon occurs, and calls this critical frequency the "singular mode". Moreover, if we increase the step size more the complex frequency disappears to revive the two real frequencies and this exchange of real to complex and vice versa occurs repeatedly. If the step size is higher than the first merging, the energy is unbounded below.

The Schiff-Snyder-Weinberg effect is the phenomenon that by varying the potential strength (system parameter), the *real frequencies (energy eigenvalues) merges to one value and then, the complex modes arise.* In cosmology, it is related to the rotating star. The role of the external electrostatic field is to decrease the mode frequency for the particle and increase (in the deep potential) the antiparticle mode frequency. The existence of singular mode implies that

the vacuum is no longer an isolated state but is degenerate with the state where the arbitrary particle-antiparticle pairs exist in a polarized way, i.e., the singular mode is the indicator for the transition to the instability [62].

Recently, it is shown that the mathematical structure of the Klein-Gordon equation with reinvestigated, and the Schiff-Snyder-Weinberg effect and quantization of this system is also suggested [44]. The Schiff-Snyder-Weinberg effect can be investigated in the BdG equation, in which apply the synthetic vector potential to make the equation of motion to be the same form with Eq. (6.29) [24]. In this section, the qualitative behaviour of the frequency behaviour on downstream Mach number is shown. In Fig. 6.12, the Schiff-Snyder-Weinberg effect occurs at $\mathfrak{m}_d = 1.1026$. In contrast to the case of [18], the two positive frequencies and two negative real frequencies merge in each. There is no mixing of positive and negative frequency, and there is pure imaginary frequency modes do not appear.

In Fig. 6.13, the Schiff-Snyder-Weinberg effect also occurs. In this case, the merging of two real frequencies occurs at zero to make two imaginary frequencies.

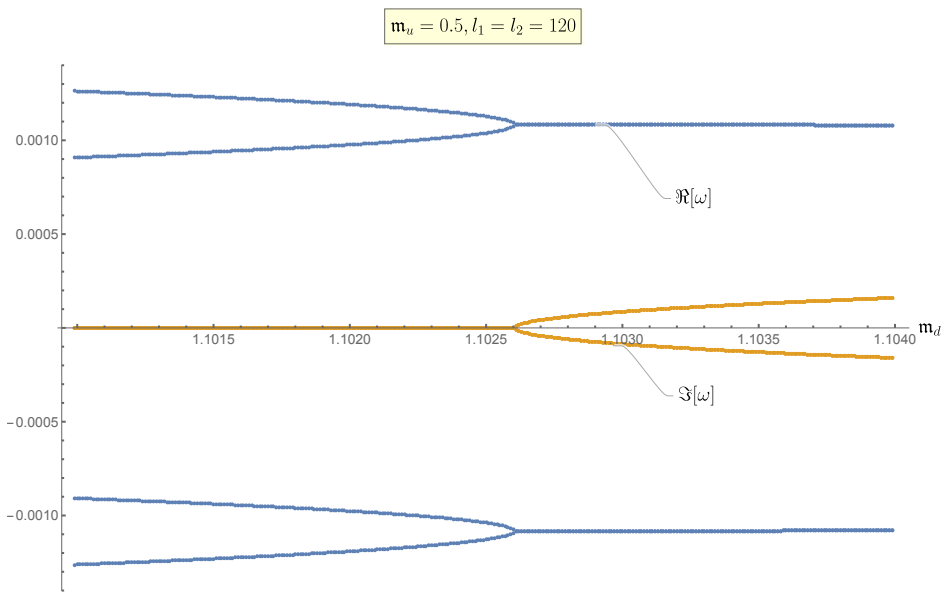

Figure 6.12 The lowest four frequencies as a function of $\mathfrak{m}_\mathrm{d}$ for fixed upstream Mach number $\mathfrak{m}_\mathrm{u} = 0.5$ and fixed system size $\ell_1 = \ell_2 = 120$. Singular mode occurs at $\mathfrak{m}_\mathrm{d} = 1.1026$. When $\mathfrak{m}_\mathrm{d} < 1.1026$, there are four real frequencies. When $\mathfrak{m}_\mathrm{d} > 1.1026$, there are four complex frequencies. The positive frequency mode does not go to the negative frequency mode.

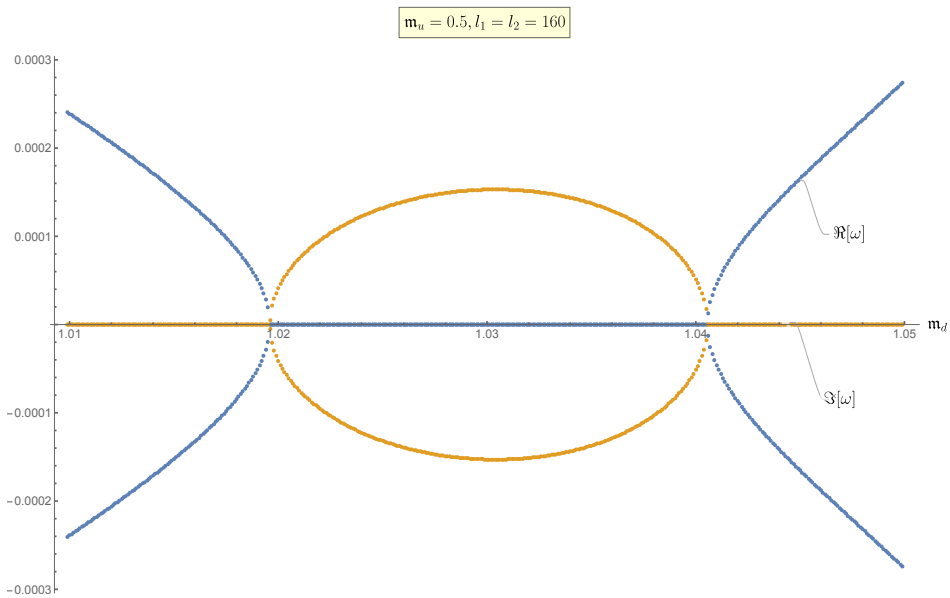

Figure 6.13 The lowest two mode frequencies for $\mathfrak{m}_\mathrm{u} = 0.5, \ell_1 = \ell_2 = 160$ as a function of $\mathfrak{m}_\mathrm{d}$. Singular mode occurs slightly below $\mathfrak{m}_\mathrm{d} = 1.02$. In this case, the merging occurs between positive and negative modes. Both frequencies approach zero to meet. They split to form real frequency again slightly above $\mathfrak{m}_\mathrm{d} = 1.04$. Note that, unlike Fulling's case, the split occurs at zero, and the positive norm and negative norm are separated.

7 Conclusion

The quantum backreaction force is shown to denote the departure from Eulerian classical hydrodynamics due to the quantum fluctuations. In the most general cases, it can be written solely in terms of quantities that have direct interpretation: The quantum depletion, the phonon flux, the leading and subleading order condensate density fluctuations, and two-point correlation functions. Furthermore, a discussion regarding the proper construction of the Cauchy problem for the backreaction analysis, and its relation with condensate preparation at an experimental level is presented.

Two finite-size Bose-Einstein condensate systems as an analogue model are investigated in this thesis. Both systems are simple and can be realized in the tabletop experiment at least approximately in near future. It is important not only because it is experimental realizable, but also because one can have a finite number of depletion to make it possible to check the validity of the Bogoliubov approximation. In analogue gravity language, a uniform finite size condensate system corresponds to the bounded homogeneous flat $(1 + 1)$-dimensional universe. On the other hand, flowing condensate with the sonic horizon, where the flow speed exceeds the sound speed, is the $(1 + 1)$-dimensional black hole. The supersonic region (downstream) is inside the black hole horizon, and the subsonic region (upstream) is outside of the horizon.

The homogeneous uniform density condensate serves the exact analytic solution. In regarding backreaction in BECs, phase diffusion plays a prominent role. Indeed, the existence of finite size interacting quasi-1D BEC is associated with the continuous decrease of the off-diagonal long-range-order, which in particular implies that the system is not stationary Accordingly, because the classical background (condensate) spontaneously degrades, one needs to specify the initial configuration of the Bose gas. In this thesis, by assuming the system starts with the noninteracting regime, the system is indeed stationary and can be taken to reside in its ground state. The interacting regime can be assessed by driving the system out of equilibrium. It is discussed that it is not possible, at least in our model, that the depletion cannot be distinguished from the condensate correction by using the existing power spectrum measurement technique. Furthermore, even though the condensate is initially at rest, backreaction from the quantum fluctuations gives rise to a condensate current. The induced current is governed by the total force which comes from the gradient of the total potential function. Also, for the condensate at rest, the classical Eulerian force in working order (N^0) is determined solely in the density $\rho = \rho_0 + \rho_\chi + \rho_\zeta$ which can be probed in the experiment. By comparing the total and classical force, one can conclude that the quantum force attenuates the classical force a lot near the condensate walls.

An immediate application of the present approach is furnished by considering its consequences in analogue gravity say for the backreaction of the emitted Hawking radiation onto the condensate background. It is also noteworthy that the connection that classical backreaction has already been studied experimentally in shallow water tanks.

In the 1D finite piecewise uniform flowing condensate model, there is a single event horizon. In the model, not like in the uniform condensate at rest model, Dirichlet boundary conditions are adopted for the condensate walls so that not only the condensate but also the fluctuations vanishes there. It is also better suited for experimental realizations since the condensate is confined in the trapping potential along its symmetry axis.

Two distinct signatures of the Hawking process emerge when the event horizon forms. The first one is the appearance of the oscillatory pattern in the depletion cloud inside the black hole which translates to distinct peaks in its power spectrum. The pattern is a new effect which is not related to the famous BCL radiation. The second one is the increase of the depletion outside of the horizon. The depletion increase is linked to radiation emitted by the black hole. More precisely, the local depletion at a region outside the black hole starts to increase as the radiation reaches that region. This represents the novel signature of Hawking radiation.

The existence of finite-size-induced dynamical instabilities is discussed. If the Bogoliubov field is not carefully quantized, the theory can represent the strong depletion which renders the Bogoliubov expansion inconsistent. The model used in this thesis evades this problem by employing a quenching from a stationary configuration in its quasiparticle vacuum to the black hole configuration. Hence, one can simulate the evolution of the depletion cloud where the instability is onset. The qualitative comparison between the Schiff-Snyder-Weinberg effect and the dynamical instability in the analogue finite-size black hole is also given.

8 Appendix

8.1 The Mathematical Structure of Spacetime

In this section, the mathematical structure of spacetime in general relativity is summarized [65, 76, 14, 6, 27]. The set is the collection of objects which satisfies the set-theoretic axiom. Let M be a set whose element is all the spacetime points and its union. Thus one can say that some points are in spacetime or not. But in classical physics, one wants to talk about more than just single points. One of the main objects in classical mechanics is the trajectory of particles (curve). The structure on a set is just another set in M which gives the relation between objects in M. When one thinks about the curve, it must be continuous in some interval. Hence, one needs a structure which can define continuity. It is called the topology. The topology is a collection of sets $\mathcal{O}$ which satisfies 3 properties.

Definition 8.1 Let M be a set. If the set $\mathcal{O}$ satisfies

(a) The empty set and the entire set is an element, i.e., $\varnothing, M \in \mathcal{O}$;

(b) Pairwise intersection of elements is an element i.e., $\forall u, v \in \mathcal{O} \implies u \cap v \in \mathcal{O}$;

(c) Arbitrary union on elements is an element i.e., $\forall i \in I : u_i \in \mathcal{O} \implies \bigcup_{i \in I} u_i \in \mathcal{O}$,

$\mathcal{O}$ is called a *topology* on M. The tuple $(M, \mathcal{O})$ is called a *topological space*.

Now, one can talk about the trajectory of particles. It is, however, not easy to treat the curve itself. Fortunately, thanks to the equivalence principle, the space is locally flat.

Definition 8.2 A topological space $(M, \mathcal{O})$ is *locally Euclidean of dimension* n if

$$\forall p \in M : \quad \exists U \in \mathcal{O} : \quad \exists x : U \to \mathbb{R}^n$$

where $p \in U$ and φ is the homeomorphism. The pair (U, x) is called a *chart*, U is called a *coordinate neighborhood*, and x is called a *coordinate map (or coordinate system) on* U.

And one can now use the coordinate system to describe the position of spacetime in a given chart. The locally-Euclidean space is called a manifold. But it contains many pathological spaces and is not so useful in describing our universe. Hence, we apply further topological conditions to the manifold, and think of it as a definition of topological manifold [71]

Definition 8.3 A *topological manifold of dimension* n is a Hausdorff, second countable, locally Euclidean space of dimension n.

Now one can describe the curve using the coordinate system in each chart. Let the curve $\gamma : I \subset \mathbb{R} \to U \subset M$. Using the chart, one can define the differentiability of the curve on the coordinate system just using undergraduate calculus. More precisely, $x \circ \gamma : \mathbb{R} \to \mathbb{R}^n$ by $t \mapsto x \circ \gamma(t)$ can be differentiated by t in elementary calculus. But, the differentiability of one chart does not guarantee the differentiability of the other chart. Hence, it means that nature knows what coordinate one uses. It is weird to accept. So, one defines the compatibility of the chart.

Definition 8.4 Two charts (U, x) and (V, y) on a topological manifold are called C^k-*compatible* if two maps $y \circ x^{-1} : x(U \cap V) \to y(U \cap V)$ and $x \circ y^{-1} : y(U \cap V) \to x(U \cap V)$ are both k times differentiable.

The collection of charts that covers the total manifold M is called an *atlas* $\mathcal{A}$. If each of the charts in the atlas $\mathcal{A}_k$ is C^k-compatible, it is called C^k-*atlas*. The maximal atlas is an atlas which is not contained in any other and is called an *maximal atlas* or a *differential structure*. In physics, one usually treats the C^∞ curve. Fortunately, there is a theorem by Whitney

Theorem 8.1 (Whitney) *Any $C^{k>1}$-atlas $\mathcal{A}_k$ contains a C^∞-atlas $\mathcal{A}_\infty$.*

Hence, one can always pick C^∞-atlas from any C^k differential structure. Hence, it is common to consider only the C^∞-atlas $\mathcal{A}_\infty$, and from now I will drop the subscript ∞ in the atlas.

Definition 8.5 A triple $(M, \mathcal{O}, \mathcal{A})$ is called a *smooth manifold (or C^∞-manifold)*.

Now one has the well-defined notion of differentiation of the curve. By using it, one can define the velocity of the curve. Note that the manifold does not have a vector space structure. Hence, one cannot define the velocity like in the undergraduate time i.e., a difference between two positions (which is ill-defined) divided by time. What one can define now is only the velocity at a given point.

Definition 8.6 Let $(M, \mathcal{O}, \mathcal{A})$ be a smooth manifold and the curve $\gamma : \mathbb{R} \to M$ be at least C^1. Suppose $\gamma(\lambda_0) = p$. The *velocity* of γ at p is the linear map

$$v_{\gamma,p} : C^\infty(M) \to \mathbb{R}.$$

The tangent space at the point p, T_pM is the collection of all tangent vectors at p.[1] One can easily check that the tangent space is the vector space. One of the astonishing points is that the dimension of the velocity is not (Length$\times$Time) but only Time^{-1} For calculation, it is worth showing the components in the specific chart. Let the chart $(U, x) \in \mathcal{A}$ and curve to be $\gamma : \mathbb{R} \to U$ with $\gamma(0) = p$. Then, $\forall f \in C^\infty(M)$,

$$\begin{aligned} v_{\gamma,p}(f) &= (f \circ \gamma)'(0) \\ &= \big((f \circ x^{-1}) \circ (x \circ \gamma)\big)'(0) \\ &= (x^i \circ \gamma)'(0)\big(\partial_i (f \circ x^{-1})\big)(x(p)) \\ &= \dot{\gamma}^i_x(0) \left.\frac{\partial}{\partial x^i}\right|_p f \end{aligned}$$

The $\dot{\gamma}^i_x(0)$ is called the component and $\left.\frac{\partial}{\partial x^i}\right|_p$ is called the coordinate basis of the velocity. Now one knows the derivatives at one point, and because the T_pM is vector space, one can also add or subtract the velocities at p.

But our spacetime is not the one point. And the most important dynamical variable in modern physics is the fields. To define the field, one derives the structure called bundle[34].

Definition 8.7 Let E, M be a manifold and $\pi : E \to M$ be a surjective map. The triple $(E, M, \pi : E \to M)$ is called the *vector bundle* if they satisfy

(a) Each set $E_p := \pi^{-1}(p)$ (called the *fiber* of E over p) is endowed with the structure of a vector space.

(b) For each $p \in M : \exists U$ which is open neighborhood of p and $\exists$ a diffeomorphism $\varphi : \pi^{-1}(U) \to U \times \mathbb{R}^k$ called a *local trivialization* of E, such that

[1] There is another definition of tangent vectors and space using the derivation at the point p. It is equivalent to the definition given here.

the following diagram commutes:

$$\begin{array}{ccc} \pi^{-1}(U) & \xrightarrow{\quad\varphi\quad} & U \times \mathbb{R}^k \\ & {\scriptstyle\pi}\searrow \quad \swarrow{\scriptstyle\pi_1} & \\ & U & \end{array}$$

where π_1 is the projection onto the first factor.

(c) The restriction of φ to each fiber. $\varphi : E_p \to p \times \mathbb{R}^k$, is a linear isomorphism.

One calls E the *total space*, M the *base manifold*, and π the *projection*.

The bundle structure allows one to extend the concept of continuous (topology) from the base manifold to the total space. The field in physics is called a section of the bundle.

Definition 8.8 If $\pi : E \to M$ is a vector bundle over M, a *section* of E is a map $F : M \to E$ such that $\pi \circ F = \mathrm{id}_M$ (identity in M).

The bundle structure allows one to extend the smoothness of the manifold to the smoothness of the section i.e., fields. Because the tangent space is also a vector space, one can define the bundle so-called the *tangent bundle* TM with it.

$$TM := T(M) := \dot{\bigcup_{p \in M}} T_p M$$

where $\dot{\bigcup}$ is the disjoint union. Note that the TM is also a manifold. Hence, one can define higher-order tangent bundles by a repeated process such as $TTM = T(TM)$.

Until now, the (tangent) vectors in each point, and the smooth vector field as a smooth section are defined in the manifold structure. There is, however, no way to compare the vectors at different points in the manifold. Especially, if one wants to differentiate the sections independent of the chart. The *connection*

in the TTM gives the way to differentiate the sections independently on the chart.

Definition 8.9 Let $\pi : E \to M$ be a vector bundle, $\mathcal{T}(M)$ be a smooth sections of TM, and $\mathcal{E}(M)$ be a space of sections on E. A *connection* in E is a map

$$\nabla : \mathcal{T}(M) \times \mathcal{E}(M) \to \mathcal{E}(M) \qquad \text{by } (X, Y) \mapsto \nabla_X Y$$

satisfying the following properties:

(a) For $f, g \in C^\infty(M) : \nabla_{fX_1+gX_2} Y = f\nabla_{X_1} Y + g\nabla_{X_2} Y$;

(b) For $a, b \in \mathbb{R} : \nabla_X(aY_1 + bY_2) = a\nabla_X Y_1 + b\nabla_X Y_2$;

(c) For $f \in C^\infty(M) : \nabla_X(fY) = f\nabla_X Y + (Xf)Y$.

A *linear connection* is just a restriction of Koszul connection.

$$\nabla : \mathcal{T}(M) \times \mathcal{T}(M) \to \mathcal{T}(M).$$

One of the most famous symbols related to the connection is the Christoffel symbol.

Definition 8.10 Let $\{E_i\}$ be a local frame i.e., $\{E_i|_p\}$ forms a basis for T_pM in each point p in an open set U. Since

$$\nabla_{E_j} E_i := \Gamma_{ij}^k E_k,$$

one calls Γ_{ij}^k the *Christoffel symbol (or connection coefficient).*

In a manifold with connection i.e., $(M, \mathcal{O}, \mathcal{A}, \nabla)$, one can tell how to move the vectors along a smooth curve in a certain way.

Definition 8.11 A vector field X is said to be *parallel transported* if $\nabla_{v_\gamma} X = 0$. Especially, if the X is v_γ itself, the equation $\nabla_{v_\gamma} v_\gamma$ is called an *auto-parallel equation.*

One can also define tensors using the connection ∇

Definition 8.12 In $(M, \mathcal{O}, \mathcal{A}, \nabla)$, a map

$$\begin{aligned} T :& \mathcal{T}(M) \times \mathcal{T}(M) \to \mathcal{T}(M) \\ & (X, Y) \mapsto T(X, Y) = \nabla_X Y - \nabla_Y X - [X, Y] \end{aligned}$$

is a $(2, 1)$-tensor field called a *torsion.*

The torsion is assumed zero in the usual theory of general relativity texts and one says in that case that spacetime is torsion-free. In this thesis, spacetime is also treated as torsion-free. Another tensor one can define with the connection is the (Riemann) curvature tensor.

Definition 8.13 In $(M, \mathcal{O}, \mathcal{A}, \nabla)$, a map

$$\begin{aligned} R :& \mathcal{T}(M) \times \mathcal{T}(M) \times \mathcal{T}(M) \to \mathcal{T}(M) \\ & (X, Y, Z) \mapsto R(X, Y)Z = \nabla_X \nabla_Y Z - \nabla_Y \nabla_X Z - \nabla_{[X,Y]} Z \end{aligned}$$

is a $(3, 1)$-tensor field called the *(Riemann) curvature endomorphism.*

Until now, the length of the vector is not defined. The length of the vectors can be determined by the metric tensor.

Definition 8.14 A *metric* on a smooth manifold $(M, \mathcal{O}, \mathcal{A})$ is a 2-tensor field g i.e., at each point $p \in M$ and $X, Y \in \mathcal{T}(M) : g(X, Y)(p) := g|_p(X|_p, Y|_p)$, satisfying

(a) Symmetric : $g(X,Y) = g(Y,X)$.

(b) Nondegenerate : $\forall 0 \neq Y|_p \in T_pM : \exists X|_p \in T_pM : g(X,Y)(p) \neq 0$.

Using the metric, one can define the speed of a particle at $p \in M$ as $\sqrt{g(v,v)(p)}$. The arc length of a curve γ (or the distance of the trajectory of a particle) L is defined as

$$L := \int \mathrm{d}\lambda \sqrt{g(v_\gamma, v_\gamma)(\lambda)} \tag{8.1}$$

where λ is a parameter for the curve. The geodesic is the curve that the length is extremum i.e., $\delta L = 0$. One must note that the manifold does not have a vector space structure, and the concept of position vector or displacement vector in our spacetime is an ill-defined concept. But, with metric, one can define the distance by the length of the curve by the above definition.

The metric is an independent structure with a connection. But, one can choose a unique linear connection from the metric if the connection is torsion-free and compatible with the metric g.

Definition 8.15 In $(M, \mathcal{O}, \mathcal{A}, \nabla, g)$, the linear connection ∇ is called *metric compatible* if for $X, Y, Z \in \mathcal{T}(M) : \nabla_X g(Y,Z) = g(\nabla Y, Z) + g(Y, \nabla Z)$, or eqivalently $\nabla g = 0$.

In this thesis, the connection is always chosen to be metric-compatible. In the metric compatible connection, the auto-parallel equation becomes the geodesic equation in a given chart i.e., in chart map x, the geodesic equation for curve γ in coordinate basis $\{\frac{\partial}{\partial x^c}\}$ is

$$0 = \nabla_{v_\gamma} v_\gamma = \left(\ddot{\gamma}^c_{(x)} + \Gamma^c_{(x)\,ab} \dot{\gamma}^a_{(x)} \dot{\gamma}^b_{(x)}\right) \frac{\partial}{\partial x^c}$$

where the subscript (x) is used to denote the chart clearly, and $\dot{\gamma} \equiv \frac{\mathrm{d}}{\mathrm{d}\lambda}\gamma(\lambda)$. Similarly, the components of the torsion tensor are

$$T^c_{ab} := T\left(\mathrm{d}x^i, \frac{\partial}{\partial x^a}, \frac{\partial}{\partial x^b}\right) = \Gamma^c_{ab} - \Gamma^c_{ba}. \tag{8.2}$$

And the torsion-free condition is just the symmetry of the subscript in the Christoffel symbol in the coordinate chart. One can also define the components of curvature endomorphism in the same way. Moreover, with metric, one can define the (Riemann) curvature tensor

Definition 8.16 The *(Riemannian) curvature tensor* is a covariant 4-tensor $Rm := R^\flat$ which is

$$Rm(X, Y, Z, W) = g\big(R(x, Y)Z, W\big).$$

Its component in coordinate basis is

$$R_{abcd} := Rm\left(\frac{\partial}{\partial x^a}, \frac{\partial}{\partial x^b}, \frac{\partial}{\partial x^c}, \frac{\partial}{\partial x^d}\right) = g_{af}\left(\frac{\partial}{\partial x^b}\Gamma^f_{cd} - \frac{\partial}{\partial x^c}\Gamma^f_{bd} + \Gamma^e_{bd}\Gamma^f_{ce} - \Gamma^e_{cd}\Gamma^f_{be}\right) \tag{8.3}$$

8.2 Calculation Details for f_{q}

In this thesis, I show only 1D quantum backreaction force. But, one can show the more general 3D dimensional expression for $f_{\mathrm{q,3D}}$. Within the Thomas-Fermi (TF) approximation, it is given in the paper [68]. I show detailed derivation for general $f_{\mathrm{q,3D}}$ here. By definition, the quantum backreaction is

$$\begin{aligned} f_{\mathrm{q,3D}} &:= \frac{\partial}{\partial t} J(\hat{\Psi}, \hat{\Psi}^\dagger) - f(J, \rho) \\ &= \frac{1}{4m^2}\left\langle \hat{\chi}^\dagger \nabla^3 \hat{\chi} - (\nabla^2 \hat{\chi}^\dagger)\nabla\hat{\chi} + H.C. \right\rangle - \frac{1}{m}\langle \hat{\chi}^\dagger \hat{\chi}\rangle \nabla U \end{aligned}$$

$$-\frac{1}{2gm}\nabla\left(g^2\langle\phi_c^2\hat{\chi}^{\dagger 2}+\phi_c^{*2}\hat{\chi}^2+4|\phi_c|^2\hat{\chi}^\dagger\hat{\chi}\rangle\right)$$
$$-\left\{-\nabla\cdot[\rho v\otimes v]-\frac{\rho}{m}\nabla\left[-\frac{\nabla^2\sqrt{\rho}}{2m\sqrt{\rho}}+U+g\rho\right]\right\}\Bigg|_\chi+\mathcal{O}\left(\frac{1}{\sqrt{N}}\right) \tag{8.4}$$

where $v := J/\rho$, and $|_\chi$ in the last line means that they contain only terms which contain ρ_χ, J_χ contributions. Because $\rho_\chi = \langle\hat{\chi}^\dagger\hat{\chi}\rangle$, the terms containing U is exactly canceled. Hence, the external potential does not affect the $f_{\mathrm{q,3D}}$ directly, and if we know all the field variables exactly, we do not need to calculate them.

The first term in the last line is

$$\nabla\cdot[\rho v\otimes v]\big|_\chi=\nabla\cdot\left[\frac{J\otimes J}{\rho}\right]\Bigg|_\chi=\nabla\cdot[J_\chi\otimes v_c+v_c\otimes J_\chi-\rho_\chi v_c\otimes v_c]+\mathcal{O}\left(\frac{1}{\sqrt{N}}\right) \tag{8.5}$$

It is easy to expand the last term in the last line

$$\rho\nabla(g\rho)=\rho_c\nabla(g\rho_\chi)+\rho_\chi\nabla(g\rho_c)=\frac{1}{g}\nabla(g^2\rho_\chi\rho_c). \tag{8.6}$$

And

$$\rho\nabla\left[\frac{1}{2}\frac{\nabla^2\sqrt{\rho}}{\sqrt{\rho}}\right]=\rho_\chi\nabla\left[\frac{1}{2}\frac{\nabla^2\sqrt{\rho_c}}{\sqrt{\rho_c}}\right]+\frac{\rho_c}{4}\nabla\left[\frac{1}{2}\frac{1}{\sqrt{\rho_c}}\nabla^2\left(\frac{\rho_\chi}{\sqrt{\rho_c}}\right)-\frac{\rho_\chi}{\rho_c^{3/2}}\nabla^2\sqrt{\rho_c}\right] \tag{8.7}$$

By substituting Eq. (8.5), Eq. (8.6), and Eq. (8.7) to Eq. (8.4), one gets

$$f_{\mathrm{q,3D}}=\nabla\cdot[J_\chi\otimes v_c+v_c\otimes J_\chi-\rho_\chi v_c\otimes v_c]-\frac{1}{2gm}\nabla\left(g^2\langle\phi_c^2\hat{\chi}^{\dagger 2}+\phi_c^{*2}\hat{\chi}^2+2|\phi_c|^2\hat{\chi}^\dagger\hat{\chi}\rangle\right)$$
$$-\frac{\rho_\chi}{m}\nabla\left[\frac{\nabla^2\sqrt{\rho_c}}{2m\sqrt{\rho_c}}\right]-\frac{\rho_c}{4m^2}\nabla\left[\frac{1}{\sqrt{\rho_c}}\nabla^2\left(\frac{\rho_\chi}{\sqrt{\rho_c}}\right)-\frac{\rho_\chi}{\rho_c^{3/2}}\nabla^2\sqrt{\rho_c}\right]$$
$$+\frac{1}{4m^2}\left\langle\hat{\chi}^\dagger\nabla^3\hat{\chi}-(\nabla^2\hat{\chi}^\dagger)\nabla\hat{\chi}+H.C.\right\rangle+\mathcal{O}\left(\frac{1}{\sqrt{N}}\right) \tag{8.8}$$

It is interesting enough, but one can go further to make a similar form in the [68]. Note that

$$\rho_c\nabla\left[\frac{1}{\sqrt{\rho_c}}\nabla^2\left(\frac{\rho_\chi}{\sqrt{\rho_c}}\right)\right]=\nabla^3\rho_\chi+\rho_c\nabla\left[\frac{\rho_\chi}{\sqrt{\rho_c}}\nabla^2\left(\frac{1}{\sqrt{\rho_c}}\right)-\frac{1}{2\rho_c}(\nabla\rho_c)\cdot(\nabla\rho_\chi)\right] \tag{8.9}$$

Direct calculation gives

$$\nabla^3\rho_\chi=\langle\hat{\chi}^\dagger\nabla^3\hat{\chi}+(\nabla^2\hat{\chi}^\dagger)\nabla\hat{\chi}+2(\nabla\hat{\chi}^\dagger)\cdot(\nabla\otimes\nabla\hat{\chi})+H.C.\rangle \tag{8.10}$$

Hence,

$$\begin{aligned}\frac{1}{4}\left\langle\hat{\chi}^\dagger\nabla^3\hat{\chi}-(\nabla^2\hat{\chi}^\dagger)\nabla\hat{\chi}+H.C.\right\rangle-\frac{\nabla^3\rho_\chi}{4}&=-\frac{1}{2}\langle(\nabla^2\hat{\chi}^\dagger)\nabla\hat{\chi}+(\nabla\hat{\chi}^\dagger)\cdot(\nabla\otimes\nabla\hat{\chi})+H.C.\rangle\\&=-\frac{1}{2}\nabla\cdot\langle(\nabla\hat{\chi}^\dagger)\otimes\nabla\hat{\chi}+H.C.\rangle\end{aligned} \tag{8.11}$$

Substitute Eq. (8.9) and (8.11) to the Eq. (8.8), one gets

$$\begin{aligned}f_{\mathrm{q,3D}}=&\nabla\cdot[J_\chi\otimes v_c+v_c\otimes J_\chi-\rho_\chi v_c\otimes v_c]-\frac{1}{2gm}\nabla\left(g^2\langle\phi_c^2\hat{\chi}^{\dagger2}+\phi_c^{*2}\hat{\chi}^2+2|\phi_c|^2\hat{\chi}^\dagger\hat{\chi}\rangle\right)\\&-\frac{\rho_c}{4m^2}\nabla\left[\frac{\rho_\chi}{\sqrt{\rho_c}}\nabla^2\left(\frac{1}{\sqrt{\rho_c}}\right)-\frac{1}{2\rho_c}(\nabla\rho_c)\cdot(\nabla\rho_\chi)-\frac{\rho_\chi}{\rho_c^{3/2}}\nabla^2\sqrt{\rho_c}\right]\\&-\frac{\rho_\chi}{m}\nabla\left[\frac{\nabla^2\sqrt{\rho_c}}{2m\sqrt{\rho_c}}\right]-\frac{1}{2m^2}\nabla\cdot\langle(\nabla\hat{\chi}^\dagger)\otimes\nabla\hat{\chi}+H.C.\rangle+\mathcal{O}\left(\frac{1}{\sqrt{N}}\right)\\=&\nabla\cdot[J_\chi\otimes v+v\otimes J_\chi-\rho_\chi v\otimes v]-\frac{1}{2gm}\nabla\left(g^2\langle\phi_c^2\hat{\chi}^{\dagger2}+\phi_c^{*2}\hat{\chi}^2+2|\phi_c|^2\hat{\chi}^\dagger\hat{\chi}\rangle\right)\\&-\frac{1}{2m^2}\nabla\cdot\langle(\nabla\hat{\chi}^\dagger)\otimes\nabla\hat{\chi}+H.C.\rangle\\&-\frac{\rho_\chi}{m}\nabla\left[\frac{\nabla^2\sqrt{\rho_c}}{2m\sqrt{\rho_c}}\right]-\frac{\rho_c}{4m^2}\nabla\left[\frac{(\nabla\rho_c)^2\rho_\chi}{\rho_c^3}-\frac{(\nabla\rho_c)\cdot(\nabla\rho_\chi)}{2\rho_c}\right]+\mathcal{O}\left(\frac{1}{\sqrt{N}}\right)\end{aligned} \tag{8.12}$$

Note that the last line vanishes when we use TF approximation. Hence, the leading order term is [68]

$$f_{\mathrm{q,3D}}^{\mathrm{TF}}=\nabla\cdot[J_\chi\otimes v_c+v_c\otimes J_\chi-\rho_\chi v_c\otimes v_c]-\frac{1}{2gm}\nabla\left(g^2\langle\phi_c^2\hat{\chi}^{\dagger2}+\phi_c^{*2}\hat{\chi}^2+2|\phi_c|^2\hat{\chi}^\dagger\hat{\chi}\rangle\right)$$

$$-\frac{1}{2m^2}\nabla\cdot\langle(\nabla\hat{\chi}^\dagger)\otimes\nabla\hat{\chi}+H.C.\rangle \tag{8.13}$$

For the 1-dimensional Bose gas, we can simply substitute $\nabla\to\partial_x$ to get $f_{\rm q}$ in our working order N^0,

$$\begin{aligned}f_{\rm q}=&\partial_x[2J_\chi v_c-\rho_\chi v_c^2]-\frac{1}{m^2}\partial_x\langle(\partial_x\hat{\chi}^\dagger)\partial_x\hat{\chi}\rangle-\frac{1}{2gm}\partial_x\left(g^2\langle\phi_c^2\hat{\chi}^{\dagger 2}+\phi_c^{*2}\hat{\chi}^2+2|\phi_c|^2\hat{\chi}^\dagger\hat{\chi}\rangle\right)\\&-\frac{\rho_\chi}{m}\partial_x\left[\frac{\partial_x^2\sqrt{\rho_c}}{2m\sqrt{\rho_c}}\right]-\frac{\rho_c}{4m^2}\partial_x\left[\frac{(\partial_x\rho_c)^2\rho_\chi}{\rho_c^3}-\frac{(\partial_x\rho_c)(\partial_x\rho_\chi)}{2\rho_c}\right]\end{aligned} \tag{8.14}$$

Note that all the terms except $\frac{1}{m^2}\partial_x\langle(\partial_x\hat{\chi}^\dagger)\partial_x\hat{\chi}\rangle$ are expressed in the measurable quantities. Using the Bogoliubov-de Gennes equation (3.34), one gets

$$\begin{aligned}-\frac{1}{m^2}\partial_x\langle(\partial_x\hat{\chi}^\dagger)(\partial_x\hat{\chi})\rangle=&\partial_t J_\chi-\frac{1}{4m^2}\partial_x^3\rho_\chi+\frac{\rho_\chi}{m}\partial_x(U+2g\rho_c)\\&+\frac{1}{2m}\left[\langle\hat{\chi}^2\rangle\partial_x(g\phi_c^{*2})+\langle\hat{\chi}^{\dagger 2}\rangle\partial_x(g\phi_c^2)\right]\end{aligned} \tag{8.15}$$

and because $\phi_c=e^{i\theta_c}\sqrt{\rho}_c$ with $\partial_x\theta_c=mv_c$, we have the relation

$$\begin{aligned}-\frac{\rho_c}{2m}\partial_x\left(g\frac{G^{(2)}}{\rho_c}\right)=&-\frac{1}{2mg}\partial_x(g^2\langle\phi_c^2\hat{\chi}^{\dagger 2}+\phi_c^{*2}\hat{\chi}^2+2\rho_c\hat{\chi}^\dagger\hat{\chi}\rangle)-igv_c(\phi_c^2\langle\hat{\chi}^{\dagger 2}\rangle-\phi_c^{*2}\langle\hat{\chi}^2\rangle)\\&+\frac{\rho_\chi}{m}\partial_x(g\rho_c)+\frac{1}{2m}\left[\langle\hat{\chi}^2\rangle\partial_x(g\phi_c^{*2})+\langle\hat{\chi}^{\dagger 2}\rangle\partial_x(g\phi_c^2)\right].\end{aligned} \tag{8.16}$$

where the two-point correlation function is (See Eq. (3.39).)

$$G^{(2)}:=\langle:(\hat{\rho}-\langle\hat{\rho}\rangle)^2:\rangle, \tag{8.17}$$

Substituting Eq. (8.15), Eq. (8.16) and continuity equation (3.44) to the (8.14), one gets

$$\begin{aligned}f_q=&-v_c\partial_t\rho_\chi-igv_c(\phi_c^2\langle\hat{\chi}^{\dagger 2}\rangle-\phi_c^{*2}\langle\hat{\chi}^2\rangle)-J_\chi\partial_x v_c\\&+\partial_x(J_\chi v_c-\rho_\chi v_c^2)-\frac{1}{2gm}\partial_x(g^2\langle\phi_c^2\hat{\chi}^{\dagger 2}+\phi_c^{*2}\hat{\chi}^2+2\rho_c\hat{\chi}^\dagger\hat{\chi}\rangle)\\&+\partial_t J_\chi-\frac{1}{4}\partial_x^3\rho_\chi+\frac{\rho_\chi}{m}\partial_x(U+2g\rho_c)+\frac{1}{2m}\left[\langle\hat{\chi}^2\rangle\partial_x(g\phi_c^{*2})+\langle\hat{\chi}^{\dagger 2}\rangle\partial_x(g\phi_c^2)\right]\end{aligned}$$

$$
\begin{aligned}
&-\frac{\rho_\chi}{m}\partial_x\left[\frac{\partial_x^2\sqrt{\rho_c}}{2m\sqrt{\rho_c}}\right]-\frac{\rho_c}{4m^2}\partial_x\left[\frac{(\partial_x\rho_c)^2\rho_\chi}{\rho_c^3}-\frac{(\partial_x\rho_c)(\partial_x\rho_\chi)}{2\rho_c}\right]\\
&=\partial_t J_\chi-v_c\partial_t\rho_\chi+\partial_x(J_\chi v_c-\rho_\chi v_c^2)-J_\chi\partial_x v_c\\
&\quad-\frac{1}{2gm}\partial_x(g^2\langle\phi_c^2\hat{\chi}^{\dagger 2}+\phi_c^{*2}\hat{\chi}^2+2\rho_c\hat{\chi}^\dagger\hat{\chi}\rangle)-igv_c(\phi_c^2\langle\hat{\chi}^{\dagger 2}\rangle-\phi_c^{*2}\langle\hat{\chi}^2\rangle)\\
&\quad-\frac{\rho_\chi}{m}\partial_x\left[\frac{\partial_x^2\sqrt{\rho_c}}{2m\sqrt{\rho_c}}\right]+\frac{\rho_\chi}{m}\partial_x(U+2g\rho_c)+\frac{1}{2m}\left[\langle\hat{\chi}^2\rangle\partial_x(g\phi_c^{*2})+\langle\hat{\chi}^{\dagger 2}\rangle\partial_x(g\phi_c^2)\right]\\
&\quad-\frac{1}{4m^2}\partial_x^3\rho_\chi-\frac{\rho_c}{4m^2}\partial_x\left[\frac{(\partial_x\rho_c)^2\rho_\chi}{\rho_c^3}-\frac{(\partial_x\rho_c)(\partial_x\rho_\chi)}{2\rho_c}\right]\\
&=\partial_t J_\chi-v_c\partial_t\rho_\chi+\partial_x(J_\chi v_c-\rho_\chi v_c^2)-J_\chi\partial_x v_c-\frac{\rho_c}{2m}\partial_x\left(\frac{gG^{(2)}}{\rho_c}\right)\\
&\quad+\frac{\rho_\chi}{m}\partial_x\left[-\frac{\partial_x^2\sqrt{\rho_c}}{2m\sqrt{\rho_c}}+U+g\rho_c\right]\\
&\quad-\frac{\rho_c}{4}\partial_x\left[\frac{1}{2}\frac{1}{\sqrt{\rho_c}}\partial_x^2\left(\frac{\rho_\chi}{\sqrt{\rho_c}}\right)-\frac{\rho_\chi}{\rho_c^{3/2}}\partial_x^2\sqrt{\rho_c}\right]
\end{aligned}
\tag{8.18}
$$

8.3 Calculation for the Homogeneous Model

Let $\tilde{F}_{n,0}$ be a solution to the equation

$$-\sigma_4\tilde{F}_{n,0}=(1,1)^{\mathrm{t}}.$$

Then $\tilde{F}_{n,0}$ is

$$\tilde{F}_{n,0}=-\frac{1}{2}(1,1)^{\mathrm{t}}.$$

Let $\tilde{F}_{n,\pm 1}$ be a solution of the equation

$$(i\partial_t\sigma_3-\sigma_4)\tilde{F}_{n,\pm 1}=e^{\pm 2i\omega_n t}(1,1)^{\mathrm{t}}.$$

Using the ansatz $\tilde{F}_{n,\pm 1}=e^{\pm 2i\omega_n t}(a,b)^{\mathrm{t}}$, we have

$$
\begin{pmatrix}
\mp 2\omega_n-1 & -1\\
-1 & \pm 2\omega_n-1
\end{pmatrix}
\begin{pmatrix}
a\\ b
\end{pmatrix}
=
\begin{pmatrix}
1\\ 1
\end{pmatrix}
\tag{8.19}
$$

Hence,

$$\tilde{F}_{n,\pm 1} = \mp \frac{e^{\pm 2i\omega_n t}}{2\omega_n}(1,-1)^{\mathrm{t}} \tag{8.20}$$

Let $\tilde{F}_{n,\pm 2}$ be a solution to the equation

$$(i\partial_t \sigma_3 - \sigma_4)\tilde{F}_{n,\pm 2} = e^{\pm 2i\omega_n t}(1,-1)^{\mathrm{t}}.$$

Using the ansatz $\tilde{F}_{n,\pm 2} = e^{\pm 2i\omega_n t}(a,b)^{\mathrm{t}}$, we have

$$\begin{pmatrix} \mp 2\omega_n - 1 & -1 \\ -1 & \pm 2\omega_n - 1 \end{pmatrix} \begin{pmatrix} a \\ b \end{pmatrix} = \begin{pmatrix} 1 \\ -1 \end{pmatrix} \tag{8.21}$$

Hence,

$$\tilde{F}_{n,\pm 2} = \frac{e^{\pm 2i\omega_n t}}{2\omega_n^2}(1 \mp \omega_n, -1 \mp \omega_n)^{\mathrm{t}}. \tag{8.22}$$

Let $\tilde{F}_{n,\pm 3}$ be a solution to the equation

$$\left(\frac{1}{2}\partial_x^2 - \sigma_4\right)\tilde{F}_{n,\pm 3} = \cos(2k_n x)(1,1)^{\mathrm{t}}.$$

Using the ansatz $\tilde{F}_{n,3} = \cos(2k_n x)(a,b)^{\mathrm{t}}$, we have

$$\begin{pmatrix} -2k_n^2 - 1 & -1 \\ -1 & -2k_n^2 - 1 \end{pmatrix} \begin{pmatrix} a \\ b \end{pmatrix} = \begin{pmatrix} 1 \\ 1 \end{pmatrix} \tag{8.23}$$

Hence,

$$\tilde{F}_{n,3} = -\frac{\cos(2k_n x)}{2(k_n^2+1)}(1,1)^{\mathrm{t}} \tag{8.24}$$

Let $\tilde{F}_{n,\pm 4}$ be a solution of the equation

$$\left(i\partial_t \sigma_3 + \frac{1}{2}\partial_x^2 - \sigma_4\right)\tilde{F}_{n,\pm 4} = \cos(2k_n x)e^{\pm 2i\omega_n t}(1,1)^{\mathrm{t}}.$$

Using the ansatz $\tilde{F}_{n,\pm 4} = \cos(2k_n x) e^{\pm 2i\omega_n t}(a,b)^{\mathrm{t}}$, we have

$$\begin{pmatrix} \mp 2\omega_n - 2k_n^2 - 1 & -1 \\ -1 & \pm 2\omega_n - 2k_n^2 - 1 \end{pmatrix} \begin{pmatrix} a \\ b \end{pmatrix} = \begin{pmatrix} 1 \\ 1 \end{pmatrix}. \tag{8.25}$$

Hence,

$$\tilde{F}_{n,\pm 4} = \frac{2\cos(2k_n x) e^{\pm 2i\omega_n t}}{3k_n^4} (\pm\omega_n - k_n^2, \mp\omega_n - k_n^2)^{\mathrm{t}}. \tag{8.26}$$

Let $\tilde{F}_{n,\pm 5}$ be a solution of the equation

$$\left(i\partial_t \sigma_3 + \frac{1}{2}\partial_x^2 - \sigma_4 \right) \tilde{F}_{n,\pm 5} = \cos(2k_n x) e^{\pm 2i\omega_n t}(1,-1)^{\mathrm{t}}.$$

Using the ansatz $\tilde{F}_{n,\pm 5} = \cos(2k_n x) e^{\pm 2i\omega_n t}(a,b)^{\mathrm{t}}$, one has

$$\begin{pmatrix} \mp 2\omega_n - 2k_n^2 - 1 & -1 \\ -1 & \pm 2\omega_n - 2k_n^2 - 1 \end{pmatrix} \begin{pmatrix} a \\ b \end{pmatrix} = \begin{pmatrix} 1 \\ -1 \end{pmatrix} \tag{8.27}$$

Hence,

$$\tilde{F}_{n,\pm 5} = \frac{2\cos(2k_n x) e^{\pm 2i\omega_n t}}{3k_n^4} (\pm\omega_n - k_n^2 - 1, \pm\omega_n + k_n^2 + 1)^{\mathrm{t}} \tag{8.28}$$

8.4 Direct Calculation of f_{cl}

One can also obtain Eq. (5.90) also by directly putting our field expansion to the definition Eq. (4.10). In our model, $\rho_0 = \text{const.}, v_0 = 0, U + g\rho_0 = \mu = \text{const.}$. Hence, in our scaling, Eq. (5.90) becomes

$$f_{\mathrm{q}} = -\frac{1}{2}\partial_x G^{(2)} - \frac{1}{4}\partial_x^3 \rho_\chi. \tag{8.29}$$

Recall that we know all the mode function Eq. (5.41), Eq. (5.42), Eq. (5.54), Eq. (5.57). Hence, the Eq. (8.17) gives us

$$\partial_x G^{(2)} = \rho_c \langle \psi^2 + \psi^{\dagger 2} + \psi^\dagger \psi \rangle$$

$$= \sum_n 2\partial_x \Re[(u_n + v_n)v_n^*]$$
$$= \frac{1}{\ell}\sum_{n=1}^{\infty} \frac{(-1)^n k_n^3 \sin(2k_n x)}{\omega_n^2}[1 - \cos(2\omega_n t)] \tag{8.30}$$

And from Eq. (5.45), one gets

$$\partial_x^3 \rho_\chi = \frac{4}{\ell}\sum_{n=1}^{\infty} \frac{(-1)^n k_n^3 \sin(2k_n x)}{\omega_n^2}[1 - \cos(2\omega_n t)]. \tag{8.31}$$

Let us put Eq. (8.30) and Eq. (8.31) to Eq. (8.29), and then one gets

$$f_{\rm q} = -\frac{3}{2\ell}\sum_{n=1}^{\infty} \frac{(-1)^n k_n^3 \sin(2k_n x)}{\omega_n^2}[1 - \cos(2\omega_n t)]$$
$$= -\frac{6}{\ell}\sum_{n=1}^{\infty} \frac{(-1)^n k_n \sin(2k_n x)}{k_n^2 + 4}[1 - \cos(2\omega_n t)]$$

which is the same as Eq. (5.90).

Bibliography

[1] Ivan Agullo: *Qft in curved space-time, from loop quantum gravity online summer school*. June 2021.

[2] A. Ashtekar, Anne Magnon, and Roger Penrose: Quantum fields in curved space-times. *Proceedings of the Royal Society of London. A. Mathematical and Physical Sciences*, **346** (1975), 375–394.

[3] Roberto Balbinot, Alessandro Fabbri, Serena Fagnocchi, Alessio Recati, and Iacopo Carusotto: Nonlocal density correlations as a signature of Hawking radiation from acoustic black holes. *Phys. Rev. A*, **78** (2 Aug. 2008), 021603(R).

[4] Roberto Balbinot, Serena Fagnocchi, Alessandro Fabbri, and Giovanni P. Procopio: Backreaction in acoustic black holes. *Phys. Rev. Lett.*, **94** (16 Apr. 2005), 161302.

[5] T. P. Billam, P. Mason, and S. A. Gardiner: Second-order number-conserving description of nonequilibrium dynamics in finite-temperature bose-einstein condensates. *Phys. Rev. A*, **87** (3 Mar. 2013), 033628.

[6] Sean M. Carroll: *Spacetime and Geometry: An Introduction to General Relativity*. Cambridge University Press, 2019.

[7] I. Carusotto, S. X. Hu, L. A. Collins, and A. Smerzi: Bogoliubov-Cherenkov Radiation in a Bose-Einstein Condensate Flowing against an Obstacle. *Phys. Rev. Lett.*, **97** (26 Dec. 2006), 260403.

[8] Y. Castin, and R. Dum: Low-temperature Bose-Einstein condensates in time-dependent traps: Beyond the $U(1)$ symmetry-breaking approach. *Phys. Rev. A*, **57** (4 Apr. 1998), 3008–3021.

[9] A. P. Chikkatur, Y. Shin, A. E. Leanhardt, D. Kielpinski, E. Tsikata, T. L. Gustavson, D. E. Pritchard, and W. Ketterle: A Continuous Source of Bose-Einstein Condensed Atoms. *Science*, **296** (2002), 2193–2195.

[10] Antonin Coutant, and Renaud Parentani: Black hole lasers, a mode analysis. *Phys. Rev. D*, **81** (8 Apr. 2010), 084042.

[11] Jonathan Curtis, Gil Refael, and Victor Galitski: Evanescent modes and step-like acoustic black holes. *Annals of Physics*, **407** (2019), 148–165.

[12] V. A. De Lorenci, and E. S. Moreira: Renormalized scalar propagator around a dispiration. *Phys. Rev. D*, **67** (12 June 2003), 124002.

[13] Salvatore De Vincenzo, and Carlet Sánchez: Point interactions: boundary conditions or potentials with the Dirac delta function. *Canadian Journal of Physics*, **88** (2010), 809–815.

[14] F. de Felice, and C.J.S. Clarke: *Relativity on Curved Manifolds*. Cambridge Monographs on Mathematical Physics. Cambridge University Press, 1992.

[15] Grace E. Field: *The latest frontier in analogue gravity: new roles for analogue experiments*. June 2021.

[16] S. Finazzi, and R. Parentani: Black hole lasers in Bose–Einstein condensates. *New Journal of Physics*, **12** (Sept. 2010), 095015.

[17] L. H. Ford: *Quantum field theory in curved spacetime*. 1997.

[18] S. A. Fulling: Varieties of instability of a boson field in an external potential. *Phys. Rev. D*, **14** (8 Oct. 1976), 1939–1943.

[19] Stephen A. Fulling: *Aspects of Quantum Field Theory in Curved Spacetime*. London Mathematical Society Student Texts. Cambridge University Press, 1989.

[20] Stephen A. Fulling: Nonuniqueness of canonical field quantization in riemannian space-time. *Phys. Rev. D*, **7** (10 May 1973), 2850–2862.

[21] L. J. Garay, J. R. Anglin, J. I. Cirac, and P. Zoller: Sonic black holes in dilute Bose-Einstein condensates. *Phys. Rev. A*, **63** (2 Jan. 2001), 023611.

[22] S. A. Gardiner, and S. A. Morgan: Number-conserving approach to a minimal self-consistent treatment of condensate and noncondensate dynamics in a degenerate bose gas. *Phys. Rev. A*, **75** (4 Apr. 2007), 043621.

[23] Alexander L. Gaunt, Tobias F. Schmidutz, Igor Gotlibovych, Robert P. Smith, and Zoran Hadzibabic: Bose-Einstein Condensation of Atoms in a Uniform Potential. *Phys. Rev. Lett.*, **110** (20 May 2013), 200406.

[24] Luca Giacomelli, and Iacopo Carusotto: Understanding superradiant phenomena with synthetic vector potentials in atomic bose-einstein condensates. *Phys. Rev. A*, **103** (4 Apr. 2021), 043309.

[25] M. D. Girardeau: Comment on "particle-number-conserving bogoliubov method which demonstrates the validity of the time-dependent gross-pitaevskii equation for a highly condensed bose gas". *Phys. Rev. A*, **58** (1 July 1998), 775–778.

[26] S. W. Hawking: Particle creation by black holes. *Communications in Mathematical Physics*, **43** (Aug. 1975), 199–220.

[27] S. W. Hawking, and G. F. R. Ellis: *The Large Scale Structure of Space-Time*. Cambridge Monographs on Mathematical Physics. Cambridge University Press, 1973.

[28] P. C. Hohenberg: Existence of long-range order in one and two dimensions. *Phys. Rev.*, **158** (2 June 1967), 383–386.

[29] M. Isoard, and N. Pavloff: Departing from thermality of analogue hawking radiation in a bose-einstein condensate. *Phys. Rev. Lett.*, **124** (6 Feb. 2020), 060401.

[30] P. Jain, A. S. Bradley, and C. W. Gardiner: Quantum de Laval nozzle: Stability and quantum dynamics of sonic horizons in a toroidally trapped Bose gas containing a superflow. *Phys. Rev. A*, **76** (2 Aug. 2007), 023617.

[31] Victor I. Kolobov, Katrine Golubkov, Juan Ramón Muñoz de Nova, and Jeff Steinhauer: Observation of stationary spontaneous Hawking radiation and the time evolution of an analogue black hole. *Nature Physics*, **17** (2021), 362–367.

[32] Yasunari Kurita, Michikazu Kobayashi, Hideki Ishihara, and Makoto Tsubota: Particle creation in bose-einstein condensates: theoretical formulation based on conserving gapless mean-field theory. *Phys. Rev. A*, **82** (5 Nov. 2010), 053602.

[33] P.-É. Larré, A. Recati, I. Carusotto, and N. Pavloff: Quantum fluctuations around black hole horizons in bose-einstein condensates. *Phys. Rev. A*, **85** (1 Jan. 2012), 013621.

[34] John M. Lee: *Riemannian Manifolds: An Introduction to Curvature*. Graduate Texts in Mathematics. Springer International Publishing, 2019.

[35] T. D. Lee, Kerson Huang, and C. N. Yang: Eigenvalues and Eigenfunctions of a Bose System of Hard Spheres and Its Low-Temperature Properties. *Phys. Rev.*, **106** (6 June 1957), 1135–1145.

[36] U. Leonhardt, T. Kiss, and P. Öhberg: Theory of elementary excitations in unstable Bose-Einstein condensates and the instability of sonic horizons. *Phys. Rev. A*, **67** (3 Mar. 2003), 033602.

[37] M. Lewenstein, and L. You: Quantum phase diffusion of a bose-einstein condensate. *Phys. Rev. Lett.*, **77** (17 Oct. 1996), 3489–3493.

[38] Stefano Liberati, Giovanni Tricella, and Andrea Trombettoni: Back-reaction in canonical analogue black holes. *Applied Sciences*, **10** (2020).

[39] Elliott H. Lieb, and Robert Seiringer: Proof of Bose-Einstein Condensation for Dilute Trapped Gases. *Phys. Rev. Lett.*, **88** (17 Apr. 2002), 170409.

[40] Elliott H. Lieb, Robert Seiringer, and Jakob Yngvason: Bosons in a trap: a rigorous derivation of the gross-pitaevskii energy functional. *Phys. Rev. A*, **61** (4 Mar. 2000), 043602.

[41] William C. C. Lima, George E. A. Matsas, and Daniel A. T. Vanzella: Awaking the Vacuum in Relativistic Stars. *Phys. Rev. Lett.*, **105** (15 Oct. 2010), 151102.

[42] William C. C. Lima, and Daniel A. T. Vanzella: Gravity-Induced Vacuum Dominance. *Phys. Rev. Lett.*, **104** (16 Apr. 2010), 161102.

[43] Raphael Lopes, Christoph Eigen, Nir Navon, David Clément, Robert P. Smith, and Zoran Hadzibabic: Quantum Depletion of a Homogeneous Bose-Einstein Condensate. *Phys. Rev. Lett.*, **119** (19 Nov. 2017), 190404.

[44] Q. Z. Lv, Heiko Bauke, Q. Su, C. H. Keitel, and R. Grobe: Bosonic pair creation and the schiff-snyder-weinberg effect. *Phys. Rev. A*, **93** (1 Jan. 2016), 012119.

[45] Jean Macher, and Renaud Parentani: Black-hole radiation in Bose-Einstein condensates. *Phys. Rev. A*, **80** (4 Oct. 2009), 043601.

[46] R.D. Mattuck: *A Guide to Feynman Diagrams in the Many-body Problem.* Dover Books on Physics Series. Dover Publications, 1992.

[47] Florent Michel, and Renaud Parentani: Nonlinear effects in time-dependent transonic flows: An analysis of analog black hole stability. *Phys. Rev. A*, **91** (5 May 2015), 053603.

[48] Florent Michel, and Renaud Parentani: Saturation of black hole lasers in Bose-Einstein condensates. *Phys. Rev. D*, **88** (12 Dec. 2013), 125012.

[49] Giovanni Modugno: The life of an analogue black hole. *Nature Physics*, **17** (Mar. 2021), 300–301.

[50] Viatcheslav Mukhanov, and Sergei Winitzki: *Introduction to Quantum Effects in Gravity.* Cambridge University Press, 2007.

[51] Juan Ramón Muñoz de Nova, Katrine Golubkov, Victor I. Kolobov, and Jeff Steinhauer: Observation of thermal Hawking radiation and its temperature in an analogue black hole. *Nature*, **569** (2019), 688–691.

[52] Nir Navon, Robert P. Smith, and Zoran Hadzibabic: Quantum gases in optical boxes. *Nature Physics*, **17** (2021), 1334–1341.

[53] J. R. M. de Nova, D. Guéry-Odelin, F. Sols, and I. Zapata: Birth of a quasi-stationary black hole in an outcoupled Bose–Einstein condensate. *New Journal of Physics*, **16** (Dec. 2014), 123033.

[54] J. R. M. de Nova, P. F. Palacios, I. Carusotto, and F. Sols: Long time universality of black-hole lasers. *New Journal of Physics*, **23** (Feb. 2021), 023040.

[55] Sam Patrick, Harry Goodhew, Cisco Gooding, and Silke Weinfurtner: Backreaction in an analogue black hole experiment. *Phys. Rev. Lett.*, **126** (4 Jan. 2021), 041105.

[56] Tobias Paul, Klaus Richter, and Peter Schlagheck: Nonlinear Resonant Transport of Bose-Einstein Condensates. *Phys. Rev. Lett.*, **94** (2 Jan. 2005), 020404.

[57] Oliver Penrose, and Lars Onsager: Bose-einstein condensation and liquid helium. *Phys. Rev.*, **104** (3 Nov. 1956), 576–584.

[58] L. P. Pitaevskii, and S. Stringari: *Bose-Einstein Condensation*. International Series of Monographs on Physics. Clarendon Press, Oxford, 2003.

[59] Caio C. Holanda Ribeiro, Sang-Shin Baak, and Uwe R. Fischer: Existence of steady-state black hole analogs in finite quasi-one-dimensional bose-einstein condensates. *Phys. Rev. D*, **105** (12 June 2022), 124066.

[60] Caio C. Holanda Ribeiro, and Daniel A. Turolla Vanzella: Analogues of gravity-induced instabilities in anisotropic metamaterials. *Phys. Rev. Research*, **2** (1 Mar. 2020), 013281.

[61] A. D. Sakharov: Vacuum quantum fluctuations in curved space and the theory of gravitation. *Dokl. Akad. Nauk Ser. Fiz.*, **177** (1967). Ed. by Yu. A. Trutnev, 70–71.

[62] Humitaka Sato, and Kei-ichi Maeda: Instability of a Quantum Field in the Curved Space-Time of a Rotating Star. *Progress of Theoretical Physics*, **59** (Apr. 1978), 1173–1187.

[63] S. Schander, and T. Thiemann: Backreaction in cosmology. *Frontiers in Astronomy and Space Sciences*, **8** (2021).

[64] L. I. Schiff, H. Snyder, and J. Weinberg: On the existence of stationary states of the mesotron field. *Phys. Rev.*, **57** (4 Feb. 1940), 315–318.

[65] Frederic P. Schuller: *Lectures from the we-heraeus international winter school on gravity and light*. a b. Feb. 2015.

[66] RALF SCHÜTZHOLD, MICHAEL UHLMANN, YAN XU, and UWE R. FISCHER: Mean-field expansion in bose–einstein condensates with finite-range interactions. *International Journal of Modern Physics B*, **20** (2006), 3555–3565.

[67] Ralf Schützhold, Michael Uhlmann, Yan Xu, and Uwe R. Fischer: Mean-field expansion in Bose-Einstein condensates with finite-range interactions. *International Journal of Modern Physics B*, **20** (2006), 3555–3565.

[68] Ralf Schützhold, Michael Uhlmann, Yan Xu, and Uwe R. Fischer: Quantum backreaction in dilute bose-einstein condensates. *Phys. Rev. D*, **72** (10 Nov. 2005), 105005.

[69] R. Seki: On Boundary Conditions for an Infinite Square-Well Potential in Quantum Mechanics. *American Journal of Physics*, **39** (1971), 929–931.

[70] M. Tettamanti, S. L. Cacciatori, A. Parola, and I. Carusotto: Numerical study of a recent black-hole lasing experiment. *EPL (Europhysics Letters)*, **114** (June 2016), 60011.

[71] Loring W. Tu: *An Introduction to Manifolds*. Universitext. Springer New York, 2010.

[72] W. G. Unruh: Experimental black-hole evaporation? *Phys. Rev. Lett.*, **46** (21 May 1981), 1351–1353.

[73] W. G. Unruh: Notes on black-hole evaporation. *Phys. Rev. D*, **14** (4 Aug. 1976), 870–892.

[74] P. B. Walczak, and J. R. Anglin: Back-reaction of perturbation wave packets on gray solitons. *Phys. Rev. A*, **86** (1 July 2012), 013611.

[75] R.M. Wald: *Quantum Field Theory in Curved Spacetime and Black Hole Thermodynamics*. Chicago Lectures in Physics. University of Chicago Press, 1994.

[76] Robert M Wald: *General relativity*. Chicago, IL: Chicago Univ. Press, 1984.

[77] Yi-Hsieh Wang, Ted Jacobson, Mark Edwards, and Charles W. Clark: Induced density correlations in a sonic black hole condensate. *SciPost Phys.*, **3** (2017), 022.

[78] Yi-Hsieh Wang, Ted Jacobson, Mark Edwards, and Charles W. Clark: Mechanism of stimulated hawking radiation in a laboratory bose-einstein condensate. *Phys. Rev. A*, **96** (2 Aug. 2017), 023616.

초 록

아날로그 중력은 휘어진 시공간에서의 물리를 실험실에서 가능한 실험으로 시뮬레이션하는 학제간 연구 프로그램이다. 본 연구는 입자간 상호작용이 접촉 상호작용인 준-1차원 유한한 크기의 보즈-아인슈타인 응축체 (BEC)에서의 측정가능한 아날로그 중력 효과를 다루고 있다. 보즈 가스의 해밀토니안이 전체 $U(1)$-대칭성이 있기 때문에, 총 입자의 수 N은 고정되어있다. 따라서, 큰 N을 가진 시스템에서, $1/\sqrt{N}$을 장의 작은 전개 매개변수로 사용할 수 있다. 이 논문에서 입자수를 보존하는 보골리우보프 전개는 $U(1)$ 대칭성을 깨는 보통의 입자수를 보존하지 않는 보골리우보프 전개에 단순하게 장의 $N^{-1/2}$-차 항을 포함하여 행해진다. 그 포함된 장은 보골리우보프 장에 의해 유도된 응축의 보정으로 해석된다. 전개의 타당성은 오로지 결손이 작다는 보골리우보프 근사에 의존한다. 그리고 분석은 타당한 영역에서 행해졌다. 특히, 타당한 영역의 시간 규모도 연구되었다.

본 연구는 극저온 가스 실험에서 실현 가능한 두 개의 유한한 크기의 시스템을 다룬다. 첫 번째로, 1차원 유한한 크기의 균일한 보즈-아인슈타인 응축이 연구되었다. 입자수를 보존하는 보골리우보프 전개를 이용하여, 운동방정식의 이 모델에 대한 $N^{-1/2}$-차 항 전개까지 정확한 모드 해를 얻을 수 있다. 응축은 처음에 상호작용하지 않으며, 바닥상태에 있다고 가정하여 잘-정의된 초기 진공상태를 보장한다. 갑자기 상호작용을 켜서, 응축은 순간적으로 평형상태에서 벗어난다. 특히,이 초기 진공 가정은 위상 분산과 그로인한 응축체 붕괴로 말미암아 생기는 상호작용하는 응축체의 모호한 진공의 정의를 피할 수 있게 해준다. 주어진

진공 상태에서 모드 전개의 정확한 해를 이용하여, 결손과 응축체 보정이 계산되었다. 결손과 응축체 보정은 파워 스펙트럼 관측을 통해서는 구분할 수 없음을 밝혔다. 게다가, 비록 초기 응축체가 정지한 상태이고 응축의 주요 항은 움직이지 않더라도, 결손된 입자들의 양자요동이 자명하지 않는 버금 차수의 응축 흐름을 만들어낸다.

더욱이, 양자 백리액션 힘이 마들룽 표현을 통해 얻을 수 있는 오일러 힘에서 벗어난 정도로 정의되었다. 또한, 주요 차수 항에서 정지한 응축체의 경우, 전개 차수 (N^0) 에서, 고전 힘이 오직 총 입자의 밀도에만 의존함을 보였다. 따라서, 총 밀도를 시간의 함수로 아는 것이 실험적으로 양자 백리액션 힘을 측정할 수 있는 실현 가능한 방법을 준다. 게다가, 고전힘과 총 힘이 보존 형태로 쓰일 수 있다. 즉, 그들에 대한 스칼라 퍼텐셜을 찾을 수 있다. 퍼텐셜이 힘보다 훨씬 빠르게 수렴하기 때문에, 고전과 총 퍼텐셜을 해석적 형태로 구하고 그들을 그릴 수 있다. 그로부터 양자 백리액션 힘이 경계면 근처에서 고전 힘을 많이 줄여준다는 것을 확인할 수 있다.

두 번째로, 1차원 유한한 크기의 부분적으로 균일한 흐름 모형을 연구했다. 흐름은 경계에 놓여진 결맞은 소스와 드레인을 통해 유지된다. 각 영역에서 마하수는 흐름 속도와 각 영역에서 음속의 비율로 정의된다. 특히, 아날로그 사건 지평선은 마하수가 1을 넘어가는 영역으로 정해진다. 해밀토니안의 에르미션아님과 관계 없이 원론적으로는 안정적인 사건 지평선 하나를 가지는 음파 블랙홀 모형이 유지될 수 있음을 보였다.

블랙홀-화이트홀 쌍에서와 같이 동적 불안정이 발생한다. 블랙홀의 생존시간이 불안정에 의해 정의되며, 시스템 매개변수에 대한 생존 시간 역시 연구되었다. 이 모델에 대한 양자 결손이 보골리우보프 이론의 타당성을 검증하고 아날로그 호킹 과정을 묘사하는 도구로 제안되었다. 사건지평선 안쪽과 바깥쪽 모두에서 호킹복사의 명백한 신호를 찾을 수 있다. 불안정과 쉬프-스나이더-와인버그 현상과의 관계가 정성적으로 연구되었다.

주요어: Bose-Einstein Condensate, Analogue Gravity
Quantum Backreaction, Depletion

학 번: 2012-20359

Acknowledgement

This thesis came out from the third project since I joined our group. Because it took a long time to choose the topic and to proceed with research, there are a lot of people I'm thankful for. I would like to take this opportunity to express my gratitude briefly.

First of all, I would like to thank professor Fischer. As an advisor, he gives many critical and exciting questions. I get a lot of motivation for research from conversations with him. I also want to say 'Muito Obrigado' to professor Caio. He is a saviour of my graduation. He is a great researcher enough to be my role model and is a good friend. 바쁘신 와중에도 심사위원장을 맡아 심사를 진행해주신 정성훈 교수님께 감사의 인사를 드립니다. 심사 전반적으로 날카로운 질문을 주신 신용일 교수님께 감사의 말씀을 드리고 싶습니다. 심사 이후에도 깊은 내공으로 주신 조언과 아이디어들을 통해 이 논문 뿐만 아니라 앞으로 진행할 연구도 더 풍성하게 생각하고 진행할 수 있게 되었습니다. 논문의 내용을 꼼꼼히 봐주시고 심사 이후에 세세한 피드백을 주신 김지훈 교수님께도 감사를 올립니다.

제가 연구실에 들어왔을 때 졸업을 앞둔 상황이었던 명균이형은 바쁜 와중에도 잊지 않고 조언을 해주셨습니다. 학교에 있는 내내 석영이형은 정말 많은 것을 챙겨 주셨습니다. 졸업이 가까워질 수록 석영이형이 얼마나 많은 것을 챙겨주셨는지를 알게 됩니다. 그래서 더욱 감사하고 그만큼 제가 후배들한테 잘

챙겨줬는지 반성하게 됩니다. 연구실 멤버중 가장 많은 추억을 공유하는 건 태웅이형입니다. 가끔 걱정되는 면도 있지만 언제나 배우는 점이 많습니다. 성호씨는 도움이 필요할 때 언제나 친절하게 저에게 많은 도움을 주곤 했습니다. 재균이는 후배임에도 확고하고 분명한 마음가짐과 가치관이 멋지고 본받고 싶은 점이 더 많습니다. 그래서 무언가 챙겨준 일이 별로 없는 것 같아 미안한 마음이 큽니다. 연구를 진행하면서 중간중간 연구에 대해서 혹은 관련된 개념에 대해서 누군가와 이야기하고 싶을 때가 많았습니다. 그때 마침 연구실에 들어온 상종이와 이야기하면서 많은 것들을 다듬어낼 수 있었습니다. 주연이와 승범이는 함께 보낸 시간이 짧아 많은 이야기를 나누지 못해 아쉽습니다. Papon is a warm-hearted friend. discussion with him is always interesting and made me think more deeply about the subject. He helped me a lot. Morgan is very enthusiastic and kind. He gave me a lot of advice about job searching.

학위과정동안 가르치는 일을 하였습니다. 특히 제가 연구에 집중하도록 배려해주고 경제적으로 도움을 준 잔디학원 여러분께 이 자리를 빌어 감사의 말씀을 드립니다. 잔디선생님, 용남식선생님, 승리형은 가르치는 즐거움 뿐만 아니라 책임감에 대해서도 많은 깨달음을 주셨습니다. 과외 학생인 동현이를 가르치면서, 학부때 가볍게 넘겼던 설명과 개념들을 즐겁게 더 꼼꼼히 볼 수 있었습니다. 천체물리에 관심이 많은 동현이가 앞으로 관심과 열정을 잃지 않고 물리를 즐겼으면 좋겠습니다.

연구를 진행하면서 필요했던 수학적 개념들은 현기에게 배운 것들이 많습니다. 그리고 광우형, 종정이형, 성우, 재훈이형이 알려주신 내용이 많은 도움이 되었습니다. 동진이형도 이론적인 개념에 많은 도움을 주었습니다. 본 논문의 연구를 진행하면서 직접적인 수치 계산을 사용하진 않았지만 중간중간 환철이형, 정환이형,장호형,보람이형,용철이형이 알려주신 개념들이 많은 도움이 되었습니다. 지금 이 자리를 빌어 감사를 전합니다.

많은 인연들이 연구를 진행하는 동안 저에게 큰 힘이 되었습니다. 동민이형은 때론 걱정과 질책을 하기도 하고, 때론 응원도 하며 저에게 많은 조언을 주었습니다. 늘 장난스레 대하지만 존경하는 형입니다. 경태, 간승, 지호, 일영이와는 학업, 진로, 미래 등 다양한 주제에 대해 많은 이야기를 나누고 도움을 받았습니다. 생각이 깊어 그만큼 고민이 많은 민주는 제가 가장 아끼고 좋아하는 후배입니다. 덩달아 고민하며 많은 것을 배우기도 하고, 즐겁게 이야기를 나누고 나면 언제나 힘이 납니다. 사랑이와 향형은 오랜 시간 친하게 지내며 서로 지켜봐 주었습니다. 진현이, 규현이, 규하, 상래는 만날 때마다 고등학교 시절로 돌아간 듯한 느낌에 들뜨게 됩니다. 용기와 창민이를 만나 이야기할 때면 제가 전혀 모르는 것들에 대한 이야기들이 많아 신기하고 즐겁습니다. 성우형을 만날때는 언제나 든든하고 마음이 편합니다. 형이 소개해준 예찬이와도 만날때면 너무나 즐겁습니다. 지현이누나는 제가 처음 이 논문에 나온 연구 주제를 받았을 때 옆에서 많은 도움을 주었습니다. 혁이, 영성이형, 태진이는 만날 때마다 웃음이 끊이지 않는 좋은 친구들입니다. 훌리아는 제가 연구를 진행하는 동안 가장 오랜 시간을 함께 했습니다. 창훈이형, 재영이형, 람이는 함께 공부하면서 서로 용기를 북돋워 주었습니다. 준상이형과는 종종 이야기를 하며 이런저런 고충을 나누었습니다. 대학원에 오고 가장 오래 보아온 인연 중 한 명인 지선이와는 틈틈이 가벼운 이야기를 하기도 하고, 때론 고민을 나누기도 했습니다. 이 자리를 빌려 모두에게 다시 한번 고맙다는 말을 전하고 싶습니다.

무엇보다 오랜 시간 저를 지켜봐 준 가족 모두에게 감사의 인사를 전하고 싶습니다. 때론 응원하고 걱정해준 엄마, 아빠, 동생 부부에게 감사의 인사를 전합니다. 바쁘단 핑계로 연락도 거의 안 하는 저를 늘 먼저 챙겨 주는 매형과 사촌들을 비롯하여 고모, 이모, 이모부, 삼촌, 모든 분들께 감사의 인사를 드립니다. 특히 저를 언제나 아껴주셨던 할머니께 이 자리를 빌어 감사의 인사를 올립니다.